UNIVERSITÀ DEGLI STUDI DI PADOVA

Dipartimento di Fisica e Astronomia "Galileo Galilei"

Master Degree in Physics

Final Dissertation

Production and Signatures of CP-even Scalars from Core-Collapse Supernovae

Thesis supervisor
Prof. Francesco D'Eramo

Thesis co-supervisor
Dr. Andrea Caputo

Candidate
Federico Pavone

Academic Year 2023/2024

Contents

Introduction

Despite representing the 27% of the energy budget of the Universe, Dark Matter composition remains one of the most fascinating open problems in Fundamental Physics. In the last five decades the collection of new indisputable evidences concerning its existence has been closely accompanied by the attempts to find a suitable model to understand its origin and microscopic nature. A widely spread assumption in the literature is that the Dark Matter is an elementary particle as much as the ones described by the Standard Model of Particle Physics. In this case, the mass range available for DM models can vary from $10^{-22}\,eV$ to be confined inside galactic halos to enormous scales as the ones of Grand Unified Theories of $10^{15}\,GeV$. This range can be significantly reduced if one considers models that have been in thermal equilibrium with the primordial bath of SM particles at some early stages of the evolution of our Universe. To compose the observed energy density of DM we observe today, at some point these thermal models have to decouple from thermal equilibrium in a process called *freeze-out*. In this scenario, DM mass must be higher than some keV to allow for structure formation and lighter than some $10\,TeV$ for perturbative unitarity.

A principle that has lead physicists in their attempt to unveil the Dark Matter mystery is the one of trying to solve the inconsistencies of the Standard Model adding new degrees of freedom which could provide a satisfying description of DM nature. This is the case of Weakly Interacting Massive Particles, which could solve the *hierarchy problem*. They constitute a thermal model with mass $m_\chi = (10\,GeV—10\,TeV)$ and an annihilation cross section of the order of typical Weak Interactions $\langle\sigma v\rangle = 1\,pb$, hence their name. This choice "miraculously" leads to the observed DM density today. Another famous example is the one of the axions, that are designed for solving the Strong CP Problem, but can also be light (e.g. with respect to WIMPs) Dark Matter candidates, thanks to their oscillations in the Friedmann-Robertson-Walker (FRW) background, in the so-called *misalignment* mechanism.

Strong bounds for QCD axions and Axion-like Particles (which in general do not solve the Strong CP problem) come from astrophysical environments such as the Sun, White Dwarves, Red Giants and Core-Collapse Supernovae. Clearly, these bounds can be applied also to other light DM candidates. For example, the absence of signals in WIMP direct detection experiments pushed phenomenologists to investigate also light thermal (thus in the $keV—10\,GeV$ region) models that interact weakly with the SM. However, they would be overproduced by the freeze-out mechanism unless they can interact also with a "mediator" that drives may be coupled to the SM through

renormalizable portal operators (Ref. [1]). These mediators may be of particular interest also for direct detection purposes, especially if they are *nucleo-philic* scalars.

In this thesis work we will study in detail a light DM mediator coupled to the SM thanks to the Higgs-portal operator $H^\dagger H$. In Chapter 5 we will introduce the problems of light thermal DM models and thus the necessity of the mediators. Then, we will show how the Higgs-portal mechanism couples the mediators to the SM and in particular to hadrons (pions and nucleons in particular). A light scalar coupled to nucleons would be massively produced in hot, dense and nucleon-rich environments such as Core-Collapse Supernovae, that we will study in Chapter 4.

Before doing so, we review the SM theory and its drawbacks in Chapter 1 in order to develop the formalism and the concepts for the following Chapters. Chapter 2 is entirely dedicated to what we know about Dark Matter and suitable models that have been proposed throughout the years. One particular model, the axion, is so fascinating that is worth going more in detail in a dedicated Chapter (3). Moreover, probably going back to Iwamoto's work in the early '80s (Ref. [2]), the techniques for studying the emission of light particles by Core-Collapse Supernovae has been developed specifically to constrain the elusive axion, as we will show in Chapter 4.

With all these premises, we can study the behaviour of the (CP-even) scalar mediator in the SN environment in Chapter 6. There, we will produce original and self-consistent bounds on the masses and couplings of the scalar. In particular, we will discuss where and how we differ from the previous literature (mainly Ref. [3]) about bounds from the luminosity of scalar production, which will be constrained with the famous Raffelt criterion (Ref. [4]). In addition to that, we will add bounds coming from Low-Energy Supernovae (following Ref. [5]), SN1987A gamma rays detected by GRS and cosmic diffuse photons coming from all past CCSN events.

Chapter 1

The Standard Model and its drawbacks

The Standard Model of Particle Physics is a Lorentz invariant QFT built upon the gauge group $SU(3)_C \times SU(2)_L \times U(1)_Y$ and the requirement of renormalizability. The fermionic content is represented in gauge group multiplets and in Weyl basis:

$$\begin{aligned} Q_L^i &\sim (3, 2, +1/6) \\ L_L^i &\sim (1, 2, -1/2) \\ u_R^i &\sim (3, 1, 2/3) \\ d_R^i &\sim (3, 1, -1/3) \\ e_R^i &\sim (1, 1, -1) \end{aligned}$$

In this notation $Q_L = (u_L, d_L)^T$ and $L_L = (\nu_L, e_L)^T$. The i apex is there to account for multiple generation for both quarks and leptons.
We will call G_μ^a the $SU(3)_C$ gauge bosons, W_μ^i the $SU(2)_L$ ones and B_μ for $U(1)_Y$. It is known that in order to maintain the gauge invariance, the lagrangian should be built using the field strength tensors and the gauge bosons must transform under the gauge transformation in the adjoint representation of the gauge group. The field strength tensor is

$$F_{\mu\nu}^a = \partial_\mu A_\nu^a - \partial_\nu A_\mu^a + g f_{bc}^a A_\mu^b A_\nu^c$$

and it is built in a way such that a gauge transformation acting on the fermionic fields

$$\psi \to \psi'(x) = U(x)\psi(x) = \exp\{-i\tau \cdot \theta(x)/2\}\psi(x)$$

with τ^i being the generators of the (in general non-abelian) gauge group, transforms with covariant derivatives as:

$$D_\mu \psi(x) \to D'_\mu \psi'(x) = U(x) D_\mu \psi(x)$$

Being as usual $D_\mu = \partial_\mu + ig\tau \cdot \mathbf{A}$. In this way the gauge fields must transform as

$$A_\mu^a(x) \to A_\mu'^a(x) = A_\mu^a(x) + \frac{1}{g}\partial_\mu \theta^a(x) - f^{abc} A_\mu^b(x)\theta^c(x)$$

With all these prescriptions gauge invariance is ensured since this way the field strength tensor is gauge invariant and also the Dirac lagrangian term $\bar{\psi} i \not{D} \psi$.
The final ingredient is the Higgs field, which is a complex scalar doublet H of $SU(2)_L$, or better

$$H \sim (1, 2, 1/2)$$

Having this in mind and defining $\widetilde{H} = i\sigma_2 H^*$, the Standard Model Lagrangian is:

$$\begin{aligned}
\mathcal{L}_{SM} = & -\frac{1}{4} G^a_{\mu\nu} G^{a,\mu\nu} - \frac{1}{4} W^i_{\mu\nu} W^{i,\mu\nu} - \frac{1}{4} B_{\mu\nu} B^{\mu\nu} \\
& + \overline{Q^j_L} i \not{D} Q^j_L + \overline{L^j_L} i \not{D} L^j_L + \overline{u^j_R} i \not{D} u^j_R + \overline{d^j_R} i \not{D} d^j_R + \overline{e^j_R} i \not{D} e^j_R \\
& + (D_\mu H)^\dagger (D^\mu H) - V(H) \\
& - Y_d^{ij} \overline{Q^i_L} H \, d^j_R - Y_u^{ij} \overline{Q^i_L} \widetilde{H} \, u^j_R - Y_e^{ij} \overline{L^i_L} H \, e^j_R + h.c.
\end{aligned} \tag{1.1}$$

In this equation a shorthand notation, which is a little imprecise, has been used. Defining $\sigma^\mu = (\mathbb{1}, \sigma^i)$ and $\overline{\sigma}^\mu = (\mathbb{1}, -\sigma^i)$, with D_μ being the covariant derivative (which of course changes for each fermionic field along with its transformation properties under the gauge group), we mean

$$\overline{\psi_L} i \not{D} \psi_L = \psi^\dagger_L i \overline{\sigma}^\mu D_\mu \psi_L \quad \text{and} \quad \overline{\psi_R} i \not{D} \psi_R = \psi^\dagger_R i \sigma^\mu D_\mu \psi_R$$

The phenomenology that can be extracted from this construction is rich and, disregarding for a while the open problems, consistent with observations: within its most successful predictions we remember the discovery of the W and Z bosons (1983), of the top quark (1995) and finally of the Higgs boson (2012).

1.1 Electroweak Spontaneous symmetry breaking and Higgs interactions

The easiest way to provide spontaneous symmetry breaking in the Higgs sector within all the previous requirements is to assume a mexican-hat potential:

$$V(H) = -\mu^2 H^\dagger H + \lambda (H^\dagger H)^2 \quad \text{with } H = \frac{1}{\sqrt{2}} \begin{pmatrix} \phi_1 + i\phi_2 \\ \phi_3 + i\phi_4 \end{pmatrix}$$

The gauge symmetry ensures that we can choose the vacuum

$$\langle H \rangle = \frac{1}{\sqrt{2}} \begin{pmatrix} 0 \\ v \end{pmatrix} \quad \text{with } \mu^2 = \lambda v^2$$

Expanding around the new vacuum as $H = (v + h)/\sqrt{2}$ we transform the Higgs lagrangian

$$\mathcal{L}_H = (\partial_\mu H)^\dagger (\partial^\mu H) + \mu^2 H^\dagger H - \lambda (H^\dagger H)^2$$

in the new lagrangian of the Higgs boson h with its mass and self interactions:

$$\mathcal{L}_h = \frac{1}{2} \partial_\mu h \, \partial^\mu h - \frac{1}{2} M_h^2 \, h^2 - \lambda \, v \, h^3 - \frac{\lambda}{4} h^4 \quad \text{where } M_h^2 = 2\lambda \, v^2 \tag{1.2}$$

Masses of the gauge bosons

In the broken phase, three d.o.f. out of four of the Higgs field seem to disappear and the only one remaining is the Higgs boson. As Goldstone theorem requires, the three broken generators must correspond to three Goldstone bosons, that we do not see explicitly in $\mathcal{L}_h$. However, in a gauge theory, thus local, we can choose the gauge in order to make the three Goldstone bosons be eaten up by the gauge bosons, which now become massive, acquiring the longitudinal d.o.f.. This particular gauge choice will be called unitary gauge, since it arises from the possibility to parametrize the Higgs field around the stable vacuum as

$$H = \frac{1}{\sqrt{2}} \begin{pmatrix} 0 \\ v+h \end{pmatrix} \exp\left\{ i \frac{\sigma^i \xi^i(x)}{2} \right\}$$

In a gauge theory we can choose functions $\theta^i(x)$ to make this expression to recast into the previous one without the exponential.
Being $D_\mu H = (\partial_\mu + ig\,\sigma^i W^i_\mu/2 + ig'\,Y_H B_\mu)H$, we see that $(D_\mu H)^\dagger (D^\mu H)$ becomes (the kinetic term of the Higgs boson was already taken into account in $\mathcal{L}_h$)

$$\mathcal{L}_{hGB} = \frac{1}{2} \begin{pmatrix} 0 & v+h \end{pmatrix} \begin{pmatrix} \frac{g}{2} W^3_\mu + g'\,Y_H\,B_\mu & \frac{g}{2}(W^1_\mu - iW^2_\mu) \\ \frac{g}{2}(W^1_\mu + iW^2_\mu) & \frac{g}{2} W^3_\mu - g'\,Y_H\,B_\mu \end{pmatrix}^2 \begin{pmatrix} 0 \\ v+h \end{pmatrix}$$

Performing all the algebra and defining $W^\pm_\mu = (W^1_\mu \mp i W^2_\mu)/\sqrt{2}$, we get

$$\mathcal{L}_{hGB} = \frac{1}{2}(v+h)^2 \left[\frac{g^2}{2} W^+_\mu W^{-,\mu} + \begin{pmatrix} W^3_\mu & B_\mu \end{pmatrix} \begin{pmatrix} \frac{g^2}{4} & -\frac{g\,g' Y_H}{2} \\ -\frac{g\,g' Y_H}{2} & g'^2 Y_H^2 \end{pmatrix} \begin{pmatrix} W^{3,\mu} \\ B^\mu \end{pmatrix} \right]$$

It is now evident that, for each value of Y_H we have a massless gauge boson, the photon, as required by the spontaneous breaking of $SU(2)_L \times U(1)_Y$ in $U(1)_{em}$. So, we will call the diagonalizing basis $(Z_\mu \;\; A_\mu)$ and define

$$(c_W =)\ \cos\theta_W = \frac{g}{\sqrt{g^2 + 4g'^2 Y_H^2}}$$

Thus,

$$\mathcal{L}_{hGB} = \left(1 + \frac{h}{v}\right)^2 \left[M^2_W\, W^+_\mu W^{-,\mu} + \frac{1}{2} M^2_Z\, Z_\mu Z^\mu \right] \tag{1.3}$$

where

$$M^2_W = \frac{g^2 v^2}{4} \quad \text{and} \quad M^2_Z = \frac{M^2_W}{c^2_W}.$$

Fermion masses

Let us, for a moment, stick to a model with one generation of fermions. Thus, the Yukawa part of the $\mathcal{L}_{SM}$ contains the interactions between the fermions and the Higgs field. *A priori* we could have used two different scalar doublets for the y_u

and y_d term, each of them making SSB and leading to fermion masses. We therefore invoke a somewhat principle of minimality, using only one scalar doublet H. Namely,

$$\mathcal{L}_Y = -y_d \overline{Q_L} H \, d_R - y_u \overline{Q_L} \widetilde{H} \, u_R - y_e \overline{L_L} H \, e_R + h.c.$$

In this simplified scenario, once one expands the Higgs field around the vacuum. very easily gets:

$$\mathcal{L}_f = -\left(1 + \frac{h}{v}\right) m_u \overline{u} u - \left(1 + \frac{h}{v}\right) m_d \overline{d} d - \left(1 + \frac{h}{v}\right) m_e \overline{e} e \tag{1.4}$$

with $m_i = y_i v/\sqrt{2}$. As it will be shown in Section 1.3 accounting for the flavour structure will lead to even more interesting consequences driven from $\mathcal{L}_Y$.
Finally, we can comment the fact that the absence of ν_R in the lagrangian leads to a null mass for neutrinos. We do not explicitly put a ν_R in the lagrangian since it is well-known that in experiments neutrinos have appeared only left-handed. However, we know that neutrinos are massive, as it will be discussed in Section 1.4: thus, we cannot settle for a null neutrino mass and we try to provide mechanisms to cure this problem.

1.2 Fermion interactions with gauge bosons

The Dirac term provides the interactions of the fermion fields with the gauge bosons. Again, to illustrate the mechanism, we stick to a one generation model. In this case we are allowed to assume that the ψ_L and ψ_R Weyl fermions are nothing else than the chiral projections of 4D fermions. In this case $\psi_L = (1-\gamma_5)\psi$ and $\psi_R = (1+\gamma_5)\psi$. The Dirac lagrangian is:

$$\begin{aligned}
\mathcal{L}_D = & \overline{Q_L} \, i\gamma^\mu \left(\partial_\mu + i g_S \frac{\lambda^a}{2} G^a_\mu + i g \frac{\sigma^i}{2} W^i_\mu + i g' Y_Q B_\mu\right) Q_L \\
& + \overline{L_L} i\gamma^\mu \left(\partial_\mu + i g \frac{\sigma^i}{2} W^i_\mu + i g' Y_L B_\mu\right) L_L \\
& + \overline{u_R} \, i\gamma^\mu \left(\partial_\mu + i g_S \frac{\lambda^a}{2} G^a_\mu + i g' Y_u B_\mu\right) u_R \\
& + \overline{d_R} \, i\gamma^\mu \left(\partial_\mu + i g_S \frac{\lambda^a}{2} G^a_\mu + i g' Y_d B_\mu\right) d_R \\
& + \overline{e_R} \, i\gamma^\mu \left(\partial_\mu + i g' Y_e B_\mu\right) e_R
\end{aligned}$$

where λ^a are the Gell-Mann matrices of $SU(3)_C$. Carrying on the algebra and passing to the diagonalizing base of the gauge bosons masses (Z_μ and A_μ), we get the lagrangian (written symbolically just for quarks; if the difference between up and down quark is unnecessary, it will be generically written ψ):

$$
\begin{aligned}
\mathcal{L} &= \overline{u}\, i\not{\partial}\, u + \overline{d}\, i\not{\partial}\, d && \text{kinetic term} \\
&- g_S \overline{\psi}\, \not{G}^a \frac{\lambda^a}{2} \psi && \text{Strong Interactions} \\
&- \frac{g}{\sqrt{2}} \left(\overline{u}_L \not{W}^+ d_L + \overline{d}_L \not{W}^- u_L \right) && \text{Charged Current Weak Interactions} \\
&- \frac{g}{c_W} \left(g_L \overline{\psi}_L \not{Z} \psi_L + g_R \overline{\psi}_R \not{Z} \psi_R \right) && \text{Neutral Current Weak Interactions} \\
&- Qe \overline{\psi}\, \not{A} \psi && \text{Electromagnetic Interactions}
\end{aligned}
\tag{1.5}
$$

The new parameters appearing are a combination of the previous ones:

$$
\begin{aligned}
e &= \frac{g}{s_W} \\
Q &= \frac{\sigma^3}{2} + Y_Q = Y_\psi \\
g_L &= \frac{\sigma^3}{2} - Q s_W^2 \\
g_R &= -Q s_W^2
\end{aligned}
$$

It is now quite evident that in order to maintain gauge invariance in $\mathcal{L}_Y$, we must also choose a suitable Y_H such that $-Y_Q + Y_H + Y_d = 0$ ($U(1)_Y$ invariance condition). This implies $Y_H = 1/2$ and we get the same from the u quark. Thus, as expected, the charge of the Higgs boson has to be zero, in accordance with the fact that it does not interact with the photon.

1.3 Flavour structure of the Standard Model

The fermionic content of the Standard model contains three generations of quark and lepton doublets, respectively:

$$
\begin{pmatrix} u \\ d \end{pmatrix} \begin{pmatrix} c \\ s \end{pmatrix} \begin{pmatrix} t \\ b \end{pmatrix} \quad \text{and} \quad \begin{pmatrix} \nu_e \\ e \end{pmatrix} \begin{pmatrix} \nu_\mu \\ \mu \end{pmatrix} \begin{pmatrix} \nu_\tau \\ \tau \end{pmatrix}
$$

Of course, the only way to get a renormalizable and gauge invariant theory allowing for interactions between different generations of fermions is given by $\mathcal{L}_{SM}$ in Equation 1.1. In particular, let us focus on the Yukawa term for quarks:

$$
\mathcal{L}_Y = -Y_d^{ij} \overline{Q_L^i} H\, d_R^j - Y_u^{ij} \overline{Q_L^i} \widetilde{H}\, u_R^j + h.c.
$$

In the broken phase, we would have mass-mixing of the kind

$$
\mathcal{L}_Y^{SSB} \supset -M_{ij}^d\, \overline{d}_L^i\, d_R^j - M_{ij}^u\, \overline{u}_L^i\, u_R^j + h.c.
$$

Employing the singular value decomposition, one can diagonalize the mass matrices using unitary rotations of the fields. In particular:

$$
q_L^i \to q_L'^i = L_q^{ij} q_L^j \quad \text{and} \quad q_R^i \to q_R'^i = R_q^{ij} q_R^j
$$

Concerning fermion interactions with gauge bosons, we see that only one term is not flavour-diagonal, that is the CCW interactions. Thus,

$$\mathcal{L}_{CCWI} = -\frac{g}{\sqrt{2}}\left(\overline{u}_L^i\,(L_u^\dagger L_d)_{ij}\,\not{W}^+ d_L^j + \overline{d}_L^i\,(L_d^\dagger L_u)_{ij}\,\not{W}^- u_L^j\right)$$

The matrix $L_u^\dagger L_d$ is a unitary matrix called V_{CKM} that allows for changes in flavour in CCW interactions. The CKM matrix is a source of CP violation, since CP invariance would require $V_{CKM} = V_{CKM}^*$, but the CKM matrix contains one (and only one) physical phase, that cannot be absorbed by a field redefinition.
Instead, in the lepton sector we do not have this effect since we do not have a matrix Y_ν to diagonalize. This translates in the fact that we can freely rotate the ν_L field such that $L_\nu = L_e$, thus making also the CCW term flavour-diagonal.

Low energy QCD and the chiral lagrangian [1]

The QCD lagrangian below the confinement scale Λ_{QCD} can be written as

$$\mathcal{L}_{\text{QCD}} = -\frac{1}{4}G^a_{\mu\nu}G^{a,\mu\nu} + \bar{\Psi}_L\, i\not{D}\Psi_L + \bar{\Psi}_R\, i\not{D}\Psi_R - \bar{\Psi}_L\, M\,\Psi_R - \bar{\Psi}_R\, M\,\Psi_L \qquad (1.6)$$

upon defining $D_\mu = \partial_\mu + ig_S\, G^a_\mu \lambda^a/2$ and

$$\Psi = \begin{pmatrix} u \\ d \\ s \end{pmatrix} \quad \text{and} \quad M = \begin{pmatrix} m_u & 0 & 0 \\ 0 & m_d & 0 \\ 0 & 0 & m_s \end{pmatrix}.$$

The heavy quarks (c, b, t) have masses above Λ_{QCD}, so they will be absent in our regime of interest. Quantum Chromodynamics does not couple different quarks, so that we can write the lagrangian in this form.
In the massless limit for quarks (which is particularly accurate when describing only the up and down quarks) this lagrangian has a global $U(3)_L \times U(3)_R$ symmetry: namely, it is possible to rotate left-handed components differently from the right-handed ones. However, even in this limit, the QCD vacuum induces a spontaneous symmetry breaking $U(3)_L \times U(3)_R \to U(3)_V$, since

$$\langle\overline{\Psi}\Psi\rangle = \langle\overline{u}u + \overline{d}d + \overline{s}s\rangle \neq 0$$

and this scalar singlet is invariant only if we rotate the left- and right-handed components by the same quantity. Goldstone theorem would then guarantee the existence of 9 Nambu-Golstone bosons coming from the breaking of $U(3)_A$ (calling $U(3)_L \times U(3)_R \equiv U(3)_A \times U(3)_V$). However, this is not the end of the story, because the difference between the quark masses brakes also $U(3)_V \simeq U(1)_B \times SU(3)_V$ into $U(1)_B$, that ensures baryon number conservation by the QCD lagrangian. Therefore, the massless Goldstone bosons, that we will call pions, are in reality just pseudo-NGBs, because the mass matrix would induce non-zero masses for them (see Appendix A for the details). Finally, as it will be discussed in Chapter 3, the boson

[1] More details can be found in Appendix A

η' associated to the $U(1)_A$ breaking is much heavier than the other quarks. This happens since $U(1)_A$ is an anomalous symmetry of the theory even in the massless quark limit. Hence, the source of symmetry breaking that generates the mass of the boson η' is not the mass matrix and we do not expect then that η' mass would be suppressed by the ratio m_q/Λ_{QCD}.
We give here an expression for the effective theory at lowest order that describes the pions, known as chiral perturbation theory (χPT):

$$\mathcal{L}_\chi = \frac{f_\pi^2}{4}\,\mathrm{Tr}\big\{\partial_\mu \Sigma^\dagger \partial^\mu \Sigma\big\} - \frac{B f_\pi^2}{2}\,\mathrm{Tr}\big\{M(\Sigma^\dagger + \Sigma)\big\} \tag{1.7}$$

where B has dimensions of a mass and

$$\Sigma = \exp\left\{\frac{i\pi^a\lambda^a}{f_\pi}\right\} = \exp\left\{\begin{pmatrix} \pi^0+\eta/\sqrt{3} & \sqrt{2}\pi^+ & \sqrt{2}K^+ \\ \sqrt{2}\pi^- & -\pi^0+\eta/\sqrt{3} & \sqrt{2}K^0 \\ \sqrt{2}K^- & \sqrt{2}\,\overline{K}^0 & -2\eta/\sqrt{3} \end{pmatrix}\right\}$$

$\mathcal{L}_\chi$ has two main advantages: it encodes in a synthetic and elegant way the symmetries of the original $\mathcal{L}_{QCD}$ and it is perturbative below Λ_{QCD} where it is accurate. From this lagrangian we will extract pion masses and their interaction with the Higgs boson in Chapter 4.

1.4 The Standard Model drawbacks

We have seen the Standard model as a beautiful theory motivated by convincing requirements as gauge symmetry and renormalizability. Many of the successes of this theory come exactly from this construction. However, we need to extend, if not modify, it in order to answer some fundamental questions that arise from observations. In this Section we will see some of the most important open problems in Particle Physics.

Dark Matter

We have gained in the last century convincing evidence that the matter present Universe is not only the one described by $\mathcal{L}_{SM}$ (in the jargon of Cosmology *baryonic*), which represents only an $\approx 5\%$ of the energy density of the Universe. Another $\approx 27\%$ is composed by a form of matter that does not interact electromagnetically, thus it is called Dark Matter. Despite its invisibility, its presence is inferred through the gravitational effects on visible matter, radiation, and the large-scale structure of the Universe, as we will delve into in Chapter 2.

The concept of Dark Matter was first proposed in the 1930s by Swiss astronomer Fritz Zwicky, who noticed that galaxies within clusters were moving faster than could be explained by the visible matter alone. After having been set aside for 40 years, the work of Zwicky gained the attention of the community thanks to Vera Rubin's observation of galactic rotation curves. In the last five decades we have collected evidence of Dark Matter presence at every cosmological scale.

However, the nature of Dark Matter remains one of the biggest open questions in Cosmology and Particle Physics. Various candidates for Dark Matter have been proposed, including Weakly Interacting Massive Particles (WIMPs), axions, and sterile neutrinos. These particles interact with ordinary matter primarily through gravity, which makes them difficult to detect directly.

Several experiments and observational strategies are currently underway to detect Dark Matter. These include direct detection experiments that attempt to observe the rare interactions between Dark Matter particles and ordinary matter, and indirect detection methods that look for the products of Dark Matter annihilations or decays. Additionally, particle accelerators like the Large Hadron Collider (LHC) seek to produce Dark Matter particles through high-energy collisions.

Understanding Dark Matter is crucial for explaining the formation and evolution of galaxies, clusters of galaxies, and the Universe as a whole. Its discovery would not only solve a key puzzle in Cosmology, but would also provide new insights into Particle Physics, potentially revealing new fundamental particles and forces. As technology and experimental techniques advance, the search for Dark Matter continues to be a dynamic and rapidly evolving field, promising exciting discoveries in the years to come.

Baryon Asymmetry

Baryon asymmetry refers to the observed disparity in the abundance of baryons compared to their antiparticles. According to the Dirac lagrangian, matter and antimatter should have been produced in equal quantities during the early stages of the universe's evolution. Instead, we observe that our Universe is predominantly composed of matter, with very little antimatter present. To be more precise investigating Big Bang Nucleosynthesis (BBN) and the Cosmic Microwave Background (CMB), we get

$$\eta_B \equiv \frac{n_B - n_{\overline{B}}}{n_\gamma} = (5.8—6.6) \cdot 10^{-10}$$

Even though we could simply accept this fact and assume that the Universe was born with, simplifying, one extra baryon for each 10^9 baryons and antibaryons (and photons), this is not convincing since inflation would have washed away this difference and reheating would have created particles and antiparticles almost in equal abundance. Therefore, we seek to find a dynamical model creating the observed asymmetry.

However, every model attempting to solve this puzzle has to satisfy three important conditions, known as Sakharov conditions:

- **B violation**: it is quite clear that our model has to treat baryons and antibaryons differently in order to provide the asymmetry.
- **C and CP violation**: even in the case of B violation, if we had a theory conserving C and CP, the rate for the production of baryons and antibaryons would be exactly the same, thus providing a symmetric Universe.

- **Out of equilibrium processes**: the production of baryons and antibaryons must happen out of equilibrium, i.e. there must exist a finite non-zero chemical potential μ_B. Otherwise, equilibrium distributions would be forced to be the same as required by $\mu_B = 0$ at equilibrium.

As we have seen in Section 1.3 the Standard Model provides sources of C and CP violation even at tree level: C is trivially violated by the chiral structure of the SM, while CP is violated by the V_{CKM}. However, it provides B violation only at loop level, thus it is an effect so suppressed that cannot give the observed η_B.

One of the most interesting scenarios is the one of baryogenesis via leptogenesis, employing the fact that B-L is a non anomalous symmetry of the SM. A viable candidate is a sterile Majorana neutrino N_R that decays out of equilibrium. This model satisfies the three Sakharov conditions and provides also a mechanism to suppress neutrino masses. The baryogenesis would take place because of the "reshuffling" of the asymmetry between baryons and leptons, conserving B-L.

Another famous model is represented by Great Unification Theories, which aim to a unification of strong and electroweak forces at very high energies ($\Lambda_{GUT} \approx 10^{16}\, GeV$). The decay of these heavy particles could satisfy Sakharov conditions. However, these theories would also lead to the proton decay, whose lifetime has been measured to be $\tau_P \gtrsim 10^{34}\, yr$ and its measure will be investigated by Hyper-Kamiokande.

Neutrino masses

Neutrinos have peculiar properties, which make them unique in the SM theory. Firstly, their mass is really small compared to the lightest non-neutrino fermion, which is the electron: this is, in a first approximation, why their mass is assumed to be 0 in the SM. Then, they are the only fermions in the SM which do not carry electric charge, hence their name. Finally, we have seen them to appear only with left-handed chirality in experiments: this justifies why we do not put a ν_R in the SM lagrangian. However, there is no symmetry preventing neutrinos to have a mass term, so the most general renormalizable mass term respecting the SM gauge group comes from:

$$\mathcal{L}_{mass,\nu} = -Y^e_{ij}\overline{L}^i H e^j_R - Y^\nu_{ij}\overline{L}^i \widetilde{H}\nu^j_R - M_{ij}(\nu^i_R)^\dagger i\sigma_2(\nu^j_R)^* + h.c.$$

It includes a Majorana mass term for the right-handed neutrino since it is chargeless under any gauge interaction in the SM, hence the name "sterile".
A beautiful explanation of the reason why we write also a Majorana mass term is also that a pure Dirac term would be really innatural, since it would require a Yukawa coupling of the order $y_\nu \approx 10^{-12}$. A Majorana mass term would cure this non-naturalness, because M_{ij} can receive huge corrections at loop level: this comes from the fact that a Majorana mass term is super-renormalizable and that there is no additional symmetry in taking $M_{ij} = 0$ (only if right-handed neutrinos do not carry any lepton number). Therefore, the masses of light neutrinos are formally m^2/M with m being the Dirac masses and M the Majorana ones. This is the famous

see-saw mechanism.

An important implication of neutrinos being massive and that, in general, their mass matrix is not flavour-diagonal is that (flavour eigenstate) neutrinos oscillate in vacuum. This solves the *solar neutrino problem*: the Sun would produce almost only electron neutrinos, but the flux of solar electron neutrinos is 1/3 of the predicted one, meaning that during their travel to Earth electron neutrinos oscillate and when they arrive at Earth they are almost with equal probability ν_e, ν_μ or ν_τ.
However, we do not know exactly the value of neutrino masses from oscillations, because these are sensitive only to $\Delta m^2_{12} = (7.50 \pm 0.20) \cdot 10^{-5}\, eV^2$ and $\Delta m^2_{23} = (2.32 \pm 0.12) \cdot 10^{-3}\, eV^2$: these differences are consistent with either $m_1 < m_2 < m_3$ (*normal hierarchy*) or $m_3 < m_1 < m_2$ (*inverted hierarchy*).

As a final comment, currently it is still unknown whether neutrinos have also a Majorana mass term: this is investigated by neutrino-less double beta ($0\nu2\beta$) decays experiments. $0\nu2\beta$ events would violate lepton number and thus would be a clear evidence that neutrinos must have a Majorana mass term.

Strong CP problem [2]

The QCD lagrangian in Equation 1.6 is CP conserving. However, an additional term, emerging at quantum level and respecting all gauge and Lorentz requirements, can be added to the lagrangian: it is known as θ-term, namely

$$\mathcal{L}_{QCD+\theta} = \mathcal{L}_{QCD} + \theta \frac{g_S^2}{32\pi^2} G^a_{\mu\nu} \widetilde{G}^{a,\mu\nu}$$

Although being a total derivative, $\mathcal{L}_\theta$ has physical implications (i.e. modifies the action), due to the non-triviality of the QCD vacuum.

The θ-term would imply a non-zero electric dipole moment for neutrons, which has not been measured. This allows to put a bound to the neutron EDM $d_n \lesssim 10^{-26}\, e{\cdot}cm$ and, comparing this value with the theoretical prediction, it implies $\theta \lesssim 10^{-10}$. The smallness of θ poses a naturalness problem, because θ is a parameter for a $U(1)$ rotation, meaning that it ranges from 0 and 2π and so, in principle, it should be a number of order one. This issue is known as the *strong CP problem*.

Among the possible solutions (see Chapter 3 for more details) the most interesting one is the Peccei-Quinn mechanism, which implies the existence of a new degree of freedom ϕ, that makes the vacuum of the theory CP conserving and whose excitation around the vacuum are called *axions*. This scenario is really appealing, because it not only solves the strong CP problem, but it also have cosmological implications, due to the fact that axions are a convincing dark matter candidate.

Experiments like CAST and the future IAXO are searching for an axion discovery taking advantage of the Primakoff process $\gamma \to \phi\, \gamma$, using the Sun as a source of photons. Axions have also been studied in astrophysical environments, which have produced convincing bounds on their couplings and mass.

[2] This will be the topic of Chapter 3.

Inflation

The Hot Big Bang model, which assumes a singularity at the beginning of our Universe and that its components were in thermal equilibrium with themselves with a temperature decreasing with the expansion of the Universe, has provided us with testable predictions, mainly the Big Bang Nucleosynthesis and the Cosmic Microwave Background, which are its most popular successes. In practice, we gained so much evidences about BBN and CMB that every theory with new Physics must reproduce these results.

However, the HBB scenario has two famous shortcomings. The first one is the *horizon problem*, which involves causal inconsistencies in the HBB model. In fact, we observe the Universe to be homogeneous and isotropic on large cosmological scales (more than $100\,Mpc$), as it is beautifully confirmed by the CMB observations, for which we have observed photons coming from the recombination epoch to share the same bleck-body spectrum, with tiny fluctuations ($\delta T/\overline{T} \simeq 10^{-5}$). The problem arises when we compare the comoving Hubble radius $r_H = 1/\dot{a}$ (which is the comoving distance of causal connection in one Hubble time) today with the on at the recombination epoch. Being

$$\dot{r}_H = -\frac{\ddot{a}}{a^2},$$

the Hubble radius has increased (as long as we assume a decelerated expansion) from recombination by a factor of order 10^6. This would imply, for example, that there is no possibility for CMB photons coming from two opposite directions in the sky to share the same distribution, because they have never been in causal contact before recombination.
The second issue is known as *flatness problem* and regards a naturalness problem in the curvature of our Universe: defining $\Omega_k = -k/a^2H^2$ as the contribution of the curvature to the energy budget of the Universe, we have measured $|\Omega_k(t_0) - 1| < 10^{-3}$. This would imply that, following back the cosmological evolution in the HBB model, at very early times (let's say the Planck time) $|\Omega_k(t_P) - 1| \lesssim 10^{-60}$, which is a pretty unnatural result.

The solution for these two problems involves an inflationary period at very early times. In a first approximation we assume that in this period the scale factor grows exponentially and, in order to solve both problems, we would need at least a 60—70 e-folds expansion. The easiest way to provide an accelerated expansion is to add a scalar ϕ (the inflaton) to the action:

$$\mathcal{S} = \int d^4x\,\sqrt{-g}\left[\frac{M_p^2}{2}\mathcal{R} + \mathcal{L}_{SM} + \frac{1}{2}g^{\mu\nu}\partial_\mu\phi\,\partial_\nu\phi - V(\phi)\right]$$

If the potential is chosen in order to satisfy the *slow-roll* conditions, then the inflaton can dominate the energy budget and produce an accelerated expansion.

This is not the end of the story, because inflation can also explain fluctuations around a homogeneous and isotropic Universe. Basically, once a fluctuation exits the horizon (i.e. its typical scale λ becomes greater than r_H), it "freezes" and remains constant until it re-enters the horizon during the "normal" phases of decelerated expansion.

Thanks to these fluctuations, matter has fallen into overdense regions, creating the structure we observe nowadays.

For the aforementioned reasons, inflation is a really motivated scenario in Cosmology. Direct evidence of inflation would come from the observation of the produced primordial gravitational waves. The hopes of the community are addressed to the next generation interferometers, which could obsreve this "smoking gun" of inflationary epoch.

Accelerated expansion and Dark Energy

A naive expectation about the evolution of the Universe is that the expansion is decelerating: this is enforced by the Einstein equation for a FRW background

$$\frac{\ddot{a}}{a} = -\frac{1}{6M_p^2}(\rho + 3P).$$

For conventional fluids like matter and radiation, we get that $\ddot{a} < 0$. Defining the deceleration parameter as

$$q_0 \equiv -\frac{\ddot{a}(t_0)}{a(t_0)H_0^2}$$

we would expect, if the Universe today was dominated by matter, that $q_0 = \Omega_M(t_0)/2$. However, by measuring deviations from the Hubble law using the light from very distant galaxies, it has been obtained $q_0 \simeq -0.55$, which means that the expansion of the Universe is accelerating. An explanation would come from the fact that the Universe today is dominated by a cosmological constant, which having $P = -\rho$, produces an accelerated exponential expansion. If we suppose that the radiation contribution to the energy density is negligible and that the Universe is flat, from $q_0 = \Omega_M(t_0)/2 - \Omega_\Lambda(t_0) = -0.55$ and $\Omega_M + \Omega_\Lambda = 1$, we get

$$\Omega_M(t_0) = 0.32 \quad \text{and} \quad \Omega_\Lambda(t_0) = 0.68.$$

The cosmological fluid causing the accelerated expansion has received the name of *Dark Energy*.

One candidate for Dark Energy is, as anticipated before, a cosmological constant Λ, which would make $A \propto \exp\{Ht\}$ with $H^2 = \Lambda/3M_p^2$. From $\Omega_\Lambda(t_0)$, we infer $\Lambda \simeq (1\,meV)^4$. The Standard Model fails completely to reproduce this result, because from the vacuum energy of the SM (which in GR has implications on Einstein equations) we get an estimate 120 orders of magnitude higher than the observed Λ.

Then, another possibility is to add another degree of freedom, which for the sake of simplicity and in order to satisfy the requirement of isotropy can be chosen as a scalar field ϕ, called *quintessence*. The lagrangian for this model is completely analogous to the one of inflation, but Dark Energy operates at energy scales much lower than inflation. In particular, also in this case we would ask for the scalar potential to satisfy the slow-roll conditions.

The hierarchy problem

The hierarchy problem arises when a bare quantity, such as a mass or a coupling, is orders of magnitudes higher than the observed value for that quantity, meaning that there has to be extreme fine-tuning between the tree-level and the loop levels in order to have a cancellation and to remain with the observed result. A famous example is the one of the Higgs mass term $\mu^2 H^\dagger H$, which is super-renormalizable and thus sensitive to the UV corrections. In the Wilsonian formalism, we can write the corrections to μ^2 as

$$\Delta\mu^2 \propto \frac{\lambda^2}{16\pi^2}\Lambda_{UV}^2$$

with y some Yukawa coupling of the Higgs. The question now becomes why corrections can become so important or equivalently why the Higgs mass is so small compared to M_p, hence the name "hierarchy problem". Clearly fermions do not suffer this kind of problem, since setting their mass to 0 enhances the symmetries of the lagrangian, because of the appearance of the chiral symmetry. Gauge boson masses, instead, are protected by gauge symmetry. Thus, the problem is particularly crude for the Higgs, since in the SM it can easily interact with anything up to the scaled of validity of the SM, i.e. $\Lambda_{UV} = M_p \sim 10^{19}\, GeV$.

The elegant solution for these problem is Supersymmetry (SUSY). It postulates for every fermion and boson of the SM the existence of a partner with the same quantum numbers and with spin $\pm 1/2$. One could easily write a superpotential encoding the interaction between a particle and its superpartner and would see that, schematically, a fermion loop would cancel a boson loop and viceversa. This would elegantly set to zero quantum corrections, thus eliminating the hierarchy problem.

Other solutions, that will not be discussed, may be: the Little Higgs Model, the Composite Higgs model or even the no Higgs model (or technicolor).

Grand Unified Theories

Grand Unified Theories historically emerge from the observed fact that the three gauge coupling of the SM gauge group approximately seem to converge in one point at some high energy scale tracing their RG evolution from M_Z. Proposed in the 1970s by Georgi and Glashow (Ref. [6]), the idea is that the SM gauge group is the result of the spontaneous breaking of a more fundamental $SU(5)$ (throughout the years also $SO(10)$ and E_6 have been proposed). In a theory with SUSY, this kind of mechanism accomplishes to unify all gauge forces at some $\Lambda_{GUT} = 10^{15}\, GeV$. Very elegantly, this theory provides explanations for the fractional charges of quarks, which is an ignored question in the SM.

GUTs also predict the existence of new particles, such as the X and Y bosons, which facilitate proton decay, a forbidden process in the Standard Model being the proton the lightest particle with $B = 1$. Although proton decay has not been detected, its observation would be a significant indicator of GUTs. Current experiments, like Super-Kamiokande in Japan, are designed to search for such rare events.

Despite their elegance, GUTs fall back into the hierarchy problem, given that again Λ_{GUT} is so much higher than the electroweak scale, hence requiring fine-tuning.

Quantum gravity

Up to this point we have completely ignored gravity, in the sense that we have treated it just as a background field. To have a holistic comprehension of Nature, however, we need to quantize it. One could in principle thing that, since we have an action for General Relativity

$$\mathcal{S} = \int d^4x \sqrt{-g} \left[\frac{M_p^2}{2} \mathcal{R} + \mathcal{L}(g_{\mu\nu}, \Phi_{SM}) \right]$$

one could simply quantize the Einstein-Hilbert lagrangian. Of course this can be done and we get exactly what we know in GR: gravity is a massless spin-2 particle! GR as a QFT however is not renormalizable, thus we can have control of the theory only up to a certain energy scale. Given a mass scale M, one should start to see quantum effects of gravity when the Compton wavelength of that scale $\lambda \sim 1/M$ is of the order of the Schwarzschild radius $r_S \sim M/M_p^2$. Therefore, GR can be treated as a good low-energy EFT for gravity only up to $M_p \sim 10^{19}\, GeV$.

Clearly, at high energies we would need to UV complete gravity. One prominent UV approach is String Theory, which postulates that the fundamental constituents of reality are one-dimensional strings rather than point particles. These strings vibrate at different frequencies, corresponding to various particles, including the graviton, which mediates gravity. Another proposed model is Loop Quantum Gravity, which suggests that spacetime is quantized, composed of discrete loops that form a spin network. Finally, Asymptotically Safe Gravity proposes that gravity becomes scale-invariant at high energies, governed by a non-trivial ultraviolet fixed point. Each of these models provides a framework to understand gravity's quantum nature, addressing issues like singularities and unifying it with other fundamental forces.

Chapter 2

Dark Matter

Among the aforementioned problems the Dark Matter one is probably the most convincing about the need to go beyond the Standard Model. In fact, in this Chapter we will see the evidences of DM existence (Section 2.1), the reasons why the SM cannot provide satisfying DM candidates (Section 2.2) and, finally, we will briefly review proposed viable models for DM (Section 2.3).

2.1 Evidences of Dark Matter

In this Section we will overview the milestones leading us to the conviction that Dark Matter exists. An important observation regards the very different lengthscales at which we have collected evidence for DM.

Zwicky's observations of the Coma cluster

In the 1930s the Swiss astronomer Fritz Zwicky, observing the Coma cluster, estimated its mass using two different techniques, which indeed were discovered to give totally different results!
The first method was to simply count the number of galaxies in the cluster, that are approximately 800, and estimate the mass of each of them as $10^9\, M_\odot$, from which he extracted

$$M_{Coma}^{(vis)} \sim 800 \cdot 10^9 \cdot M_\odot \sim 1.6 \cdot 10^{42}\, kg$$

which will be called the visible mass of the cluster since it is inferred by the electromagnetic radiation emitted by the galaxies.
The other method, instead, aims at measuring the mass from the gravitational force. Firstly, Zwicky measured using the Doppler effect that the typical dispersion velocities of galaxies inside the cluster is $v \sim 10^3\, km/s$. Then, he estimated the mass assuming the cluster is a virialized object, thus

$$2K + V \sim 0 \tag{2.1}$$

with K being the total kinetic energy of the cluster and V the total potential energy. Then,

$$K = \sum_i \frac{1}{2} m_i v_i^2 \sim \frac{1}{2} M_{Coma} v^2$$

While V is computed assuming that the galaxies are uniformly distributed and the cluster has spherical symmetry with radius $R_{Coma} \sim 10^6\, l.y.$. Thus,

$$V = -\sum_{i<j} \frac{G m_i m_j}{r_{ij}} \sim -\frac{3}{5} \frac{G M_{Coma}^2}{R_{Coma}}$$

Then, using the virial theorem (Eq. 2.1), he obtained

$$M_{Coma}^{(grav)} \sim \frac{5}{3} \frac{R_{Coma}}{G} v^2 \sim 2.4 \cdot 10^{44}\, kg.$$

Hence, he obtained $M_{Coma}^{(grav)} \gg M_{Coma}^{(vis)}$ with a difference two orders of magnitude, unjustified even by the rough assumptions that were used. This fact can be equivalently paraphrased affirming that the galaxies are moving too fast with respect to the total visible mass of the cluster.

Galactic rotation curves

Zwicky's work gained popularity only in the '70s with Vera Rubin's studies on galactic rotation curves. The rotation velocity of stars in spiral galaxies were measured via the Doppler shift of the $21\, cm$ line of neutral hydrogen hyperfine transition. To make a rough estimate for the theoretical expectation we assume spherical symmetry, which is reasonable since the mass in spiral galaxies is almost entirely concentrated around the central "bulb". Thus, from Newtonian mechanics

$$\frac{v^2(r)}{r} = G \frac{M(r)}{r^2}$$

In the central region ($r \ll r_c$) we assume an uniform matter distribution, thus $M(r) \propto r^3$, while for $r \gg r_c$ we expect $M(r)$ to be a constant. So, our prediction is

$$v(r) \propto \begin{cases} r & r \ll r_c \\ r^{-1/2} & r \gg r_c \end{cases}$$

However, as we can see in Figure 2.1 this is not what happens: for larger radii the velocity profile is constant, compatible with a density profile $\rho(r) \propto r^{-2}$. The conclusion is that there is an invisible halo surrounding the galaxy and extending far beyond the visible radius of the galaxy: in fact, typical optical radii for spiral galaxies are of the order of $10\, kpc$ (the Milky way has $r_{MW} \sim 12\, kpc$), while halos extend all the way down to $200\, kpc$.

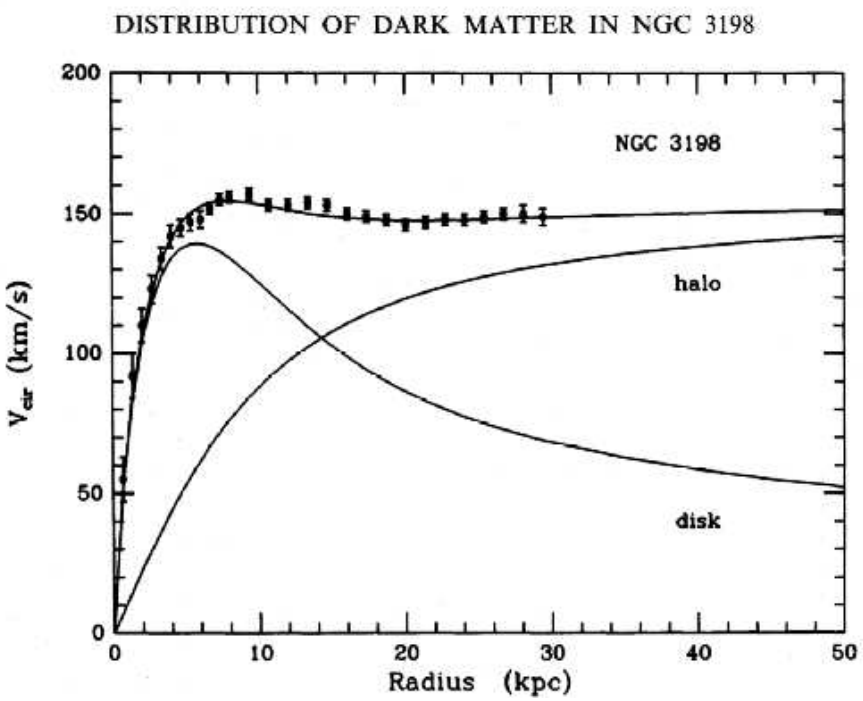

Figure 2.1: Rotation curve of NGC 3198 Galaxy.

Gravitational lensing

We mention another evidence of the existence of DM, represented by gravitational lensing around heavy objects, as predicted by General Relativity. The effect depends on the mass of the objects bending light, so, comparing the observed effect with the expectation due to visible matter, we can infer if there is some form of invisible matter. This is exactly what has been done for halos of galaxies and clusters of galaxies and, at this point not surprisingly, lensing measurements confirmed that there is an enormous amount of Dark Matter in these systems.

CMB and Dark Matter density

The largest scale we can investigate via electromagnetic radiation is the Cosmic Microwave Background, which originated when electrons and protons decoupled from the photon bath, allowing for recombination to happen. A key point of the CMB radiation is that it is extremely isotropic, with anisotropies expressed by typical variation of the blackbody temperature of $\delta T/T \sim 10^{-5}$.
However, CMB anisotropies are crucial in order to understand the composition of the Universe at the time of CMB and thus infer the densities of the species today. In particular, we are interested to measure the Ω parameters of the various species, being

$$\Omega_i = \frac{\rho_i}{\rho_c} \quad \text{with} \quad \rho_c(t) = \frac{3H^2}{8\pi G}$$

The crucial consideration is the different behaviour between baryonic matter (in this context it is the matter coupled to the photon bath during CMB and BBN, disregarding its baryonic or leptonic nature) and dark matter. In fact, we have to consider that anisotropies were generated as remnants of the inflationary epoch, so naively one would expect that matter would have fallen in overdense regions from underdense ones. This is true for dark matter, which has never been in thermal equilibrium with photons or, even if it was, had already decoupled at the times of BBN and CMB. Baryonic matter, instead, was tightly bound to photons by Compton and Coulomb processes, so the collapse was balanced by radiation pressure.
Having this in mind, the observable that was examined was the CMB power spectrum (Figure 2.2) measured by the Planck satellite. In particular, the angular power spectrum is defined as

$$\langle \delta T(\theta_i, \phi_i) \delta T(\theta_j, \phi_j) \rangle = \sum_l (2l+1) C_l P_l(\cos\theta_{ij})$$

Variations in Ω_B and Ω_{DM} produce different modifications of the power spectrum below and, fitting Planck data, the following results have been obtained

$$\Omega_B\, h^2 = 0.02233 \pm 0.00015$$
$$\Omega_{DM}\, h^2 = 0.1428 \pm 0.0012$$

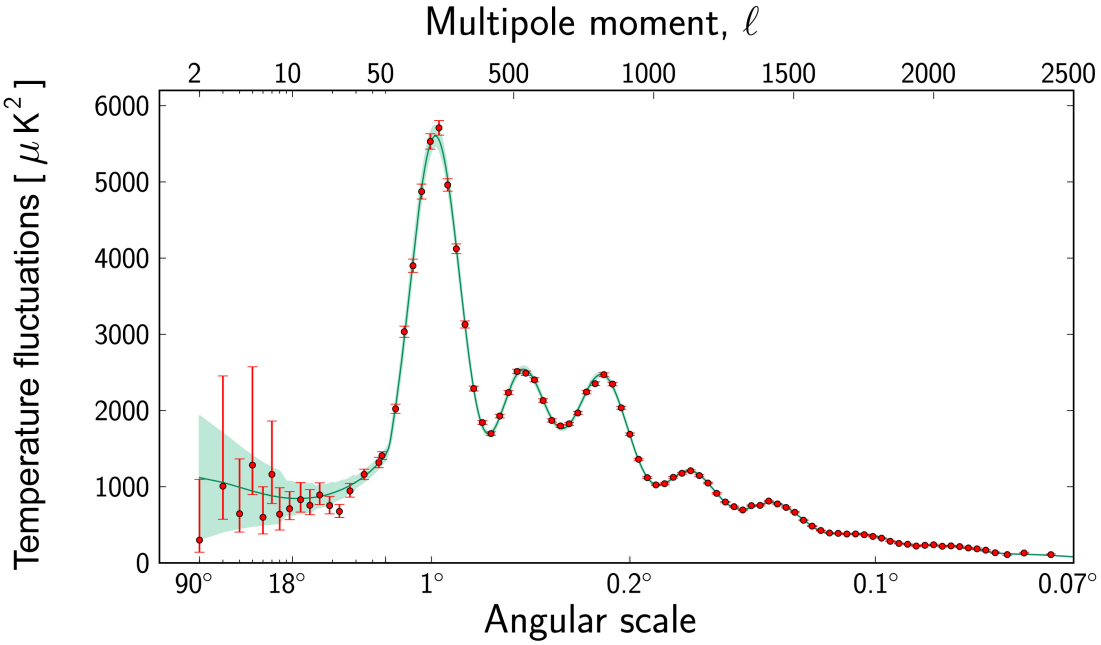

Figure 2.2: Fit of the angular power spectrum with data obtained by Planck satellite. Credits to ESA and the Planck collaboration.

2.2 Conditions for Dark Matter

Nowadays, we still do not know what is the mysterious Dark Matter, even though the community is convinced about its existence. However, by simple arguments, we can rule out easily all the SM particles. In fact Dark matter has to be:

- **Dark**: it means it does not interact electromagnetically, thus it has to be EM chargeless. Easily we rule out the quarks, the charged leptons and the W bosons. It is arguable if the DM can be a colored chargeless particle, like a neutral quark q_0. However, in this case it easily happens that below confinement, a neutral meson would appear and it would mix with the π^0, which is coupled to photons via the anomalous $\pi^0\,\gamma\,\gamma$ interactions.
- **Matter**: it must behave as a pressureless fluid, in other words as non-relativistic matter, at least at the time of BBN and CMB. This must happen because if DM was radiation at the time of CMB, it would have elapsed the fluctuations above the flat FLRW background, in the case DM was decoupled from the photon bath at recombination, or it would have been an additional relativistic degree of freedom at recombination coupled to photons, thus changing the degrees of freedom at that time $g_*(T_d)$. CMB observation are consistent with non-relativistic Dark Matter at the time of CMB formation. Thus we exclude photons, since it is obviously still relativistic, and neutrinos, since the would have elapsed cosmological structures.
- **Stable**: Dark Matter is essential for structure formation, because, since it behaves as non-relativistic matter before all other standard components of the Universe (namely light nuclei, electrons, photons and neutrinos), it provides a "depression" for these objects in which to fall once they have decoupled and become non relativistic. This is fundamental for the formation of galaxies and larger cosmological structures. Clearly, DM has to be there long enough to create structure and we still observe it in halos around galaxies. For the formation of structure as we see it today, the typical requirement is that the DM lifetime $\tau_{DM} \gtrsim 200\tau_H$. We finally exclude the Z and h bosons.

As we will see in Section 2.3, there is space for a plethora of models satisfying these requirements. The main categorization of Dark Matter candidates can be made asking whether or not DM particles ever reached thermal equilibrium with the photon bath in the history of the Universe. These models are called thermal models. They are characterized by the fact that the relic density is set by the decoupling (or freeze-out) from equilibrium. Heuristically, one should compare the typical interaction rate that keeps the particle in equilibrium $\Gamma = n\langle\sigma v\rangle$ with the expansion rate of the Universe H. The freeze-out condition is the simply

$$\Gamma(T_{FO}) \simeq H(T_{FO}).$$

Then, the relic abundance is found considering that the comoving number density $Y \equiv n/s$ (with s being the entropy density) is constant when number and entropy changing processes have stopped. Therefore, in general

$$\Omega_{DM} \equiv \frac{\rho_{DM}}{\rho_c} = \frac{m_{DM}\, Y_{FO}\, s_0}{\rho_c} \tag{2.2}$$

with $s_0 = 2890\, cm^{-3}$.

Bounds on Dark Matter masses

Simple bounds on DM masses can be inferred by the requirement that DM is confined in halos around galaxies. This gives bounds on the minimum masses that they can have.

If the DM is a boson, then the only thing we can ask is that its de Broglie wavelength λ_{DM} is smaller that the typical radius R_d of dwarf galaxies, which are the smallest objects in which we see the Dark Matter presence, so that DM is confined inside the halo. Heuristically, taking as momentum of the particle $m_{DM}\, v_{DM}$ and approximating v_{DM} with the escape velocity from such a system, one finds

$$m_{DM} \gtrsim 10^{-22}\, eV.$$

In the case of fermions, the constraint is much more severe, being related to the Pauli exclusion principle, and it is known as Tremaine-Gunn bound. In this case, the typical assumption is that DM is in its lowest excited state, so that if we compare the Fermi velocity of the system, with the typical escape velocity, one easily finds that

$$m_{DM} \gtrsim (10\text{—}100)\, eV.$$

This result depends on the actual model one takes for fermions and for the galaxy, bot all the models agree with the bound as order of magnitude. So, this is one good indication that neutrinos cannot be DM particles, since recent results (Ref. [7]) constrain the sum of neutrino masses to $\sum m_\nu \lesssim 0.2\, eV$.

Bounds on Dark Matter charge

It is obvious that the fact that Dark Matter is invisible puts only an upper bound to its charge. Experimental searches for heavy hydrogen $DM\, e^-$ conclude that

$$q_{DM} \lesssim \begin{cases} 10^{-6} & m_{DM} = 10\, GeV \\ 10^{-4} & m_{DM} = 10\, TeV \end{cases}$$

Often, as in this case, limits are weaker for heavier models, because the number density of dark matter is inversely proportional to its mass!

Bounds on DM self-interactions

DM is typically assumed to be collisionless, since it forms spherically shaped halos which otherwise would become disks, as for the baryonic matter. Constraints on DM self-interactions can be derived from observations of systems, such as the Bullet Cluster (Figure 2.3). It is the event of two clusters colliding and by the obtained image it can be observed that the baryonic components of the clusters do not simply merge, as the DM halos instead do, but they slow down and heat up. As a

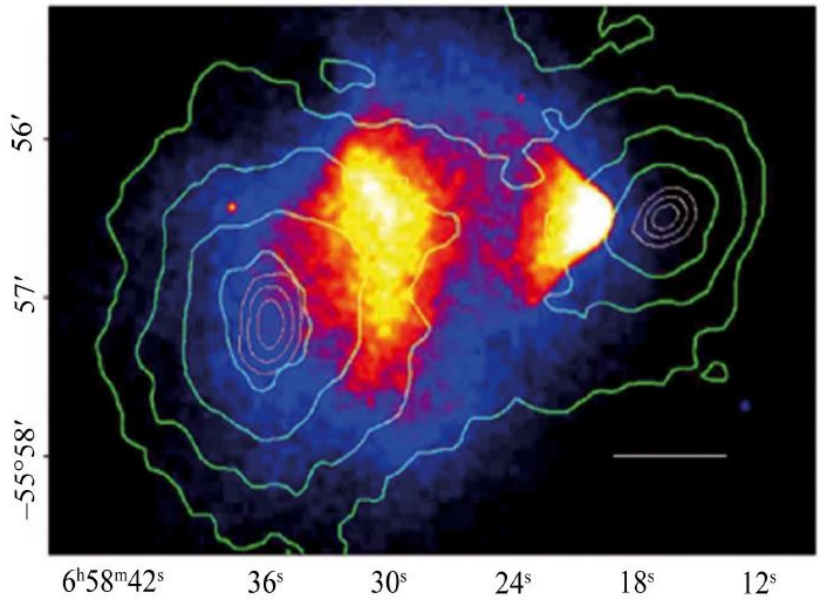

Figure 2.3: The Bullet cluster and its halo

consequence, the Bullet Cluster is an evidence that DM should be collisionless and non-baryonic.

An upper bound on DM self-interactions can be imposed, assuming that at most one self-interaction happened during the lifetime of a typical galaxy, like the Milky Way. Plugging that $\rho_{DM}^{MW} \approx 0.3\, GeV\, cm^{-3}$ and $v = v_{esc} \approx 200\, km/s$ and $\tau_{MW} \approx 10^{10}\, yrs$, from

$$\rho_{DM}^{MW} \frac{\sigma_{DM}}{m_{DM}} v_{esc}\, \tau_{MW} \lesssim 1 \quad \text{one gets} \quad \frac{\sigma_{DM}}{m_{DM}} \lesssim 1\, cm^2/g$$

Hot relics and Neutrino Dark Matter

Thermal models can be distinguished in hot models, if the decoupling happens when the particle is still relativistic, and cold models, in the opposite case.

Clearly, for an hot relic, the mass of the particle is irrelevant for the freeze-out process, which is dominated by the temperature T. Thus at the freeze-out

$$Y_{FO} = \frac{45\zeta(3)}{2\pi^4} \frac{g_{eff}}{g_{*s}(T_{FO})} \approx 0.0026\, g_{eff} \left(\frac{106.75}{g_{*s}(T_{FO})} \right)$$

Plugging the result in Equation 2.2, we easily get

$$\Omega_{DM} \simeq 0.076 \left(\frac{g_{eff}}{g_{*s}(T_{FO})} \right) \left(\frac{m_{DM}}{eV} \right)$$

The first parenthesis is a number of order (0.01—1), thus we have a hot relic DM if the mass is in the ballpark $(10—100)\, eV$. This is too high for neutrinos, for which we pointed out $\sum m_\nu \lesssim 0.2\, eV$, hence neutrinos cannot constitute entirely the Dark Matter abundance we have measured.

However, hot relics carry an important issue with themselves, which makes them unappealing Dark Matter candidates: they tend to destroy the primordial fluctuations, which is in contrast with the observations. In fact, after having decoupled, they "freely-stream" along FRW geodesics, thus moving away from overdense regions toward underdense ones. This elapses primordial perturbations and is dramatically in contrast with observations. To see it we compare the typical free-stream scale λ_{FS} from decoupling to matter-radiation equality, when cosmological perturbations start to grow significantly, with the typical radius of a galactic halo $\approx 0.1\,Mpc$. Assuming the hierarchy $T_{FO} \gg T_{NR} > T_{MRE}$, with $T_{NR} \simeq m_{DM}$ is the temperature at which the relic becomes non-relativistic, a direct computation gives

$$\lambda_{FS} \simeq 0.1\,Mpc \left(\frac{1\,keV}{m_{DM}}\right) \left(\frac{T_{MRE}^{DM}}{T_{MRE}}\right) \left[1 + \log\left(\frac{T_{NR}}{T_{MRE}}\right)\right].$$

Here, the ratio in the second parenthesis accounts for the fact that it could be that at MRE, the hot relic and the photons may have different temperatures: it is anyway an order one factor. Thus, for particles with masses below the keV, the free-streaming elapses a typical galactic halo, which is in contrast with observation. We have seen that to account for DM, hot relics must have masses of some (10—100) eV, hence we conclude that hot relic are not good DM candidates. To be more precise, it would be better to compare tha mass-scale washed out $M_{FS} \propto \rho_{DM}\lambda_{FS}^3$ with the typical mass of a galactic halo. The bound obtained is nevertheless the same. However, we have seen that neutrinos cannot account for all the DM abundance, but do free-stream after having decoupled. From the argument of the mass comparison it is possible to see why the free-streaming of neutrinos is not a problem, since nowadays $\rho_\nu \ll \rho_{DM}$.

2.3 Candidates for Dark Matter

In this Section we will briefly review the main models that have been proposed as DM candidates.

Weakly Interacting Massive Particles

Weakly interacting massive particles (WIMPs) often emerge in supersymmetric theories, suitable for solving the hierarchy problem (e.g. of the Higgs mass problem). In many theories the lightest of them is the neutralino, with a mass of $100\,GeV$—$10\,TeV$, which, being protected by a symmetry, called R-parity, is also stable. Of course, due to SUSY prescriptions, it typically interacts with a cross-section typical of weak interactions, hence the name. Namely, calling the WIMP particle χ

$$\sigma(\chi\chi \to SM\,SM) \sim 1\,pb.$$

These choice ensures the thermalization in the early Universe, making WIMPs a thermal model. For the given values of masses and annihilation cross section (which in a first approximation can be seen as the only process causing the departure from equilibrium), one obtains

$$x_{FO} = \frac{m_\chi}{T_{FO}} \simeq 20\text{—}25$$

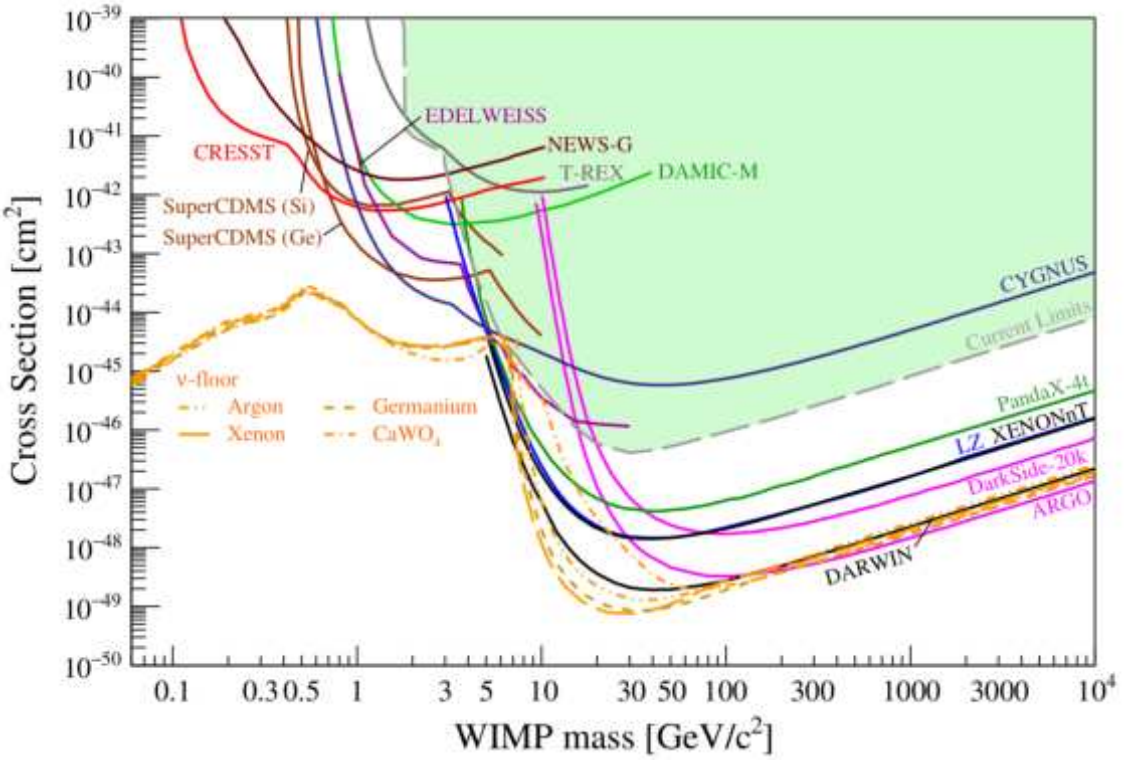

Figure 2.4: WIMP bounds updated to 2021. Figure appears in Ref. [8]

quite independently of the exact parameters. This justifies the assumption used to compute x_{FO} that WIMPs decouple when non-relativistic, thus they are considered cold relics. Now, one can write the comoving number density as

$$Y_\chi(T_{FO}) = \frac{2.3}{\pi} \frac{x_{FO}}{m_\chi} \frac{g_*^{1/2}(T_{FO})}{g_{*s}(T_{FO})} \frac{1}{M_p \langle \sigma v \rangle}$$

Using it to determine the relic density, we obtain

$$\Omega_\chi h^2 = 0.12 \left(\frac{x_{FO}}{25}\right) \left(\frac{106.75}{g_*(T_{FO})}\right)^{1/2} \left(\frac{0.7\, pb}{\langle \sigma v \rangle}\right)$$

We have beautifully obtained the observed relic density of DM and, moreover, the result is almost independent of the WIMP mass! This approximated result is reproduced even by a more accurate computation, considering the freeze-out as non instantaneous, which involves the Boltzmann equation. This result has been referred to as "the WIMP miracle".

The drawback of this model is that we have not observed supersymmetric partners at colliders and WIMPs should have been revealed at the LHC scales. Direct searches of WIMPs are usually conducted with scattering on heavy nuclei of noble gases. Bounds (Figure 2.4) have been put almost to the "neutrino floor", i.e. the region where the signal would be indistinguishable from a neutrino scattering on the nuclei.

Axions

Axions appear as a new degree of freedom aimed at solving the Strong CP problem [1]. They emerge as pseudo Goldstone bosons from the breaking of the Peccei-Quinn symmetry at some high-energy scale f_a, which ensures that the Strong CP problem is elegantly solved by the axions. As WIMPs do, they not only solve a drawback of the SM, but they provide in a natural way a convincing Dark Matter candidate. Axions, however, are not thermal models, since they behave as non-relativistic Dark Matter thanks to a mechanism known as *misalignment*. The quest for axion discovery is now a popular topic of Phenomenology and Experimental Physics and we redirect to Section 3.5 for a brief review of experimental setups and achievements (Figure 3.2).

ALPs

Axion-like particles are light pseudoscalars that, as much as axion do, thanks to the misalignment mechanism can be Dark Matter candidates. The difference with the QCD axion is that ALPs are nor required to solve the Strong CP problem, hence they are less constrained in the parameter space, since the mass and the coupling to photons do not have to satisfy the QCD axion relation $m_a \propto g_{a\gamma}$. The exclusion plot in Figure 3.2 applies to ALPs and the QCD axion landscape is highlighted in yellow.

Scalars [2]

For thermal DM χ with masses below the GeV it is well-known that the freeze-out process in the Standard Model would lead to an overproduction of χ (see Ref. [9]), unless it has a SM neutral mediator ϕ, that opens new interaction channels and could then deplete the overabundance. In this case typically these mediators can mix with renormalizable portal operators like $\overline{L}H$, $B_{\mu\nu}$ or $H^\dagger H$. This portal has the effect of coupling the scalars to all the SM (or better, to all that is coupled to the portal operators). Light scalar mediators would then be abundantly produced in astrophysical environments as will be the topic of Chapter 6.

Sterile neutrinos

As we discussed in Section 1.4 when discussing neutrino masses, sterile neutrinos can naturally set the masses of the light neutrinos to be as small as we know, if their mass is really high, potentially at the GUTs scales, which is the famous see-saw mechanism. The heavy neutrinos would the interact only via the Yukawa interaction with the lepton doublets and the Higgs doublet. It is really weakly interacting, so it appears to be a good DM candidate, which has never become thermal, but the stability is not satisfied if the masses are greater than $1\,keV$ (see Ref. [10] for more details). Thus, sterile neutrinos do not accomplish to both solve the problem of neutrino masses and of DM, so they appear as less motivated candidates.

[1] More on the Strong CP problem and the axion in Chapter 3

[2] Light DM scalars will be the topic of Chapter 5

Asymmetric Dark Matter

In this framework, motivated by the fact that $\rho_{DM} \sim 5\rho_B$, i.e. that the two energy densities are very similar, it is supposed that the Dark Matter density has been generated via a process similar to baryogenesis, that is equivalent to say that also DM experiences a particle-antiparticle asymmetry (see Ref. [11]). The main idea is that visible matter (VM) and DM are connected in an original gauge group $G_V \times G_D$ and there are various possibilities to engineer that only the visible baryon number B_V, or the B_D, or a non-trivial combination of the two, or even that they are both broken. Then, various possibilities realize the particle-antiparticle symmetry breaking, ensuring that the relic abundance of DM should be the same (order of) the VM one, thanks to the original shared symmetry.

Chapter 3

The Strong CP Problem and the Axion

In this Chapter we will study more in detail the Strong CP Problem (Section 3.1), as a SM drawback emerging from the QCD structure itself. Then, we will focus on the axion (Section 3.3), which elegantly solves the Strong CP problem, but is also a viable DM candidate (Section 3.4), which makes it an even more interesting scenario.

3.1 The Strong CP Problem

The Strong CP problem emerges from the symmetries of the QCD lagrangian (see also Section 1.3):

$$\mathcal{L}_{QCD} = -\frac{1}{4} G^a_{\mu\nu} G^{a,\mu\nu} + \bar{\Psi}_L \, i\not{D} \Psi_L + \bar{\Psi}_R \, i\not{D} \Psi_R - \bar{\Psi}_L \, M \, \Psi_R - \bar{\Psi}_R \, M \, \Psi_L .$$

As we pointed out, for $m_q \to 0$, $\mathcal{L}_{QCD}$ has a global symmetry group at classical level $SU(3)_L \times SU(3)_R \times U(1)_B \times U(1)_A$. In particular, remembering that $\Psi = (u, d, s)^T$, we know that $U(1)_B$ acts vectorially, meaning that it rotates the left- and the right-handed components by the same quantity, while $U(1)_A$ is axial, meaning that it rotates the left- and the right-handed (Weyl) fermions with opposite sign:

$$U(1)_B : \quad \Psi \to e^{i\alpha} \Psi \qquad\qquad U(1)_A : \quad \Psi \to e^{i\alpha\gamma_5} \Psi .$$

As a frequent topic of many QFT textbooks (e.g. Ref. [12]) is that if one applies an axial rotation, the path integral measure is not invariant, and one gets [1]

$$\mathcal{L}_{QCD} \to \mathcal{L}_{QCD} + 2\alpha \frac{g_S^2}{32\pi^2} G\widetilde{G}$$

It is then evident that we have to add the θ-term in the lagrangian because it is not forbidden by gauge symmetry and it is renormalizable; moreover, we do not get

[1] The following conventions are hereby adopted $\varepsilon^{0123} = -1$ and $G\widetilde{G} \equiv \frac{1}{2} G^a_{\mu\nu} \widetilde{G}^{a,\mu\nu}$. Moreover, in this Chapter gluons will be indicated as A^a_μ to ease readability.

enhanced symmetry setting $\theta = 0$, since a term like $\mathcal{L}_\theta$ is generated anyway by the anomaly of $U(1)_A$. At this point, it is also evident that θ is not physical, because a chiral rotation shifts it. Thus, we now discuss the implications of adding to our lagrangian

$$\mathcal{L}_\theta = \theta \frac{g_S^2}{32\pi^2} G\widetilde{G}.$$

An important observation is that $\mathcal{L}_\theta$ is the total derivative of a current (Chern-Simons) K^μ:

$$G\widetilde{G} = \partial_\mu K^\mu = \partial_\mu \, \varepsilon^{\mu\nu\rho\sigma} \left(A^a_\nu G^a_{\rho\sigma} + \frac{g_S}{3} f^{abc} A^a_\nu A^b_\rho A^c_\sigma \right).$$

Hence it is reasonable to expect that this term has no physical implications, since a total derivative vanishes on the boundary, hence does not contribute to the action. However, being QCD a non-abelian theory, its vacuum has a non trivial structure, due to possible gauge choices not connected to the identity. Of course, a reasonable condition for the vacuum is $A^a_\mu = 0$, but then pure gauge choices $A'_\mu = -ig_S \Omega^\dagger \, \partial_\mu \Omega$ are equivalent to the zero-field vacuum. It can be shown (Ref. [13]) that a gauge choice Ω_1, which is not connected to the identity, generates:

$$\frac{g_S^2}{32\pi^2} \int d^4x \, G\widetilde{G} \bigg|_{\Omega_1} = 1$$

Defining $\Omega_n = (\Omega_1)^n$ with $n \in \mathbb{Z}$ and evaluating the integral on Ω_n, we obtain that the result is n. Choosing the temporal gauge $A^a_0 = 0$, we have that $K^i = 0$, so

$$\nu = \frac{g_S^2}{32\pi^2} \int d^4x \, G\widetilde{G} \bigg|_{\Omega_\nu} \quad \Longrightarrow \quad \frac{g_S^2}{32\pi^2} \int d^4x \, \partial_0 K^0_\nu = \frac{g_S^2}{32\pi^2} \int d^3x K^0_\nu \big|^{t=+\infty}_{t=-\infty} = \nu$$

Thus, ν has the interpretation of the winding number of a solution that is A_n for $t \to -\infty$ and $A_{n+\nu}$ at $t \to +\infty$.

Let us now call $|n\rangle$ the vacuum configuration related to the gauge choice Ω_n and be U_1 the unitary transformation related to Ω_1 that acts on these states. Without loss of generality, we can take

$$U_1 \, |n\rangle \equiv |n+1\rangle \, .$$

Thus, the vacuum is not gauge invariant! A vacuum choice which is gauge invariant is the θ-vacuum

$$|\theta\rangle \equiv \sum_n e^{-in\theta} \, |n\rangle \quad \Longrightarrow \quad U_1 \, |\theta\rangle = e^{i\theta} \, |\theta\rangle$$

We now point out that using a θ-vacuum for $\mathcal{L}_{QCD}$ is completely equivalent to adding the θ-term:

$$\langle\theta| \, \mathcal{O} \, |\theta\rangle = \sum_{m,n} e^{i(m-n)\,\theta} \, \langle m| \, \mathcal{O} \, |n\rangle = \sum_{\nu,n} e^{i\nu\theta} \, \langle n+\nu| \, \mathcal{O} \, |n\rangle$$

From what we have seen above, both terms in the sum imply a transition for a certain vacuum state $|n\rangle$ to $|n+\nu\rangle$. We can eliminate the sum over n by passing to the path integral:

$$\sum_{\nu,n} e^{i\nu\theta} \, \langle n+\nu| \, \mathcal{O} \, |n\rangle = \sum_\nu \int \mathcal{D}A \, \delta \left(\nu - \int d^4x \, \theta \frac{g_S^2}{32\pi^2} G\widetilde{G} \right) \mathcal{O} \, e^{i \int d^4x \, \mathcal{L}_{QCD} + \mathcal{L}_\theta}$$

With the δ, we can eliminate also the sum over ν and we remain exactly with what we have claimed. This is an unequivocal proof that the θ-term must be included in our lagrangian.

However, θ itself is not physical, because a chiral rotation modifies it. If we switch on the quark masses, we immediately notice that axial rotations are no more a symmetry of the QCD lagrangian and, in particular, they produce a complex phase for the mass matrix. We can now write:

$$\mathcal{L}_{QCD} = -\frac{1}{4} G^a_{\mu\nu} G^{a,\mu\nu} + \bar{\Psi}_L \, i \not{D} \Psi_L + \bar{\Psi}_R \, i \not{D} \Psi_R - \bar{\Psi}_L \, M e^{i\theta_q} \, \Psi_R - \bar{\Psi}_R \, M e^{-i\theta_q} \, \Psi_L .$$

Thus, for a quark axial rotation of angle α:

$$\theta \to \theta + 2\alpha \quad \text{and} \quad \theta_q \to \theta_q + 2\alpha$$

The combination $\overline{\theta} = \theta - \theta_q$ is finally independent on quark chiral rotations: hence, it is physically observable.

At low energy the CP violation of the θ-term is reflected in a CP violating coupling between pions and nucleons: namely, assuming now to be in the $SU(2)$ limit,

$$\mathcal{L}_{\pi N} = \pi^a \, \overline{\Psi} \, (i \gamma_5 g_{\pi N} + \overline{g}_{\pi N}) \, \tau^a \, \Psi$$

Without focusing on the details of the computations, an interaction diagram like in Figure below generates an electric dipole moment for the neutron.

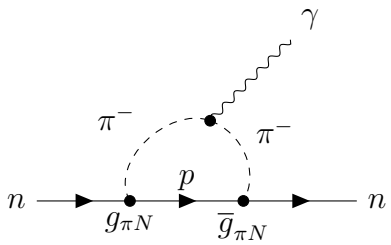

The effective lagrangian describing it can be written as

$$\mathcal{L}_{nEDM} \supset d_n \, F_{\mu\nu} \, \overline{n} \, \gamma^{\mu\nu} i \gamma_5 \, n$$

Of course $d_n \propto g_{\pi N} \overline{g}_{\pi N}$, but we can also estimate it in NDA since it must be proportional to $\overline{\theta}$ and it must be zero when at least one quark is massless. This happens because $\theta_q \simeq \arg\det M$, thus a massless quark would make the θ-term unphysical again and we could simply rotate it away. Thus,

$$d_n \simeq \overline{\theta} \, \frac{m_q}{m_N} \frac{1}{m_N} .$$

A correct computation, which takes care of regularizing well the divergence of the loop with the cutoff m_N, obtains $d_n \approx 3 \cdot 10^{-16} \, \overline{\theta} \, e \cdot cm$. Comparing this result with the experimental uncertainty (indeed, we do not measure any electric dipole moment for the neutron), it has been obtained $d_n^{exp} \lesssim 10^{-26}$. The simple consequence is that

$$\overline{\theta} \lesssim 10^{-10} .$$

Then, the Strong CP problem arises: one possibility is that we have two unnaturally small independent parameters θ and θ_q; the other possibility is that we have an extreme fine tuning between these two variables, which is equally unattractive.

3.2 Non-axionic solutions to the Strong CP problem

Before passing to the most popular solution to the Strong CP problem, the axion, we revise briefly some non-axionic solutions that have been proposed throughout the years.

The first one, that we have already mentioned, is to take (at least) one massless quark. In this case we cannot reabsorb eventual chiral rotations of the massless quark(s) and this would mahe θ unphysical. In principle, we could actually solve the Strong CP problem if $m_u \lesssim 10^{-10}\, m_d$, as the neutron EDM is proportional to $m_u m_d/(m_u + m_d)$. However, the up quark mass is a fraction of order 1/2 of the down mass. Thus, this possibility is experimentally excluded.

Another possibility is to exploit RG evolution of CP violating interactions, supposing that at some RG scale $\overline{\theta} = 0$. The only other CP violating phase of the SM comes from φ_{CKM}, the physical phase of the CKM matrix. Treating $\overline{\theta}$ and φ_{CKM} as spurions of the CP symmetry and expressing the β function of $\overline{\theta}$ as a function of possible CP violating interactions, i.e. the Yukawas and the $SU(2)_L$ gauge ones, it has been obtained that the first non-zero contribution is:

$$\beta_{\overline{\theta}} \propto g^2 \arg \mathrm{Tr}\{Y_u^4\, Y_d^4\, Y_u^2\, Y_d^2\}$$

An exact computation at leading order would require going at 7 loops in the SM computation, which is definitely not convenient. For more details see Ref. [14].

Finally, there are models which P and CP are assumed as good symmetries in the UV and are then broken at the EW scale[2]. For theories asking that P is a good symmetry, however, $\overline{\theta}$ can be made vanishing at tree level, but would receive loop corrections from the very same construction of symmetrizing the SM theory (e.g. we would need to add a right-handed Higgs). CP models are built in a way to make $\overline{\theta}$ and φ_{CKM} vanish in the UV. However, the CKM phase is huge compared to $\overline{\theta}$: this is why these theories are very fragile, because of many coincidences between physical scales have to happen in order to accomplish this result. These theories are nowadays unappealing with respect to the axion, which we will now discuss.

3.3 The Axion solution

The axion solution solves the Strong CP problem in a very clean and fascinating way. In fact, if at EW scales we have an additional degree of freedom ϕ such that

$$\mathcal{L}_{SM+\phi} \supset \frac{1}{2}\partial_\mu\phi\, \partial^\mu\phi + \left(\frac{\phi}{f_a} + \overline{\theta}\right) \frac{1}{32\pi^2}\, G\widetilde{G},$$

the Strong CP problem is solved dynamically choosing $\langle\phi\rangle = -\overline{\theta} f_a$. This is beautifully guaranteed by the Vafa-Witten theorem (Ref. [16]), that states that P cannot be spontaneously broken in QCD. As a consequence, the VEV of any term in front of $G\widetilde{G}$ is null, since, symbolically, $E(0) \leq E(\theta)$ for each θ.

[2]See Ref. [15] for more details on these models.

We have discovered that adding the axion field ϕ, on the vacuum of the theory, no θ-term appears, hence no neutron EDM: this solves the Strong CP problem. Now, more properly, the axions will be excitations above the CP symmetric vacuum, that we will nevertheless denote as ϕ. The lagrangian for these particles is then

$$\mathcal{L}_{SM+\phi} = \mathcal{L}_{SM} + \frac{1}{2}\partial_\mu\phi\,\partial^\mu\phi + \frac{\phi}{f_a}\,\frac{1}{32\pi^2}\,G\widetilde{G}$$

At energies below Λ_{QCD} the axion takes a potential due to its interactions with pions. We illustrate this in the chiral lagrangian with 2 generations, for the sake of simplicity. we employ the fact that a chiral rotation of quarks can transfer the CP violation to the quark mass matrix M. Thus, the rotation needed to make the $G\widetilde{G}$ term disappear is realized by

$$\Psi \to \exp\left\{-i\frac{\phi}{2f_a}\gamma_5\,Q_a\right\}\Psi \quad \text{such that} \quad M \to e^{i\frac{\phi}{2f_a}\,Q_a}\,M e^{i\frac{\phi}{2f_a}\,Q_a} \tag{3.1}$$

with Q_a an arbitrary matrix in flavour space that satisfies $\mathrm{Tr}\{Q_a\} = 1$ (as the axial anomaly involves traces over flavor, Lorentz and gauge indices). A convenient choice in order to find the axion potential is: $Q_a = diag\{1/2, 1/2\}$. With this choice we can extract the axion-pions potential from the chiral lagrangian term (Appendix A)

$$-\frac{B f_\pi^2}{2}\,\mathrm{Tr}\left\{M\,e^{i\frac{\phi}{2f_a}}\,\Sigma^\dagger + \Sigma\,M\,e^{-i\frac{\phi}{2f_a}}\right\}$$

A direct computation gives

$$V(\phi,\pi^a) = -m_\pi^2 f_\pi^2\sqrt{\cos^2\frac{\phi}{2f_a} + \left(\frac{m_u - m_d}{m_u + m_d}\right)^2\,\frac{\pi_0^2}{\pi^2}\,\sin^2\frac{\phi}{2f_a}}\,\cos\left(\frac{\pi}{f_\pi} - \varphi(\phi)\right)$$

where $\pi^2 = \pi_0^2 + 2\pi^+\pi^-$ and $\tan\varphi(\phi) = \frac{m_u - m_d}{m_u + m_d}\,\frac{\pi^0}{\pi}\tan\phi/2f_a$. Clearly, there is an absolute minimum for $\phi = 0$ and $\pi^a = 0$, so that, as Vafa-Witten theorem requires, the vacuum of the theory is CP conserving. Moreover, this potential generates the mass term for the axion: namely,

$$m_a^2 = \frac{m_\pi^2 f_\pi^2}{f_a^2}\frac{m_u m_d}{(m_u + m_d)^2} \quad \text{hence } m_a \approx 5.7\,meV\,\left(\frac{10^9\,GeV}{f_a}\right)$$

The use of χPT is the justified if $f_a \gtrsim 1\,GeV$.

Until now, we have treated the topic as if quarks were only coupled to gluons. However, they transform under the full SM gauge group: a chiral rotation of quarks would then generate terms of the kind

$$\theta\frac{g_S^2}{32\pi^2}G\widetilde{G} + \theta_1\frac{g^2}{32\pi^2}W\widetilde{W} + \theta_2\frac{g'^2}{32\pi^2}B\widetilde{B}$$

Being $U(1)_{B+L}$ anomalous under $SU(2)_L \times U(1)_Y$, we can nevertheless set freely θ_1 to 0. Of course, θ_2 does not contribute to the action, being $U(1)_Y$ an abelian group: this is important, because θ_1 and θ_2 being unphysical means that we do not have

an Electroweak CP problem. If we now work in the broken phase of the SM, this means that we have an axion coupling to the photons that is conventionally written as

$$\mathcal{L}_{\phi\gamma} = \frac{1}{4}\, g_{a\gamma} F\widetilde{F} \tag{3.2}$$

Therefore, if the axion has an original $g^0_{a\gamma}$ coming for a suitable UV model, the chiral rotation in Equation 3.1, would then induce an axion-photon coupling of the kind:

$$g_{a\gamma} = g^0_{a\gamma} - (2N_c)\frac{e^2}{8\pi^2\, f_a}\,\mathrm{Tr}\{Q_a\, Q^2_{em}\}$$

with Q_{em} being the generator of $U(1)_{em}$, which lives in the diagonal subgroup of $SU(3)_V \times U(1)_B$. A convenient choice is to choose Q_a such that it eliminates the mass mixing between the axion and the neutral pion, because otherwise whenever we need the coupling $g_{a\gamma}$, we cannot forget to add the mass mixing to the pion and then the vertex $\pi^0\,\gamma\,\gamma$. The choice that allows us to do that is

$$Q_a = \frac{M^{-1}}{\mathrm{Tr}\{M^{-1}\}}.$$

UV Models for the Axion: PQ mechanism

So far, we have discussed how an additional degree of freedom, the axion, which has a coupling with $G\widetilde{G}$ solves the Strong CP problem and which is its effective lagrangian at energies below the confinement scale. Now we want to briefly review the UV models that can generate the axions. The most famous way to generate the axion with the properties we have required is the *Peccei-Quinn mechanism*: the SM has to be extended with a new global symmetry $U(1)_{PQ}$ that has to be anomalous under $SU(3)_C$ and spontaneously broken at some energy scale that we will identify with our f_a. The anomaly under $SU(3)_C$ generates the $G\widetilde{G}$ term and the spontaneous breaking of $U(1)_{PQ}$ guarantees the existence of one new degree of freedom, the pseudo-NGB (of course, we do not have an exact symmetry) that will be the axion.

The first proposed model that encodes the PQ mechanism is the Peccei-Quinn-Weinberg-Wilczek model (Refs. [17, 18]), which postulates another Higgs doublet such that in the Yukawa sector

$$\mathcal{L} \supset -Y^{ij}_u\, \overline{Q}^i_L\, H_u u^j_R - Y^{ij}_d\, \overline{Q}^i_L\, H_d d^j_R + h.c.$$

For this kind of theory, however, the PQ breaking scale is below the EW scale, which makes the axion coupling to the SM not suppressed enough: this would lead to unobserved decays $K \to \pi\phi$. For this reason PQWW models are somewhat excluded.

The idea that SM quarks carry the anomaly, which is the essential idea of PQWW models, is promoted also by Dine-Fischler-Srednicki-Zhitnitsky (DFSZ) model, which gives also name to this entire class of models. The model (Ref. [19],Ref. [20]) consists of the extension of the Higgs doublet to $H_u \sim (1, 2, -1/2)$, $H_d \sim (1, 2, +1/2)$

and a brand new $\Phi \sim (1,1,0)$, which allows to decouple PQ and EW scales. Then, the potential for these scalars

$$V(H_u, H_d, \Phi) = V(|H_u|^2, |H_d|^2, |H_u^\dagger H_d|, |(H_u H_d)|, |\Phi|^2) - \lambda (H_u H_d)(\Phi^\dagger)^2$$

Here, by $(H_u H_d)$ it is meant the contraction of the doublets with the totally anti-symmetric tensor ε^{ij} of $SU(2)_L$. For suitable forms of the potential, all three scalars take a VEV. The axion is contained in H_u and H_d, so that it will be coupled to the SM fermions. The obtained low-energy lagrangian for the axion would then be

$$\mathcal{L}_{DFSZ} \supset N \frac{\alpha_S}{8\pi} \frac{\phi}{v_{PQ}} G\widetilde{G} + E \frac{\alpha}{8\pi} \frac{\phi}{v_{PQ}} F\widetilde{F} + N \frac{\partial_\mu \phi}{2 v_{PQ}} \sum_f c_f \, \overline{f} \gamma^\mu \gamma_5 f$$

Finally, we discuss another class of UV completions, named after the Kim-Shifman-Vainshtein-Zakharov model (KSVZ) (Ref. [21, 22]). In this models we add new colored quarks which will provide the $G\widetilde{G}$ term for the axion. Thus, we extend the SM with a new complex scalar $\Phi \sim (1,1,0)$ and a new quark $\psi \sim (3,1,0)$, both charged under $U(1)_{PQ}$ and such that ψ_L and ψ_R have different charges, in order to generate the axial anomaly. A Lagrangian for this theory would be

$$\mathcal{L}_{KSVZ} = \partial_\mu \Phi^* \, \partial^\mu \Phi + \overline{\psi} \, i \not{D} \, \psi - (y_\psi \overline{\psi}_L \Phi \, \psi_R + h.c.) - V(\Phi)$$

If $V(\Phi)$ is built in order to spontaneously brake at v_{PQ}. Because of Goldstone theorem, the axion now lives in the exponential representation of the broken symmetry, that means that the Yukawa assumes the form

$$\mathcal{L} \supset \frac{y_\psi v_{PQ}}{\sqrt{2}} \overline{\psi}_L \, e^{i \frac{\phi}{v_{PQ}} \gamma_5} \psi_R + h.c.$$

Then, with a chiral rotation, we can transfer the axion to the $G\widetilde{G}$ term as we are now used to. As a last comment, we notice that that if we want $v_{PQ} \gg v_{EW}$, the new quarks must be really massive and, in practice, we do not see them in colliders.

3.4 Axion Cosmology

In this Section we will discuss the cosmological relevance of the axion scenario. In fact, the axion is also a viable Dark Matter candidate, a fact that makes this particle so popular in Phenomenology.

We want to study what happens when we couple the axion field to a FLRW background (this is why we did not call the axion a, since now on $a(t)$ will be the scale factor of our metric) $ds^2 = -dt^2 + a(t)^2 d\vec{x} \cdot d\vec{x}$. For consistency we will assume the axion field to depend only on time and we will treat its cosmological evolution in a semi-analytical way. We study the Klein-Gordon equation of motion in a FLRW background, namely

$$\ddot{\phi} + 3H\dot{\phi} + V'(\phi) = 0$$

In the previous Section we have seen that the axion has a (small) mass, so we will approximate the potential to be quadratic and, when in contact with a thermal bath at temperature T, with a T dependence: $V(\phi) = m_\phi(T)^2\phi^2/2$, with

$$m_\phi(T) = \begin{cases} m_\phi & T < \Lambda_{QCD} \\ m_\phi \left(\frac{\Lambda_{QCD}}{T}\right)^{\frac{n}{2}} & T > \Lambda_{QCD} \end{cases}$$

The n in the exponent is fitted with lattice data and we will take $n = 6.84$ (Ref. [23]).

In both cases, the KG equation is the one of a damped oscillator with a (time-dependent) friction H, which in our case is the Hubble parameter. We identify two regimes in the damped oscillator, in analogy with Classical Mechanics: the field is stuck by Hubble friction or the field oscillates and is slowly damped. Clearly, we need to compare $H(T)$ and $m_\phi(T)$ to understand which phase dominates. We will call T_{osc} the temperature such that $3H(T_{osc}) = m_\phi(T_{osc})$. Assuming that $T_{osc} > \Lambda_{QCD}$ we find T_{osc} by comparing

$$3\frac{g_*(T_{osc})\,T_{osc}^2}{\sqrt{3}\,M_p} = m_\phi(T_{osc}) \Longrightarrow T_{osc} \simeq 1.18 \left(\frac{10^{12}\,GeV}{f_a}\right)^{0.185} GeV$$

which *a posteriori* motivates the assumption $T_{osc} > \Lambda_{QCD}$. At high temperatures H is big, while $m_\phi(T)$ is suppressed, thus today we are in the oscillatory phase of the axion field and we want to compute its energy density. The energy density of a scalar field in a FLRW background is simply

$$\rho_\phi = \frac{1}{2}\dot{\phi}^2 + V(\phi),$$

which, in analogy with Classical Mechanics is a kinetic plus a potential term. In the oscillatory phase we can use the virial theorem and easily show that

$$\dot{\rho}_\phi = -3H\rho_\phi.$$

We have just shown that nowadays the axion field behaves exactly as Cold Dark Matter!

However, we want to reproduce also the Dark Matter abundance. To do it we notice that in a first approximation, we can treat the axion field as stuck at the initial value ϕ_i it gets after PQ symmetry breaking until it starts to oscillate at $T = T_{osc}$. Then, very rapidly the mass overtakes the friction and we can approximate the amplitude of oscillations to be damped in a timescale much bigger than the period of oscillation. We can then use the adiabatic invariant, in analogy with Classical Mechanics,

$$I = \frac{1}{2\pi}\oint d\theta\, p_\theta(\theta) = \frac{a^3\, m_\phi(T)\theta^2}{2}$$

where $\theta = \phi/f_a$ and p_θ is the conjugated momentum to θ in the "KG" lagrangian

$$\mathcal{L} = a^3\left(\frac{1}{2}\dot{\theta}^2 - \frac{1}{2}\,m_\phi^2\,\theta^2\right).$$

Then, using the adiabatic invariant above, we easily that

$$\theta_0 \simeq \left(\frac{T_0}{T_{osc}}\right)^{\frac{3}{2}} \left(\frac{\Lambda_{QCD}}{T_{osc}}\right)^{\frac{n}{4}} \theta_i$$

Since θ_i comes from the SSB of the $U(1)_{PQ}$ symmetry, it is natural for θ_i to have a value of order π. Being $T_0 \approx 2.7 \cdot 10^{-4}\, eV$, it is clear that the background solution in a FLRW background does not generate a Strong CP problem (we verified it previously only in a $T = 0$ theory). Now, thanks to the virial theorem we easily get the abundance of axion matter today:

$$\Omega_\phi \equiv \frac{\rho_\phi}{\rho_{cr}} = \frac{m_\phi^2\, f_a^2\, \theta_0^2}{\rho_{cr}} \simeq 0.3 \left(\frac{f_a}{10^{11}\, GeV}\right)^{1.185}$$

This is approximately the observed result, for a value of f_a which is not ruled out by experiments or astrophysical bounds (see Section 3.5). Thus, the axion well reproduces the DM abundance, which is quite an astonishing result! For this precise reason, in the current jargon axion means two things:

- QCD axion: it solves the Strong CP problem and it is a good DM candidate. It is characterised by the relation $m_a = f_a^{-1} \propto g_{a\gamma}$.
- ALPs: axion-like particles are more general pseudoscalars which are not required to solve the Strong CP problem, but can be good DM candidates. For them the mass and the coupling are two independent variables.

In our discussion we have an undetermined quantity θ_i, about which we can comment further. In fact, there are two different scenarios depending on whether the PQ mechanism is realized before or after the onset of inflation. This uncertainty is enforced by the fact that, up to now, we do not know the energy scale of inflation E_{INF}. If the PQ transition happens before inflation, the comoving Hubble radius at that time was (as required by the inflationary model) larger (or equal) to the current one. Thus, there is no way that causal regions with different θ_i have interacted and, as a result, we remain with an unspecified θ_i, which we assume of order 1. On the other hand, if inflation ended before the SSB of PQ symmetry, then different field values have interacted and it is conceivable to take

$$\theta_i^2 = \langle \theta^2 \rangle = \frac{\pi^2}{3}.$$

Of course, the treatment that has been discussed here is only a first approximation: the oscillation does nor begin all in a sudden and one has to perform a numerical integration; the potential is in general anharmonic, so not every θ_i contributes the same to the axion relic density; finally, the mechanism through which we have computed the axion relic density, known as *misalignment mechanism*, is not the only contribution, as one should consider also decays of topological defects of the PQ phase transition, which are nevertheless difficult to compute.

We have to check the last ingredient before saying that the axion is a good Dark Matter candidate: its stability. The axion (at least in a reasonable range of f_a) can

decay only through $\phi \to \gamma\,\gamma$ and $\phi \to \overline{\nu}\nu$. The latter presents some issues. The first one is to be strongly model dependent, being the couplings of the axion to fermions inherited mostly by the structure of the UV model, intead of by the PQ mechanism. Secondly, we know that (at least two) neutrinos are massive, thus the decay may be kinematically forbidden. Ultimately, the axion couples derivatively to the fermionic axial current $j_A^\mu = \overline{f}\gamma^\mu\gamma_5 f$. Integrating by parts, the axion couples then to $\partial_m u j_A^\mu$ which classically is

$$\partial_\mu\, j_A^\mu = 2im\overline{f}\gamma_5 f.$$

Thus the coupling of the axion to neutrinos is suppressed by a m_ν/f_a. Hence, the more likely the decay is kinematically allowed, the higher is the price to pay in terms of suppression, which is quadratic in m_ν/f_a. It is therefore reasonable to assume that the axion decays only to photons.

To compute the decay rate $\Gamma(\phi \to \gamma\,\gamma)$, we use the axion-photon coupling as defined in Equation 3.2. Very famously, the result becomes

$$\Gamma(\phi \to \gamma\,\gamma) = \frac{g_{a\gamma}^2\, m_\phi^3}{64\pi}$$

For $g_{a\gamma}$ there is a model-dependent component

$$g_{a\gamma}^0 = \frac{\alpha}{2\pi f_a}\frac{E}{N}$$

with $E/N = 0$ in the KSVZ model and $E/N = 8/3$ in the DFSZ. Considering now the term obtained from the chiral rotation that eliminates the mass mixing between the axion and the pion and working in $N_f = 2$, we find

$$g_{a\gamma} = \frac{\alpha}{2\pi f_a}\left(\frac{E}{N} - \frac{2}{3}\frac{4m_d + m_u}{m_u + m_d}\right)$$

This now sets the benchmark result (for which we remember that $m_s \propto f_a^{-1}$)

$$\tau_\phi = 1.3 \cdot 10^{28}\left(\frac{f_a}{10^9\, GeV}\right)\, yrs,$$

which is an astonishing amount of time, 18 orders of magnitude bigger that the life of our Universe! Therefore, the axion is enough long-lived to be a good DM candidate.

3.5 Axion searches and bounds

Due to its enormous lifetime is practically impossible to see an axion decay in the lab. To hope for an axion detection (or, in the the opposite case, to put bounds) an interesting idea is to use the so called helioscopes. In fact, due to the axion-photon coupling, in presence of a strong magnetic field, we can possibly hope for a Primakoff process (Figure 3.1) $\gamma\, N \to \phi\, N$, i.e. a photon conversion into an axion in presence of an external field (here indicated as a heavy nucleon). Of course, the photons are the ones coming from the Sun, hence the name. The main experiment

in this case is CAST (CERN Axion Solar Telescope), which has put the bound $g_{a\gamma} \lesssim 6 \cdot 10^{-11}\, GeV^{-1}$. If we model the coupling as $g_{a\gamma} = \alpha/(2\pi f_a)$, we translate the CAST result as $f_a \gtrsim 10^8\, GeV$. Future experiments, like the International Axion Observatory (IAXO), will go even further this result.

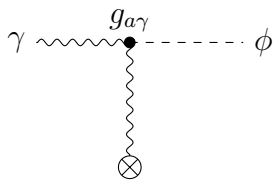

Figure 3.1: Primakoff process.

Another possibility is to produce axions in the laboratory (e.g. via inverse Primakoff) and then detect them with the same technique. One example are the "Light Shining through a Wall" experiments (e.g. ALPS I): axions are produced in the presence of a strong magnetic field, passes through a wall (impenetrable for photons) and gets converted back into photons. Clearly, the price to pay is in terms of the rate of the process, which in this case is proportional ti $g_{a\gamma}^4$. The bound is therefore weaker:

$$g_{a\gamma} \lesssim 6 \cdot 10^{-8}\, GeV^{-1}$$

Last but not least, axions could be produced naturally in highly energetic and dense astrophysical objects, such as stars and their remnants. Typical considerations involve the fact that if the star (take e.g. the Sun) radiates invisible light particles, its lifetime would be nevertheless affected and we can put a bound. We have also bounds thanks to the Supernova 1987A, studying the gamma rays we received from that event. These arguments will be the topic of the next Chapters (4 and 6) and for a detailed review, one can take Ref. [24] as a reference.

An important observation is that typically these bounds are made for a generic ALP, so that we can treat the mass and the coupling to photons as independent variables. The following plot (Figure 3.2), represents our current axion bounds in terms of mass and photon couplings.

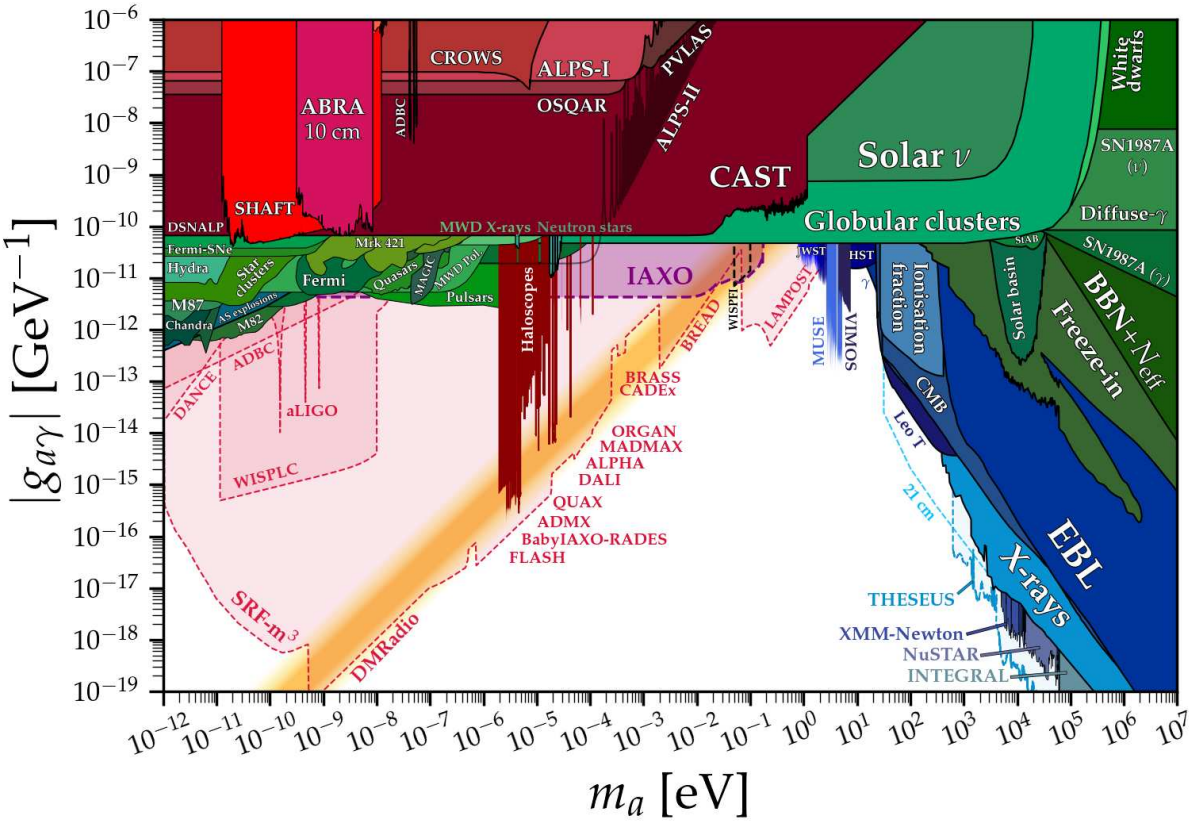

Figure 3.2: Exclusion plot for a ALPs. In red: lab experiments. In green: astrophysical bounds. In blue: cosmological bounds. In yellow: the landscape of the QCD axion. In pink: proposed new experiments.

Chapter 4

Supernova Physics and Light Particles Emission

In this Chapter we briefly review the standard lore about Core-Collapse Supernovae (Section 4.1), with a particular attention to neutrino emissions. New feebly interacting particles may affect the process of cooling, as it will be discussed in Section 4.2, where we will present the so-called Raffelt criterion (see Ref. [4]). Then, we explicitly compute the emissivity of a particle in the constant matrix element approximation, which leads to an analytic result: this reproduces Ref. [25] (Section 4.3). Finally (Section 4.4) , we apply the previous reasoning to the case of an ALP emission from a Proto-Neutron Star (PNS), to get a clue about astrophysical bounds discussed in Section 3.5.

4.1 Supernova Physics

Stars with masses $M \gtrsim 8M_\odot$ have enough energy to ignite the CO core and, by a sequence of fuel exhaustions, which imply contraction, thus temperature increase, thus the activation of new heavier nuclei burning phases, the star reaches a point in which the core is composed by elements in the Fe group. These elements saturate the nuclear binding energy, therefore fusion reactions cannot occur anymore. The Fe core mass increases thanks to the outer burning shells and, being degenerate, shrinks, until it exceeds the Chandrasekhar limit of $M_{Ch} \simeq 1.4M_\odot$ (which happens for $M \gtrsim 8M_\odot$). At this point, the core becomes unstable and, since there is no nuclear burning supporting it, the collapse begins. We can divide it in four subsequent phases phases, which added together last more or less 5—10 s and are considered the standard lore of Type II Supernova event (also called Core-Collapse SN) and the relic is a PNS or a black hole, for even larger masses (supposedly for $M \gtrsim 25M_\odot$). During this time interval the star radiates the gravitational binding energy of the core, which by a naive Newtonian argument is found to be

$$E_b \simeq \frac{3}{5}\frac{GM_{core}^2}{R} \approx 1.6 \cdot 10^{53} \left(\frac{M_{core}}{M_\odot}\right)^2 \left(\frac{10\,km}{R}\right) erg/s$$

mainly in the form of neutrino radiation. The first observation of the expelled neutrinos happened in the 1987, when the blue supergiant Sanduleak, located in the Large Magellanic Cloud, exploded in the event which is now known as SN 1987A.

The first phase is the collapse of the core, which is triggered by the onset of the $\gamma + {}^{56}\mathrm{Fe} \rightarrow 13\alpha + 4n$ reaction of iron photo-dissociation, that consumes $124.4\,MeV$ of energy. This implies the electron thermal pressure reduction. Once the collapse has started, the electron density has to increase, enhancing the electron Fermi momentum: in practice, beta decays become statistically forbidden, since the electrons would receive a momentum well inside the Fermi sphere. At this moment, electron absorption on heavy nuclei can take place and is not counterbalanced by beta decays. Thus, neutrinos are created in this process and in the first tens of ms can escape freely.
The innermost part of the core undergoes an homologous collapse Ref. [26], i.e. it maintains its internal structure (for example its density profile) the same, while shrinking. The typical ratio between the infalling velocity and the radius is $v/r \approx 400\text{—}700 s^{-1}$. The inner core is thus defined as the region for which the infalling velocity is subsonic, meaning that the inner core is in good contact within itself. The outer layers of the core will simply free-fall.
Clearly, as the density keeps increasing, neutrino interactions with nuclei becomes more efficient, until a density of $10^{12}\,g/cm^3$ (for a characteristic $10\,MeV$ neutrino), when they will be trapped. At this point, there is a typical radius R_ν, which contains the so called *neutrinosphere*, above which neutrinoes freely stream outside the star and below which neutrinos move by diffusion. In approximately $100\,ms$, the inner core collapses into the neutrinosphere.
Shortly after, the inner core reaches the nuclear density $\rho_0 \simeq 3 \cdot 10^{14}\,g/cm^3$, where the equation of state stiffens. This creates a shock at the edge of the inner core, which stores the energy of the outer layers and soon starts propagating outwards: we can naively think as if the outer layer crashed onto the inner core and release its kinetic energy in the shock. This is called "bounce and shock" scenario and was firstly proposed by Colgate and Johnson in 1960.

The outgoing shock carries enough energy to dissociate the heavy nuclei in its passage. This has the effect of reducing the efficiency of neutrino trapping, which now can escape more easily. Then, the protons coming from dissociated nuclei quickly netronize thanks to electron capture, which allows for a sudden production of ν_es, causing a burst called "prompt ν_e burst". As a result, the bloated outer layers of the core settle in $\lesssim 1\,s$ onto the surface of the inner core. The object now created is the Proto Neutron Star, which has a typical radius of $20\,km$ and a temperature of $30\text{—}40\,MeV$.

Because it dissociates nuclei, the shock stalls for some hundredths of ms at a constant radius. However, it is revived by accretion of the infalling material and by absorption of some neutrino energy. One can see by numerical simulation (as Janka and Müller did in 1993, well shown in Ref. [27] Ch.11 pp 402-403) that a small change in the neutrino luminosity from the central compact object drives dramatically different endings for the shock wave. If $L_\nu \gtrsim 2.2 \cdot 10^{52}\,erg/s$ the shock can travel again outwards and, since the binding energy of the progenitor star in realistic models is

some $10^{50}\,erg$ [1](see Ref. [28]), the star will be completely disrupted by the shock.

Finally, the PNS undergoes a phase of Kelvin-Helmoltz cooling, which means that it cools down by neutrino emission at the surface. Neutrinos are in fact trapped inside the PNS and their travel towards the surface is diffusive. At this point neutrinos undergo many different reactions (see Table 2 and Figure 3 of Ref. [29]), so that it emits neutrinos and antineutrinos of all flavors with the same luminosity. This is enforced by the fact that ν_e emissions allow for the deleptonization of the PNS. Now, the lepton number of the PNS is 0 and positrons can make their appearance: Thus, neutral current weak interaction of $e^+\,e^-$ will create couples of $\nu\overline{\nu}$ of all flavors, along with proton nucleon bremsstrahlung. In this phase, lasting approximately $10\,s$ neutrinos are produced at some tenths of B/s. Neutrino driven winds in this phase are supposed to lead to heavier than iron elements nucleosynthesis, mainly through slow (s-) and rapid (r-) processes.

At the and of these processes we end up with a $10\,km$ Neutron Star, that has emitted in more or less $10\,s$ its $\approx 300\,B$ binding energy in the form of (anti)neutrinos. Only a small fraction $O(1\%)$ of this incredible amount of energy is necessary to eject the progenitor mantle and, also, a small fraction is lost in electromagnetic radiation, making SNe by far the most luminous stellar events in the Universe. The peak of explosion luminosities outshines the entire galaxy of the SN event.

4.2 Light particles emission and bounds

The existence of new BSM particle may affect stellar evolution, given that the emission of invisible particles leads to a faster energy loss. In a virialized thermal object like a star, an energy loss implies a contraction, which implies a temperature increase, which implies faster fuel consumption. For example, for our Sun, we suppose that it loses energy mainly through electromagnetic radiation, thus we define the relative contribution of some "exotic" radiation (for many more details on this topic see Section 1.3 of Ref. [27])

$$\delta_x = \frac{L_x}{L_x + L_\gamma}.$$

Naively, one thinks that $\delta T/T \simeq -\delta_x$, where we mean that exotic particles imply the reduction of typical timescales of physical processes, e.g. the hydrogen burning phase of our Sun. We know the solar luminosity $L_\odot$ and we know, for our solar models, that the Sun is halfway through its main-sequence evolution. The only reasonable bound we can put is thus $L_x \lesssim L_\odot$. This kind of bounds are now famous as Raffelt bounds or Raffelt criterium (see e.g. Ref. [4]).

In the case of PNS cooling a particle coupled somehow to nucleons can be produced efficiently due to the enormous density $\rho_0 \approx 3 \cdot 10^{14}\,g/cm^3$ and temperature of $T \approx 30\,MeV$. A well-established estimate for the duration of the cooling phase has

[1]Now on, we will prefer the Bethe as energy unit of measure: $1\,B = 10^{51}\,erg$

been computed in Ref. [30]:

$$t_E = 10\,s \left(\frac{R_{PNS}}{10\,km}\right)^2 \left(\frac{\rho}{2\rho_0}\right)^{2/3}$$

with ρ being the central density. Clearly, the production of new particles cools the PNS faster than the characteristic $10\,s$ of neutrinos. The SN 1987A event is the only one for which we have detected the emitted neutrinos on Earth and from its data at Kamiokande detector Ref. [31], at IMB Ref. [32] and at Baksan Ref. [33] (one can also see data in Ref. [27] Ch. 11 pp. 419-420), we can say that the cooling lasted for more than $5\,s$, allowing us to put a Raffelt bound of the kind

$$L_x \lesssim L_\nu \approx (3\text{—}5) \cdot 10^{53}\, erg/s \tag{4.1}$$

from the best fit of the ν signal data. The exact luminosity value depends on the model one uses for the partition of the energy between the flavours, but the ballpark is within the values in brackets.

Then, once we have a BSM Particle Physics model for a new particle, we can put bounds on its masses and coupling from a PNS by imposing the Raffelt bound (Equation 4.1). If one assumes spherical symmetry and free streaming of the particle(s) produced, the luminosity will simply be

$$L_x = \int_0^{R_{NS}} dr\, \dot{\epsilon}_x(r) 4\pi r^2. \tag{4.2}$$

The quantity $\dot{\epsilon}$ is called emissivity and thus represents the emitted energy per unit time and volume of the produced particle(s) and it can be computed starting from the matrix element of the event $\mathcal{M}$, as we will do in the following Section.

4.3 Emissivity of light particles

Having in mind the axion production from nucleons, in this Section we reproduce the result of Brinkmann and Turner Ref. [25] for a PNS in the one-zone assumption, which means that we will assume constant T and n in the whole core of the collapsed star. Moreover, we will work under the assumption that there are only neutrons, which have temperature $T = 30\,MeV$ and density stiffened to the nuclear density $n = 10^{38}\,cm^{-3}$. To reproduce Brinkmann and Turner, we assume a constant matrix element (see Ref. [25] for their motivation). Thus, the emissivity for the process $n\,n \to n\,n\,a$ is defined as

$$\dot{\epsilon} = \int \frac{d^3p_1}{(2\pi)^3\,2E_1} \frac{d^3p_2}{(2\pi)^3\,2E_2} \frac{d^3p_3}{(2\pi)^3\,2E_3} \frac{d^3p_4}{(2\pi)^3\,2E_4} \frac{d^3q}{(2\pi)^3\,2E_s} \cdot S \cdot (2\pi)^4 \delta^{(4)}(p_i - p_f) \cdot \\ \cdot |\mathcal{M}|^2 \cdot E_S \cdot f(E_1)\, f(E_2)\, (1 - f(E_3))\, (1 - f(E_4))$$

Following the prescriptions shown in Appendix B, we get the expression (identical to Equation 7a and 7b of Ref. [25]).

$$\dot{\epsilon} = S|\mathcal{M}|^2\, m^{0.5}\, T^{6.5}\, I(y)$$

with $y = \frac{\mu - m}{T}$ and $I(y)$ defined as

$$I(y) = \frac{1}{2^{3.5}\pi^7} \int_0^{+\infty} du_+ \, du_- \int_0^{u_-} du_3^* \, (u_+ u_- u_3^*)^{1/2} (u_- - u_3^*)^2$$
$$\times \frac{1}{e^{2(u_+ + u_- - y)} - 1} \frac{1}{\sqrt{u_+ u_-}} \log \left[\frac{\cosh\left(\frac{(u_+^{1/2} + u_-^{1/2})^2}{2} - \frac{y}{2} \right)}{\cosh\left(\frac{(u_+^{1/2} - u_-^{1/2})^2}{2} - \frac{y}{2} \right)} \right]$$
$$\times \frac{1}{1 - e^{-2(u_+ + u_3^* - y)}} \frac{1}{\sqrt{u_+ u_3^*}} \log \left[\frac{\cosh\left(\frac{(u_+^{1/2} + u_3^{*,1/2})^2}{2} - \frac{y}{2} \right)}{\cosh\left(\frac{(u_+^{1/2} - u_3^{*,1/2})^2}{2} - \frac{y}{2} \right)} \right]$$

In the limits in which the nucleons are very degenerate or very non-degenerate, we get an analytic result, identical to Equations 5a and 6a of Ref. [25] (see Appendix B).

$$\dot{\epsilon}(ND) = \frac{S|\mathcal{M}|^2}{4 \cdot 35 \cdot \pi^{6.5}} \, m^{0.5} \, T^{6.5} \, e^{2y}$$
$$\dot{\epsilon}(D) = \frac{31\sqrt{2}}{64 \cdot 3780\pi} S|\mathcal{M}|^2 \, m^{0.5} \, T^{6.5} \, y^{1/2}$$

We are finally able to reproduce Figure 2 of Ref. [25] with both analytic and numerical integrations of $I(y)$:

4.4 Axion emission and cooling bounds

We now want to do better, without approximating the matrix element as a constant. So, we have to model the axion-nucleon coupling: the most convenient choice is a pseudovector coupling to a nucleon N

$$\mathcal{L}_{a\,N} = \frac{g_{aN}}{2m_N} \, \partial_\mu a \, \overline{N} \gamma^\mu \gamma_5 N$$

which upon integration by parts becomes $\mathcal{L}_{a\,N} = -i g_{aN} a \overline{N} \gamma_5 N$. For a process in which the ALP is produced only by one kind of nucleon, which is a good approximation in the PNS environment were neutrons are more abundant than protons, we can study the axion emission from an elastic scattering of the kind $n(p_1)\, n(p_2) \to n(p_3)\, n(p_4)\, a(q)$. There are 8 diagrams contributing to this specific process, 4 "direct" in Figure 4.2 and 4 with exchanged momenta p_3 and p_4, thus with a minus sign (which agrees with Ref. [25], that corrects Iwamoto's Ref. [2]).

For the One Pion Exchange potential, we use the pseudoscalar coupling (Equation A.2)

$$\mathcal{L}_{OPE} = -i \, f \frac{2m_N}{m_\pi} \pi^a \overline{\psi} \gamma_5 \tau^a \psi.$$

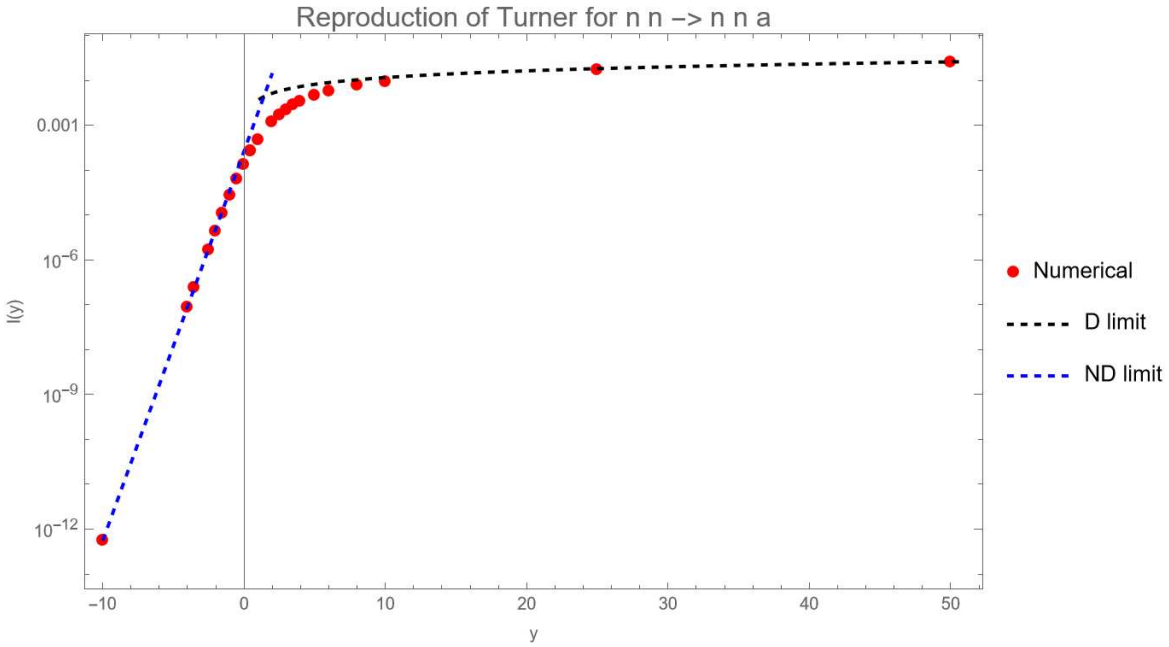

Figure 4.1: Constant matrix emission for $n\,n \to n\,n\,a$ in the NR regime and one zone and one nucleon assumption.

Thus, defining $k = p_2 - p_4$ and $l = p_2 - p_3$, we can compute the squared matrix element (averaged over axion's directions) in the degenerate limit ($\mathbf{k}\cdot\mathbf{l} \ll |\mathbf{k}||\mathbf{l}|$) for nucleons and non-relativistic kinematics (Appendix C). The leading order in the NR expansion leads to (in agreement with p. 2347 of Ref. [25]):

$$\sum_{spins} |\mathcal{M}|^2 = \frac{256}{3}\frac{g_{aN}^2 f^4 m_N^2}{m_\pi^4}\left[\frac{\mathbf{k}^4}{(\mathbf{k}^2+m_\pi^2)^2} + \frac{\mathbf{l}^4}{(\mathbf{l}^2+m_\pi^2)^2} + \frac{\mathbf{k}^2\mathbf{l}^2}{(\mathbf{k}^2+m_\pi^2)(\mathbf{l}^2+m_\pi^2)}\right] \tag{4.3}$$

For this squared matrix element we can thus compute the emissivity in a quasi[2]-analytic form in the degenerate limit (see Appendix B for more details):

$$\dot{\epsilon}_a(D) = \frac{32\cdot S}{3(2\pi)^8}\frac{m^2 f^4 g_{an}^2}{m_\pi^4}\frac{T^3}{m\,p_F}\int_0^{+\infty} d\omega\,\omega^2 F(\omega/T)\int_{k^2+l^2\le 4p_F^2} dk\,dl\,\frac{2m}{\sqrt{1-\dfrac{k^2+l^2}{4p_F^2}}}\times$$
$$\times\left[\frac{k^4}{(k^2+m_\pi^2)^2} + \frac{k^2l^2}{(k^2+m_\pi^2)(l^2+m_\pi^2)} + \frac{l^4}{(l^2+m_\pi^2)^2}\right]$$

The value of the Fermi momentum $p_F \approx 300\,MeV$ is determined directly from the number density of the PNS of $n = 10^{38}\,cm^{-3}$ form $p_F = (3\pi^2 n)^{1/3}$. In the following expression $y_\pi = m_\pi/2p_F \ll 1$, thus making sense of the quasi-analytic expression that agrees with Iwamoto Ref. [2]

$$\dot{\epsilon}_a(D) = \frac{31}{3780\pi}\frac{g_{an}^2}{m_\pi^4}\,m^2\,T^6\,p_F\,F(y_\pi)$$

[2]Actually the mixed term in $\mathbf{k}$ and $\mathbf{l}$ is not analytic, but for the values of m_π and p_F we have in mind one can numerically show that it contributes approximately as much as the other two terms, which of course contribute the same.

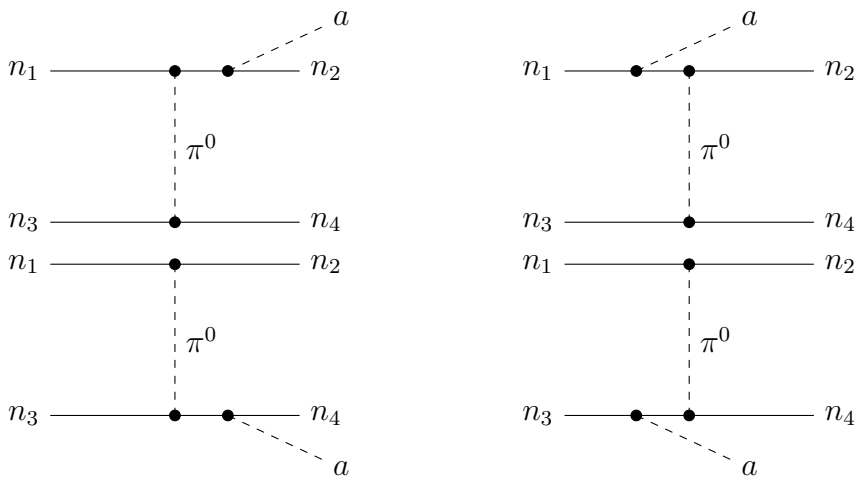

Figure 4.2: Contributing diagrams to $n(p_1)\, n(p_2) \to n(p_3)\, n(p_4)\, a(q)$ + exchange diagrams of p_3 and p_4 with a minus sign.

with $F(y_\pi) = 1 - \dfrac{3}{2} y_\pi \arctan \dfrac{1}{y_\pi} + \dfrac{1}{2} \dfrac{y_\pi^2}{1 + y_\pi^2}$.

Plugging the numerical values for a one-zone approximated PNS with radius $R \simeq 10\, km$, one gets that $L_a \lesssim L_\nu \approx 3 \cdot 10^{53}\, erg/s$ if

$$g_{aN} \lesssim 7 * 10^{-10} \left(\frac{30\, MeV}{T} \right)^2 \left(\frac{300\, MeV}{p_F} \right).$$

Chapter 5

Light scalar models

Light CP-even scalars often appear in the literature as sub-GeV thermal Dark Matter mediators, as it will be discussed in Section 5.1. This mediators could couple to the rest of the SM via renormalizable portal interactions, which are appealing because of their somewhat minimal number of free parameters required. In particular, we will study an Higgs-portal mechanism and its consequences in the couplings of the DM mediator (that we will call ϕ) in Section 5.2. Our goal, as will be discussed in Chapter 6, is to produce ϕ inside Core-Collapse Supernovae, thus in a baryon-dominated environment. Since the Higgs-portal mechanism provides a mass mixing $\phi - h$, it is necessary to discuss how the SM Higgs couples to nucleons, which will be straightforwardly translated in a result for the scalars (Section 5.3).

5.1 Why scalars?

The mass range in which thermal weakly interacting DM can live spans from the keV region, below which structure formation is elapsed by free-streaming (Section 2.2), to $10\,TeV$ for perturbative unitarity. As it is possible to see in Figure 2.4, $10\,GeV$—$10\,TeV$ WIMP DM still did not produce a signal, even with an highly increasing sensitivity, pushing the bound towards the neutrino fog.

Below this region, there are still well-motivated models reproducing the DM cosmic abundance, as asymmetric DM (Ref. [11]) or freeze-in (Ref. [34]). As pointed out in Ref. [35], WIMP targets for nuclear recoils can be arranged to be sensitive to lower energy deposition, hence to lighter DM. For sub-GeV DM there are proposals for direct detection experiments on lighter nuclei, such as liquid helium detectors, bond breaking in molecules and defect creation in crystal lattices. For MeV—GeV DM the energy deposition is such that the effect is more visible in scattering off electrons, which could produce signals using semiconductors, atoms, graphene or scintillators.

However, as it will be shown in a moment, sub-GeV DM of this kind would be overproduced unless it has a mediator, allowing it to decay in SM particles. Models with nucleo-philic or lepto-philic mediators are particularly appealing for direct detection, since one can think of possible renormalizable operators coupling them to

the SM, thus leading to bounds on the mediator itself, along with its astrophysical bounds, which will be the scope of this thesis work (Chapter 6).

Overproduction of sub-GeV DM and mediators

In Sections 2.2 and 2.3 we have discussed how the freeze-out process of thermal DM sets the DM relic density. If we now suppose that DM is composed by a light fermion χ (we are thinking to m_χ below the EW scale), a condition that ensures the stability of DM is that χ has a conserved charge, coming from whatever symmetry. For a thermal model, we need to ensure that χ has some form of interactions with the SM[1]. Clearly, the presence of a symmetry leads us to consider only annihilation processes $\chi\overline{\chi} \to SM\,SM$, and we assume weak interactions (or weaker), so that the coupling is at most G_F. We are now going to show that these considerations for light thermal DM inevitably lead to an overabundance in its relic density (as shown in Ref. [9]).

In fact, we have seen in Sections 2.1 and 2.2 that cosmological structure formation forbids hot thermal relics, thus we want to study the freeze-out process when χ is already non-relativistic. In this framework, the thermal averaged cross section can be written as

$$\langle \sigma v \rangle \simeq \frac{G_F^2 m_\chi^2}{16\pi}$$

of course we are not considering order one factors, which are not relevant for the discussion. Using the NR equilibrium number density expression

$$n_\chi^{(eq)} = g_\chi \left(\frac{m_\chi T}{2\pi}\right)^{3/2} e^{-m_\chi/T}$$

and remembering that $x \equiv m_\chi/T$, we can find the freeze-out temperature simply by requiring $\Gamma_{ann}(T_{FO}) \simeq H(T_{FO})$. From

$$\Gamma_{ann}(T_{FO}) = n_\chi^{(eq)}(T_{FO})\langle \sigma v \rangle \simeq \frac{\pi}{3\sqrt{10}} \frac{g_*^{1/2}(T_{FO})\, T_{FO}^2}{M_P} = H(T_{FO})$$

The estimate that can be obtained is

$$x_{FO} \simeq 15 + 3\,\log 10 \cdot \log_{10}\left(\frac{m_\chi}{1\,GeV}\right)$$

The Cold DM condition requires $x_{FO} \gg 1$, thus weakly interacting sub-GeV thermal DM can hardly be a cold relic. Moreover, this would lead to an overabundant DM relic density: by employing the fact that $Y_\chi \equiv n_\chi/s$ is constant, we get

$$\Omega_{DM}\, h^2 = \frac{m_\chi Y_\chi(T_{FO}) s_0}{\rho_c(t_0)/h^2}$$

[1]This is not necessary, since DM may thermalize and freeze-out in the dark sector. However, if we hope for a directly detectable model, we cannot prescind some form of interactions with the SM.

Being $s_0 \approx 2890\, cm^{-3}$ and $\rho_c(t_0) \approx 1.05 \cdot 10^{-5}\, h^2\, GeV/cm^3$, we get an estimate

$$\Omega_{DM}\, h^2 = 540 \left(\frac{g_*^{1/2}(T_{FO})}{g_{*s}(T_{FO})}\right) \left(\frac{x_{FO}}{15}\right) \left(\frac{1\, GeV}{m_\chi}\right)^2$$

While the first two parentheses are always factors of order 1 (in particular, the first is order one below EW scale), the relic density is dramatically influenced by the mass of m_χ, and sub-GeV DM is definitely incompatible with $\Omega_{DM}^{(obs)}\, h^2 \approx 0.12$. This makes even more evident why WIMP particles are chosen to have masses definitely above $10\, GeV$.

However, the overabundance could be depleted if there was a new mediator, coupling the DM to the SM (as discussed in detail in Ref. [1]). A DM mediator ϕ can keep DM in thermal equilibrium longer via the processes in Figure 5.1.

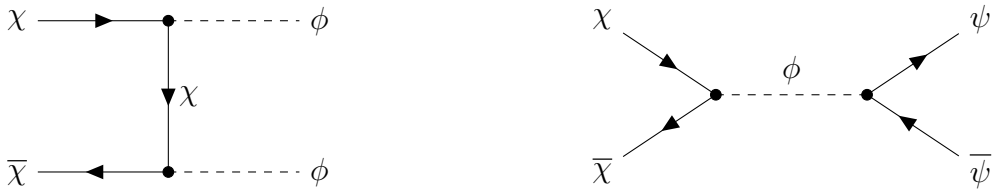

Figure 5.1: On the left: the t-channel interaction with mediators. On the right: s-channel interaction. ψ is a SM fermion.

In fact ϕ can easily talk with the SM model thanks to renormalizable portal operators. In this thesis work we assume a scenario for a Higgs-portal mechanism (Section 5.2), through which we can easily model ϕ—SM interactions. Then, one can easily engineer the coupling g_χ between χ and ϕ in order for the cross section to reproduce the relic density.

Brief review of scalar mediator landscapes

There is a plethora of models of Dark Matter candidates χ and mediators ϕ, which can produce, depending on the case, bounds from direct detection on Earth, Astrophysics or Cosmology. Having in mind a typical NR direct detection cross section of

$$\sigma_{DD} = \frac{4\pi \alpha_\chi\, \alpha_T}{(m_\phi^2 + \mathbf{q}^2)^2} \mu_{T\chi}^2,$$

where α_χ accounts for $\phi - \chi$ interactions and α_T for $\phi-$target interactions. $\mathbf{q}$ is a typical exchanged momentum in NR elastic scattering and $\mu_{T\chi}$ is the reduced mass for target-DM interactions. For Earth-based direct detection, the typical velocity of DM particles is $v \lesssim 10^{-3}$ (the escape velocity from the Milky Way), thus $\mathbf{q} \lesssim 10^{-3} m_\chi$. Mediators can be thus divided in two main categories:

- **Massive** mediators: If mediators have typical masses $m_\phi \gg |\mathbf{q}|$ (we take as a benchmark value $m_\phi \gg 1\, MeV$), their σ_{DD} is strongly influenced by the mass. In this regime typically scalars are not produced inside stars (could be only during Core-Collapse Supernovae), this does not constrain the $\phi-$SM

interactions, so that α_T can become as large as 10^{-9}. Plugging the numbers, we can write

$$\sigma_{DD}^{massive} = 2 \cdot 10^{-40}\, cm^2 \left(\frac{\alpha_\chi \alpha_T}{10^{-16}}\right) \left(\frac{\mu_{T\chi}}{m_e}\right)^2 \left(\frac{5\, MeV}{m_\phi}\right)^4 .$$

Thus, for massive models, the rate remains quite low, even for large couplings. A mild bound of (as in Ref. [35])

$$\alpha_\chi \lesssim 0.02 \left(\frac{1\, keV}{m_\chi}\right)^{1/2} \left(\frac{m_\phi}{1\, MeV}\right)^2$$

comes from DM self-interactions.

- **Massless** mediators: If we take a massless mediator, with a benchmark momentum transfer in DD experiments of $|\mathbf{q}| \lesssim 1\, MeV$, one has strong constraints from Astrophysics ($\alpha_T \lesssim 10^{-25}$), since scalars would be easily produced in stellar environments. The DD cross section can be parametrized as

$$\sigma_{DD}^{massless} = 1 \cdot 10^{-39}\, cm^2 \left(\frac{\alpha_\chi \alpha_T}{10^{-30}}\right) \left(\frac{\mu_{T\chi}}{m_e}\right)^2 \left(\frac{1\, keV}{|\mathbf{q}|}\right)^4 .$$

Massless mediators would be thus much more easily detectable even with small couplings to DM. However, Massless mediators would be thus much more easily detectable even with small couplings to DM. However, the strongest bound on α_χ is put by DM self-interactions, which in the massless mediator limit become very important:

$$\alpha_\chi \lesssim 6 \cdot 10^{-10} \left(\frac{m_\chi}{1\, MeV}\right)^{3/2} .$$

Clearly, these microscopic details depend, in general, on the microscopic model one assumes for the DM particle (whether it is a scalar or a fermion) and on the mediator portal operators with the SM. Proposed portal operators involve $\overline{L}H$, the hypercharge field $B_{\mu\nu}$ or the Higgs $H^\dagger H$ (the topic of Section 5.2). Depending on the model, one has more nucleo-philic or lepto-philic scalars, which indicate which is the suitable physical system in which to obtain the bounds.

5.2 Higgs-portal mechanism

The portal mechanism assumed in this thesis work assumes that the SM sterile Φ couples with the Higgs doublet H through the most general renormalizable potential:

$$\begin{aligned} \mathcal{V}_{H\Phi} = {} & \mu_H^2 H^\dagger H + \lambda_H (H^\dagger H)^2 \\ & + B_\Phi \Phi + \frac{\mu_\Phi^2}{2}\Phi^2 + \frac{A_\Phi}{6}\Phi^3 + \frac{\lambda_\Phi}{24}\Phi^4 \\ & (A_{\Phi H}\Phi + \frac{\lambda_{\Phi H}}{2}\Phi^2) H^\dagger H \end{aligned} \tag{5.1}$$

Without loss of generality one can assume that Φ does not take a VEV, thus leading to $B_\Phi = -A_{\Phi H} v^2/2$, with v being the EW scale of SSB ($v \approx 246\,GeV$). Parametrizing

$$H = \frac{1}{\sqrt{2}} \begin{pmatrix} 0 \\ v + \widetilde{h} \end{pmatrix},$$

it is a direct computation to show that the mass potential is

$$\mathcal{V}_M = \frac{1}{2} \begin{pmatrix} \widetilde{h} & \Phi \end{pmatrix} \begin{pmatrix} 2\lambda_H v^2 & A_{\Phi H} v \\ A_{\Phi H} v & \mu_\Phi^2 + \dfrac{\lambda_{\Phi H} v^2}{2} \end{pmatrix} \begin{pmatrix} \widetilde{h} \\ \Phi \end{pmatrix}$$

Of course, this lagrangian can be diagonalized in order to remove the mass mixing. Thus, we can choose

$$\begin{pmatrix} \widetilde{h} \\ \Phi \end{pmatrix} = \begin{pmatrix} \cos\theta_c & \sin\theta_c \\ -\sin\theta_c & \cos\theta_c \end{pmatrix} \begin{pmatrix} h \\ \phi \end{pmatrix}, \tag{5.2}$$

so that h is the physical SM Higgs boson with a mass

$$m_h^2 = \frac{1}{2}\left(T + \sqrt{T^2 - 4D}\right)$$

with $T = 2\lambda_H v^2 + \mu_\Phi^2 + \dfrac{\lambda_{\Phi H} v^2}{2}$ and $D = 2\lambda_H v^2(\mu_\Phi^2 + \dfrac{\lambda_{\Phi H} v^2}{2}) - A_{\Phi H}^2 v^2$.

We do not focus on the details of how the θ_c angle depends on the $\mathcal{V}_{H\Phi}$ parameters, but we will use these angles for describing the coupling of the scalar ϕ to the SM. The recipe is quite straightforward: if in the SM something is coupled with the Higgs boson, for example $h\,\overline{\psi}\psi$, to get how the scalar couples to ψ, we simply substitute h with $\widetilde{h}$, since $h\,\overline{\psi}\psi$ comes from something like "$\overline{L}_\psi H \psi$". Finally, one substitutes to $\widetilde{h}$ the $\phi \sin\theta_c$ from Equation 5.2. At a computational level, this means that if the physical Higgs boson has some interaction with coupling g in the SM without Φ, then, when we switch on Φ, the coupling of ϕ to the same operator will be $g \sin\theta_c$.

5.3 Higgs interactions with hadrons

One could naively think that the interactions of the Higgs boson h with hadrons, since the Higgs does not couple to gluons, would be well described by the interaction with constituent light quarks. Thus, one would expect a coupling for processes like $h\overline{N}N$ and $h\pi\pi$ of the order of the Yukawas of light quarks $y_q \simeq 10^{-5}$. However, this is not the case, since Higgs interactions with heavy quarks efficiently produce an effective Higgs-gluon coupling through the triangle diagram(s):

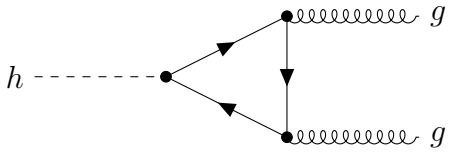

Considering this effective interaction, we can get, with some effort, the effective interactions of the Higgs with hadrons.

Higgs interactions with nucleons

The discussion follows the key passages of Refs. [36] and [37]. Phenomenologically, the Higgs couples to nucleons via

$$\mathcal{L}_{hN} = -\frac{h}{v} \langle N | \sum_h m_h \overline{h} h \, | N \rangle$$

with negligible momentum transfer. The light quarks contributions can be clearly neglected[2]. When we integrate out heavy quarks, we have essentially that, at leading order in a $1/m_h$ heavy quark expansion

$$\sum_h m_h \overline{h} h \to -\frac{2}{3} \frac{\alpha_S}{8\pi} G^a_{\mu\nu} G^{a\,\mu\nu} \tag{5.3}$$

This can be linked to the nucleon masses, since

$$m_N \overline{\psi_N} \psi_N = \langle N | \, \theta^\mu_\mu \, | N \rangle \, .$$

The trace of the energy-momentum tensor in QCD, considering the triangle diagram is

$$\theta^\mu_\mu = m_u \overline{u} u + m_d \overline{d} d + m_s \overline{s} s + \sum_h m_h \overline{h} h + \frac{\beta(\alpha_S)}{4\alpha_S} G^a_{\mu\nu} G^{a\,\mu\nu} \tag{5.4}$$

with $\beta(\alpha_S) = -(9 - \frac{2}{3} n_h) \frac{\alpha_S^2}{2\pi}$.

It is therefore evident that the heavy quark expansion cancels the contribution coming from Equation 5.3 cancels the heavy quark contribution in the gluon term of Equation 5.4. Now, neglecting light quark masses, we simply get:

$$m_N \overline{\psi_N} \psi_N = -9 \frac{\alpha_S}{8\pi} \langle N | \, G^a_{\mu\nu} G^{a\,\mu\nu} \, | N \rangle \, . \tag{5.5}$$

Now, substituting Equations 5.3 and 5.5 in $\mathcal{L}_{hN}$, one gets

$$\mathcal{L}_{hN} = -\frac{h}{v} \frac{2 n_h}{27} m_N \overline{\psi_N} \psi_N . \tag{5.6}$$

We will call y_{hN} the quantity

$$y_{hN} \equiv \frac{2 n_h}{27} \frac{m_N}{v} \approx 8.4 \cdot 10^{-4}$$

which will be our effective Higgs-nucleon coupling. As we have seen this is almost two orders of magnitude more than what we would have predicted from the light quark Yukawas. We finally comment the fact that, neglecting the light quark masses, the nucleon interaction with the Higgs boson has an isospin symmetry, as expected since quark masses are the source of isospin symmetry breaking.

[2] The strange quark is neither too heavy nor too light, so our assumption to consider it light is somewhat arbitrary.

Higgs interactions with pions

This discussion follows the key passages of Ref. [38]. In the SM a single Higgs boson couples to a certain operator as

$$\mathcal{L}_{eff} = \frac{h}{v} m \frac{\partial \mathcal{L}}{\partial m}$$

with m being the mass of a certain field in $\mathcal{L}$. The effect of light quarks on Higgs-pion coupling is easy to compute: taking the quark mass term (see also A)

$$\frac{B f_\pi^2}{2} \operatorname{Tr}\{M(\Sigma^\dagger + \Sigma)\} \tag{5.7}$$

and applying the recipe this leads to

$$\mathcal{L}_{eff,light} = \frac{B f_\pi^2}{2} \frac{h}{v} \operatorname{Tr}\{M(\Sigma^\dagger + \Sigma)\}. \tag{5.8}$$

The heavy quark contribution is evaluated in an EFT fashion, by employing that

$$m_h \frac{\partial}{\partial m_h} = m_h \frac{\partial \alpha_S}{\partial m_h} \frac{\partial}{\partial \alpha_S} + m_h \frac{\partial m_l}{\partial m_h} \frac{\partial}{\partial m_l}.$$

At leading order in perturbation theory, we have that the RG evolution of α_S is

$$\frac{6\pi}{\alpha_S(\mu)} = 3b \log \frac{\mu}{\Lambda_{QCD}} - 2 \sum_h \Theta(\mu - m_h) \log \frac{\mu}{m_h} + O(\alpha_S(\mu))$$

while the light quark evolution with respect to m_h is of order α_S^2. Performing explicitly the computation, one gets at leading order in perturbation theory

$$m_h \frac{\partial}{\partial m_h} = \frac{2}{3b} \Lambda_{QCD} \frac{\partial}{\partial \Lambda_{QCD}}.$$

Finally, by NDA, the χPT parameters f_π and B must be proportional to the only energy scale relevant to the process, thus Λ_{QCD}. This means that (for $\mathcal{L}_\chi$ as in Equation 1.7)

$$\Lambda_{QCD} \frac{\partial \mathcal{L}_\chi}{\partial \Lambda_{QCD}} = f_\pi \frac{\partial \mathcal{L}_\chi}{\partial f_\pi} + B \frac{\partial \mathcal{L}_\chi}{\partial B}.$$

An explicit calculation, leads to the final result:

$$\mathcal{L}_{eff,heavy} = \frac{2 n_h}{3b} \left[\frac{h}{v} \frac{2 f_\pi^2}{4} \operatorname{Tr}\{\partial_\mu \Sigma^\dagger \, \partial^\mu \Sigma\} + \frac{3 B f_\pi^2}{2} \frac{h}{v} \operatorname{Tr}\{M(\Sigma^\dagger + \Sigma)\} \right],$$

to which we add the light quarks contribution in Equation 5.8, obtaining

$$\mathcal{L}_{h\pi} = \frac{n_h}{3b} \frac{h}{v} f_\pi^2 \operatorname{Tr}\{\partial_\mu \Sigma^\dagger \, \partial^\mu \Sigma\} + \frac{B f_\pi^2}{2} \frac{h}{v} (1 + 2 \frac{n_h}{b}) \operatorname{Tr}\{M(\Sigma^\dagger + \Sigma)\}. \tag{5.9}$$

From this lagrangian any amplitude concerning *one* Higgs boson coupling with an even number of pions (for parity invariance), thus this is an interesting and powerful result.

Explicit result for the DM mediator ϕ interacting with the pions

Following the recipe exposed in Section 5.2, we can explicitly find the interactions of the DM scalar mediator ϕ with the pions from the lagrangian $\mathcal{L}_{h\pi}$ (Equation 5.9), simply by substituting the h with $\phi \sin\theta_c$.

If we now want to extract the $h\pi^a\pi^a$ interaction, we would need to expand $\Sigma = \exp\{i\pi^a\sigma^a\}$[3] in order to get two pionic fields, thus at first order in the kinetic-like term and at second order in the mass-like term.

From the first term, we get

$$\mathcal{L}^{(1)}_{\phi\pi\pi} = \frac{n_h}{3b}\frac{\phi \sin\theta_c}{v} 2\partial_\mu\pi^a\,\partial^\mu\pi^a.$$

Integrating by parts twice, it becomes

$$\mathcal{L}^{(1)}_{\phi\pi\pi} = \frac{2n_h}{3b}\frac{\sin\theta_c}{v}\left[\frac{1}{2}\pi^a\pi^a\Box\phi - \phi\pi^a\Box\pi^a\right]$$

Acting with the equations of motion:

$$\mathcal{L}^{(1)}_{\phi\pi\pi} = \frac{2n_h}{3b}\frac{\sin\theta_c}{v}\phi\pi^a\pi^a\left[-\frac{1}{2}m_\phi^2 + m_\pi^2\right]$$

For the other term, by the definition of pion masses in Appendix A, one gets:

$$\mathcal{L}^{(2)}_{\phi\pi\pi} = -\frac{1}{2}\frac{\sin\theta_c}{v}(1 + 2\frac{n_h}{b})\, m_\pi^2\phi\pi^a\pi^a.$$

Putting all together and plugging the values $n_h = 3$ and $b = 11 - 2n_l/3 = 9$, one gets

$$\mathcal{L}_{\phi\pi\pi} = -\frac{1}{9v}\left(m_\phi^2 + \frac{11}{2}m_\pi^2\right)\phi\sin\theta_c\left(\pi_0^2 + 2\pi^+\pi^-\right). \tag{5.10}$$

[3]For the sake of simplicity, for our scopes we show the result for $N_f = 2$.

Chapter 6

Supernova emission of CP-even scalars

In this Chapter we will apply the considerations of Chapters 4 and 5 about the scenario in which a DM mediator CP-even scalar ϕ, coupled to the SM thanks to Higgs-portal operators discussed in detail in Section 5.2, has nucleo-philic couplings coming from the Higgs-nucleon interaction described in Section 5.3. This would imply an efficient production of these scalars in very hot and dense environments, such as a cooling Proto-Neutron Star. We will compare our results with the existing literature, especially with the ones presented in Ref. [3], trying to stress where there is agreement and where we differ.

In Section 6.1 we will discuss the amplitudes relevant for the cooling process $N\,N \to N\,N\,\phi$ (with N being a nucleon) and find an approximate analytic bound, which is possible only in the $m_S \ll T \simeq 30\,MeV$ limit. Then we will show a full numeric bound for a one-zone PNS with only neutrons.

If coupled to the SM, the scalar ϕ may decay through every process which is kinematically allowed and is inherited by the Higgs boson interactions with the SM. General decays in Low-Energy Supernovae will be discussed in Section 6.2. Decays of the scalar which involve photons can be constrained from the gamma rays detected during the SN 1987A event on Earth, as discussed in Section 6.3, and by the extra-galactic photons flux, which is the topic of Section 6.4.

6.1 Production of scalars and cooling bound

As we briefly sketched in Section 4.1 the last phase of the Core-Collapse process is the Kelvin-Helmoltz cooling, in which the PNS radiates the enormous gravitational binding energy lost in the collapse mainly in the form of (anti)neutrinos of all flavors. During this phase, the temperature is about $T \simeq 30\,MeV$ and the nucleon number density is of the order of $n \simeq 10^{38}\,cm^{-3}$, which is of the order of the nuclear density. It is fair to say that the PNS is almost entirely composed of neutrons. Since the nucleon masses are much higher than the temperature, it is reasonable to treat the

nucleons as non-relativistic particles. Moreover, at nuclear densities the Fermi momentum $p_F = (3\pi^2 n)^{1/3} \simeq 300\, MeV$, which is much greater than the temperature, so it seems conceivable to approximately adopt a degenerate gas model. In this scenario, ϕ scalars can be easily produced in nucleon elastic scattering, thanks to both their coupling to nucleons and pions inherited by the Higgs-hadrons interactions (Section 5.3). The relevant diagrams are therefore:

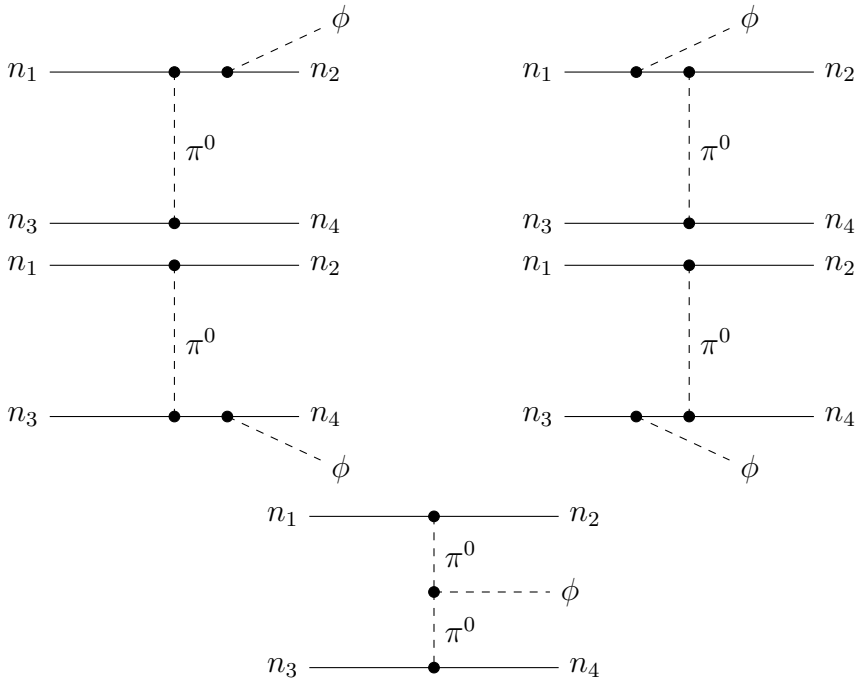

Figure 6.1: Contributing diagrams to $n(p_1)\, n(p_2) \to n(p_3)\, n(p_4)\, \phi(q)$ + exchange diagrams of p_3 and p_4 with a minus sign. Diagrams in which the scalar is emitted from nucleons are called (a) and (b) on the left, (c) and (d) on the right, the one with emission from pions is called (e).

The interaction potential driving the emission is given by Equations A.2, 5.6 and 5.10:

$$\mathcal{L} \supset -i\, f \frac{2m_N}{m_\pi} \pi^a \overline{\psi} \gamma_5 \tau^a \psi \; - \phi \sin\theta_c \left(A_\pi \left(\pi_0^2 + 2\pi^+ \pi^- \right) + y_{hN} \overline{\psi_N} \psi_N \right)$$

For later convenience we call the salar-pions coupling

$$A_\pi \equiv \frac{1}{9v} \left(m_\phi^2 + \frac{11}{2} m_\pi^2 \right).$$

Some considerations about the amplitudes

The matrix elements for $n\, n \to n\, n\, \phi$ are explicitly:

$$M_a = -iG\, y_{hN} \left[\overline{u}(p_3)\frac{i(\not{p}_3 + \not{q} + m_N)}{(p_3+q)^2 - m_N^2}\gamma_5\, u(p_1)\right] \frac{i}{k^2 - m_\pi^2}\, [\overline{u}(p_4)\gamma_5 u(p_2)]$$

$$M_b = -iG\, y_{hN}\, [\overline{u}(p_3)\gamma_5\, u(p_1)]\, \frac{i}{k^2 - m_\pi^2} \left[\overline{u}(p_4)\frac{i(\not{p}_4 + \not{q} + m_N)}{(p_4+q)^2 - m_N^2}\gamma_5 u(p_2)\right]$$

$$M_c = -iG\, y_{hN} \left[\overline{u}(p_3)\gamma_5\frac{i(\not{p}_1 - \not{q} + m_N)}{(p_1-q)^2 - m_N^2}\, u(p_1)\right] \frac{i}{k^2 - m_\pi^2}\, [\overline{u}(p_4)\gamma_5 u(p_2)]$$

$$M_d = -iG\, y_{hN}\, [\overline{u}(p_3)\gamma_5\, u(p_1)]\, \frac{i}{k^2 - m_\pi^2} \left[\overline{u}(p_4)\gamma_5\frac{i(\not{p}_2 - \not{q} + m_N)}{(p_2-q)^2 - m_N^2} u(p_2)\right]$$

$$M_e = -iG\, A_\pi\, [\overline{u}(p_3)\gamma_5 u(p_1)]\, \frac{i}{(k+q)^2 - m_\pi^2}\, \frac{i}{k^2 - m_\pi^2}\, [\overline{u}(p_4)\gamma_5 u(p_2)]$$

with $G = (2m_N/m_\pi)^2\, f^2\, \sin\theta_c$ and $k = p_2 - p_4$. Of course, we have to consider the u-channel exchanging p_3 and p_4, in which a minus sign has to be added: namely $M'_a = -M_a(p_3 \leftrightarrow p_4)$ and so on.

We refer to Appendix D for an explicit expression of the total squared matrix (averaged over ϕ directions in analogy with Equation 4.3 for the axion) in the degenerate and non-relativistic limit. Thereafter, we explicitly show how it compares with previous literature of Refs. [3, 1, 39].

We hereby comment the main differences:

- with Ref. [3]: there is a minor difference concerning the fact that their coupling A_π is

  $$A_\pi^{(BMZ)} = \frac{2}{9v}\left(m_\phi^2 + \frac{11}{2}m_\pi^2\right).$$

  Then, more importantly, they show that in the vanishing limit for the mass of the scalar m_S[1] the square of the sum of the amplitudes concerning emission from nucleonic legs, as their interference term with the diagrams concerning emission from the pionic propagator, vanish. One can explicitly have a confirmation of this fact in their Eq. A.15 and their Fig. 2. In Appendix D we show that this is definitely not true and their result comes from a non consistent NR expansion of the nucleon legs propagators in the emission by nucleons.

- with Ref. [39], which is the result then used in Eq. 34 of Ref. [1]: they do not consider emission from nucleon propagators, even though *a posteriori* one could not neglect it. Then, only the term in their squared amplitude going as E_S^{-2} agrees with ours, while the other (without an explicit E_S dependence) is different. Quite strangely, they do not use this last piece for computing their emissivity (Eqs. 20 and 21 of Ref. [39], reported in Eq. 34 of [1]).

With respect to Ref. [3] ("BMZ"), the important consequence is the fact that BMZ obtain an amplitude such that in the massless scalar limit, the emission from nucleon legs is null. This is not what we get and *a priori* we do not see any symmetry enhancement in sending the mass of the scalar to zero. The interactions of the scalar

[1]For consistency with the literature, we will often call the scalar ϕ also S.

with nucleons is inherited by the SM Higgs-nucleon interactions through the mixing angle $\sin\theta_c$, which in general does not vanish if m_ϕ does.

Explicit emissivity in the massless limit

In the massless limit, the squared amplitudes fully written in Equations D.1, D.2 and D.3 simplify and we can treat them analytically to get an insight about the results, before passing to fully numeric evaluations.

Bare pionic emission

We start from the pure pion emission amplitude (squared) I_π:

$$I_\pi(k,l,E_S) = 4A_\pi^2\left[\frac{\mathbf{k}^4}{(\mathbf{k}^2+m_\pi^2)^4}+\frac{\mathbf{l}^4}{(\mathbf{l}^2+m_\pi^2)^4}+\frac{\mathbf{k}^2\mathbf{l}^2}{(\mathbf{k}^2+m_\pi^2)^2(\mathbf{l}^2+m_\pi^2)^2}\right]$$

We can now pass to compute the emissivity (see Appendix B and, in particular, B.1) remebering that, for $\mathcal{M}$ a function only of k, l and E_S,

$$\dot\epsilon = \frac{SG^2}{8(2\pi)^8}\frac{T^3}{m_N\,p_F}\int_0^{+\infty} dE_S\,E_S^2F(E_S/T)\int_{K^2+l^2\le 4p_F^2} dk\,dl\,\frac{2m_N}{\sqrt{1-\dfrac{k^2+l^2}{4p_F^2}}}\,|\mathcal{M}|^2$$

with $F(\omega/T)=\dfrac{\omega}{6T^3}\dfrac{4\pi^2T^2+\omega^2}{e^{\omega/T}-1}$.

Plugging explicitly $|\mathcal{M}|^2 = G^2I_\pi$, in the approximation in which the mixed term in $\mathbf{k}$ and $\mathbf{l}$ is equal to the other two (which must evidently be equal to each other), we get an analytic expression ($y_\pi = m_\pi/2p_F$):

$$\dot\epsilon_\pi = \frac{SG^2}{(2\pi)^8}T^6\,p_F\left(\frac{11}{9v_{EW}}\right)^2\frac{124\pi^6}{6\cdot 315}\cdot\frac{\pi}{32}\left[\frac{y_\pi^2(1-3y_\pi^2)(y_\pi^2+3)}{(y_\pi^2+1)^3}+3y_\pi\arctan\frac{1}{y_\pi}\right] \quad (6.1)$$

Interference term

In this case the dependence of the squared amplitude on the energies and momenta is the same as for I_π. Namely,

$$I_{int} = -\frac{16}{3}A_\pi\,y_{hNN}\frac{m_\pi^2}{m_N}\left[\frac{\mathbf{k}^4}{(\mathbf{k}^2+m_\pi^2)^4}+\frac{\mathbf{l}^4}{(\mathbf{l}^2+m_\pi^2)^4}+\frac{\mathbf{k}^2\mathbf{l}^2}{(\mathbf{k}^2+m_\pi^2)^2(\mathbf{l}^2+m_\pi^2)^2}\right]$$

Thus, using the computation for $\dot\epsilon_\pi$

$$\dot\epsilon_{int} = -\frac{SG^2}{(2\pi)^8}T^6\,p_F\left(\frac{176}{54v_{EW}m_N}\right)y_{hNN}\frac{124\pi^6}{6\cdot 315}\cdot\frac{\pi}{32}\left[\frac{y_\pi^2(1-3y_\pi^2)(y_\pi^2+3)}{(y_\pi^2+1)^3}+3y_\pi\arctan\frac{1}{y_\pi}\right] \quad (6.2)$$

Bare nucleonic emission

In the case of emission from nucleons, we can write $I_N = I_S + I_0 + I_2 + I_4$.

- I_S terms have a E_S^{-2} explicit dependence, which is an interesting feature of our model, that for masses $m_S \ll T$ makes the emission spectrum non-thermal (we discuss it in Appendix E). In this case, (notice that we are using adimensional k and l)

$$I_S = \frac{16}{15E_S^2} y_{hNN}^2 \left(\frac{2p_F}{m_N^4}\right)^4 \left[\frac{k^2l^2(k^4+l^4+k^2l^2)}{(k^2+y_\pi^2)^2(l^2+y_\pi^2)^2}\, y_\pi^4 + \frac{3k^4l^4(k^2+l^2)}{(k^2+y_\pi^2)^2(l^2+y_\pi^2)^2}\, y_\pi^2 + \frac{3k^6l^6}{(k^2+y_\pi^2)^2(l^2+y_\pi^2)^2}\right] \tag{6.3}$$

  In this case it is noticeable that the energy dependence changes! The only analytic result can be obtained in the limit $y_\pi \to 0$, which is nevertheless a good assumption in a PNS ($y_\pi \simeq 0.24$):

$$\dot{\epsilon}_S = \frac{SG^2}{(2\pi)^8} \frac{16}{5} y_{hNN}^2\, T^4\, p_F \left(\frac{2p_F}{m_N}\right)^4 \frac{11\pi^4}{90} \frac{\pi}{30} \tag{6.4}$$

- I_0 is a term that explicitly goes as $E_S^0 m_\pi^0$:

$$I_0 = \frac{16}{15} \frac{y_{hNN}^2}{m_N^2} \left[\frac{k^8}{(k^8+y_\pi^2)^4} - \frac{k^4l^4}{(k^2+y_\pi^2)^2(l^2+y_\pi^2)^2} + \frac{l^8}{(l^2+y_\pi^2)^4}\right]$$

  This can be integrated analytically as usual assuming that the mixed term is equal to the other two "unmixed":

$$\dot{\epsilon}_0 = \frac{SG^2}{(2\pi)^8} \frac{16}{15} \frac{y_{hNN}^2}{m_N^2}\, T^6\, p_F\, \frac{124\pi^6}{6\cdot 315} \frac{\pi}{96} \left[\frac{105y_\pi^6 + 280y_\pi^4 + 221y_\pi^2 + 48}{(y_\pi^2+1)^3} - 105y_\pi \arctan\frac{1}{y_\pi}\right] \tag{6.5}$$

- I_2 can be written as

$$I_2 = \frac{16}{15} \frac{y_{hNN}^2}{m_N^2}\, y_\pi^2 \left[\frac{2k^6}{(k^2+y_\pi^2)^4} - \frac{k^4l^2+k^2l^4}{(k^2+y_\pi^2)^2(l^2+y_\pi^2)^2} + \frac{2l^4}{(l^2+y_\pi^2)^4}\right]$$

  Thus, as usual, assuming the mixed term behaves as the others

$$\dot{\epsilon}_2 = \frac{SG^2}{(2\pi)^8} \frac{16}{15} \frac{y_{hNN}^2}{m_N^2}\, T^6\, p_F\, \frac{124\pi^6}{6\cdot 315} \frac{5\pi}{16} \left[y_\pi \arctan\frac{1}{y_\pi} - \frac{15y_\pi^6 + 40y_\pi^4 + 33y_\pi^2}{15(y_\pi^2+1)^3}\right] \tag{6.6}$$

- $I_4 = \frac{64}{15} \frac{y_{hNN}^2}{m_N^2}\, y_\pi^4 \left[\frac{k^4}{(k^2+y_\pi^2)^4} + \frac{l^4}{(l^2+y_\pi^2)^4}\right]$. So,

$$\dot{\epsilon}_4 = \frac{SG^2}{(2\pi)^8} \frac{64}{15} \frac{y_{hNN}^2}{m_N^2}\, T^6\, p_F\, \frac{124\pi^6}{6\cdot 315} \frac{\pi}{48} \left[\frac{y_\pi^2(1-3y_\pi^2)(y_\pi^2+3)}{(y_\pi^2+1)^3} + 3y_\pi \arctan\frac{1}{y_\pi}\right] \tag{6.7}$$

We can now give the numerical expression for all these pieces, which give benchmark values for the emissivities in the massless limit. For a $T = 30\,MeV$, $p_F = 300\,MeV$ PNS it results in:

$$\begin{aligned}
\dot{\epsilon}_\pi &= 0.11\,\sin^2\theta_c\,MeV^5 \\
\dot{\epsilon}_{int} &= -0.010\,\sin^2\theta_c\,MeV^5 \\
\dot{\epsilon}_S &= 0.38\,\sin^2\theta_c\,MeV^5 \\
\dot{\epsilon}_0 &= 0.047\,\sin^2\theta_c\,MeV^5 \\
\dot{\epsilon}_2 &= -0.013\,\sin^2\theta_c\,MeV^5 \\
\dot{\epsilon}_4 &= 0.015\,\sin^2\theta_c\,MeV^5
\end{aligned} \tag{6.8}$$

Cooling bound

As discussed in Sections 4.1 and 4.2, the neutrino luminosity has been observed to be $L_\nu = (3\text{—}5)\cdot 10^{53}\,erg/s = (1.2\text{—}2)\cdot 10^{38}\,MeV^2$. Thus, adding all the contributions in Equation 6.8, we impose the Raffelt criterion $L_\phi \lesssim L_\nu$, by simply applying the relation between luminosity and emissivity in Equation 4.2. The summation gives

$$\dot{\epsilon}_{tot} = 0.55\sin^2\theta_c\,MeV^5 \tag{6.9}$$

For a one-zone PNS model, we can thus estimate the scalar luminosity as $L_\phi = \dot{\epsilon}_{tot}\frac{4}{3}\pi R_*^3$, with $R_* \sim 10\,km$. The Raffelt criterion then is computed from [2]:

$$0.55\cdot\sin^2\theta_c\frac{4\pi}{3}(5.1\cdot 10^{16})^3\,MeV^2 \lesssim 1.2\cdot 10^{38}\,MeV^2$$

This implies $\sin\theta_c \lesssim 6.2\cdot 10^{-7}$.

If, as in Ref. [3], we considered only the emission from the pionic propagator, we would have obtained an emissivity (which is $\dot{\epsilon}_\pi$) about 5 times lower, which would have implied $\sin\theta_c \lesssim 1.4\cdot 10^{-6}$. We cast back into BMZ result when we use their coupling A_π which is twice as big as ours. Given that $\dot{\epsilon}_\pi \propto A_\pi^2\sin^2\theta_c$, the sine we obtain is precisely BMZ's one: $\sin\theta_c{}^{(BMZ)} \lesssim 7\cdot 10^{-7}$. Hence, for a coincidence of numerical factor, our result is quite similar to BMZ one.

A numeric result, which takes in consideration both the effects of the scalar and the pion masses in the amplitudes and in the phase space, is shown in Figure 6.2.

6.2 Low-Energy Supernovae bound

Core-Collapse SNe (CCSNe) cover wide ranges of energies and luminosities. As briefly discussed in Section 4.1, the SN explosion energy is of the order of 1—2 B. If new degrees of freedom are produced in the PNS, but decay inside the progenitor star, they contribute to the explosion energy, thus their energy deposition may constrain the masses and couplings of the new Physics[3].

[2] We make evident the transformation from km to MeV^{-1}.

[3] For a more detailed discussion we refer to Ref. [5]

To better constrain this scenario, one can use the lowest energy SN cases, called Low-Energy SNe (LESNe). Observationally, they have ^{56}Ni masses of some $10^{-3}\,M_\odot$, are even 100 times dimmer than "normal" CCSNe and 2—3 times slower photospheric expansion velocities. These evidences point out to a SN explosion energy of only $0.1\,B$, as observed for example from the reconstruction of SN1054 (the event that lead to the Crab Nebula), for which we refer to [40].

If the scalar decay products quickly thermalize in the medium when the scalar decays inside the progenitor star, then one could say that all the energy of the scalar contributes to the SN explosion energy, thus, calling E_{mantle} the deposited energy of the scalars in the mantle, one can say that LESNe imply $E_{mantle} \lesssim 0.1\,B$. Explicitly, E_{mantle} can be computed as

$$E_{mantle} = \Delta t \int_{m_S}^{+\infty} dE_S \, \frac{dL_S}{dE_S} \left[\exp\{-R_{NS}/\lambda_S\} - \exp\{-R_*/\lambda_S\} \right]. \tag{6.10}$$

$\Delta t \simeq 3\,s$[4] is approximately the production time of the scalars during the collapse phases, L_S is the luminosity of the scalar (thus related to its production), $R_{NS} \simeq 20\,km$ is the radius of the PNS and $R_* \simeq (3\text{—}100) \cdot 10^{12}\,cm$ is the radius of the progenitor. Some approximations are made, which make our formula differ from Eq. 1 of Ref. [5]. Firstly, the production is assumed as constant in time. Then, we are using a one-zone PNS model, which allows us to neglect where in the PNS the scalar is produced: in the exponential involving R_*, which sets the "probability" that a particle decays inside the progenitor, this can be done quite safely, due to the many orders of magnitude between R_* and R_{NS}; the exponential containing R_{NS}, instead, reminds us that the particle has to decay outside the PNS to enforce the argument. Since, the particle is produced inside the PNS, one should include a geometrical factor in the first exponential of Equation 6.10. However, we do not put it and leave this piece as an approximate benchmark suppression factor.

The term λ_S is the mean free path for decays, thus defined as:

$$\lambda_S \equiv \gamma\beta\tau_S = \frac{\gamma\beta}{\Gamma_S}$$

with $\gamma = E_S/m_S = (1-\beta^2)^{-1/2}$ is the Lorentz boost factor. The total decay rate of the scalar is the sum of many contributions, each of them inherited by the Higgs interactions with the SM through the mixing. We report the main contributions (in the scalar's rest frame) here (for a reference: Ref. [3] Eqs. 3.1-3.5 and Sec. 6.3 of Ref. [41]):

$$\Gamma_0(S \to \gamma\,\gamma) = \frac{\alpha_{em}^2 m_S^3 \sin^2\theta_c}{256\pi^3 v_{EW}^2} \Big| \sum_f N_C^f Q_f^2 A_{1/2}(\tau_f) + A_1(\tau_W) \Big|^2$$

$$\Gamma_0(S \to e^+\,e^-) = \frac{m_S m_e^2 \sin^2\theta_c}{8\pi v_{EW}^2} \left(1 - \frac{4m_e^2}{m_S^2}\right)^{3/2}$$

[4] Which is in the range of the duration of a CCSNe event ($\Delta t \lesssim 10\,s$) and is consistent with Ref. [5].

$$\Gamma_0(S \to \mu^+ \mu^-) = \frac{m_S m_\mu^2 \sin^2\theta_c}{8\pi v_{EW}^2}\left(1 - \frac{4m_\mu^2}{m_S^2}\right)^{3/2}$$

$$\Gamma_0(S \to \pi^a \pi^a) = \frac{\sin^2\theta_c}{27 \cdot 64\pi m_S v_{EW}^2}\left(m_S^2 + \frac{11}{2}m_\pi^2\right)^2\left(1 - \frac{4m_\pi^2}{m_S^2}\right)^{1/2}$$

Note that we have corrected Eqs. 3.4 and 3.5 of Ref. [3] since their A_π is twice as ours.

We have said that the bound we will consider is $E_{mantle} \lesssim 0.1\,B$. The greater is $\sin\theta_c$ (now on, for readability purposes, we will call it s_c), then the grater are the production ($L_S \propto s_c^2$) and the decay rate $\Gamma_S \propto s_c^2$. Therefore, there is an upper bound on s_c at a given mass. However, if s_c increases too much, it may happen that $\lambda_S \lesssim R_{NS}$, then the particles do not release energy in the mantle, since the tend to decay inside the PNS. Thus, it will not be possible to exclude very high values of s_c with this argument. These very high values are however often excluded with rare meson decays and beam dump experiments. Finally, if $\lambda_S \gg R_*$ it is possible to expand both exponentials in Equation 6.10, leading to a much easier to evaluate

$$E_{mantle}^{low} = \Delta t \int_{m_S}^{+\infty} dE_S \frac{dL_S}{dE_S}\frac{R_* \Gamma_S}{\gamma\beta}. \tag{6.11}$$

When new decay channels activate, such as for $m_S > 2m_e$, there is an abrupt increase in Γ_S. So, for the aforementioned reasons the exclusion plot (Figure 6.2) will move downwards, because the scalar is more likely to decay in the progenitor star (since λ_S decreases), but also inside the PNS.

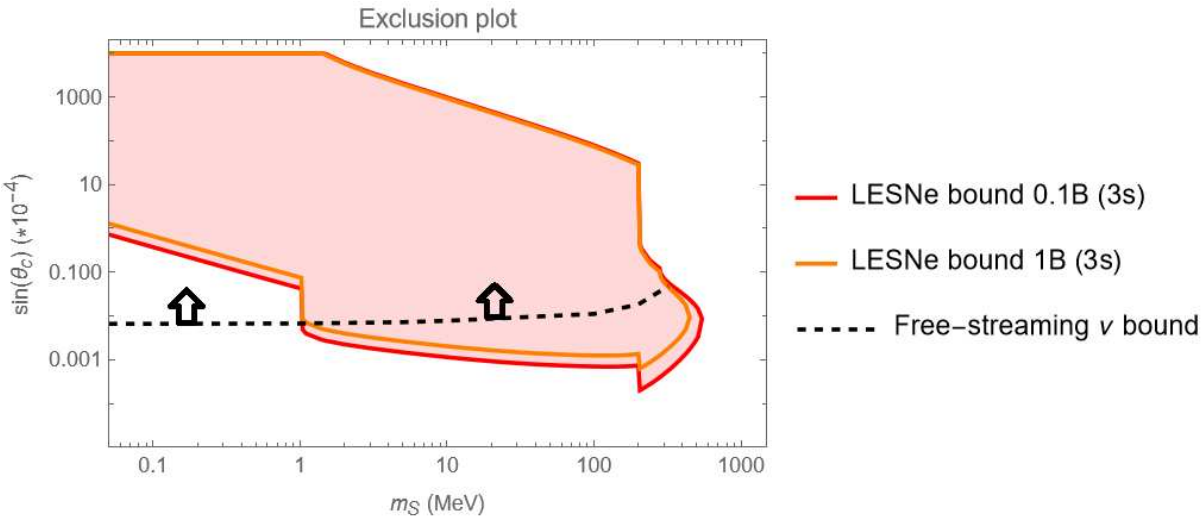

Figure 6.2: Exclusion plot given by LESNe and Raffelt criterium from neutrino luminosity L_ν assuming freely streaming scalars. For the latter, clearly, the excluded region is the upper part.

In the plot right above we truncated by hand the curve of the free-streaming bound (dashed black line) since free-streaming of neutrinos is physically not possible for the region *above* the LESNe excluded zone, for the fact that scalars would decay inside the PNS, thus making it impossible to apply the Raffelt criterium. Clearly this

would be automatically taken into account if one considered decays and trapping when computing L_ϕ.

6.3 Gamma ray bound

If the scalar, once having left the progenitor star, can decay into photons, these could either be detected as gamma rays, if coming from a near-galactic SN event (such as SN1987A), or contribute to the extra-galactic photons background, as discussed in Section 6.4. We hereby follow the discussion of Ref. [42] and apply it to our specific model.

In this Section we consider the bound coming from SN1987A gamma rays. Photons produced in the decay of scalars would have been detected by the Gamma-Ray Spectrometer (GRS) on board of the Solar Maximum Mission (SMM) satellite. The data collected by GRS since the arrival of the first IMB neutrino from SN1987A have been taken for $t_f = 223.2\,s$, after which SMM passed through the South Atlantic radiation anomaly (more details on the background would have been required, so data from photons arrived later are discarded). The collected data acquired from GRS during the $223.2\,s$ are exposed in Table 6.1.

Channel	**Energy band**	**Gamma fluence limits** [cm^{-2}]	
	[MeV]	$10\,s$ [43]	$223.2\,s$ [44]
1	4.1—6.4	0.9	6.11
2	10—25	0.4	1.48
3	25—100	0.6	1.84

Table 6.1: GRS 3σ upper fluence limits for the two indicated time intervals after the arrival of the first neutrino from SN1987A at IMB.

We can study the fluence on Earth of the photons assuming that the scalars are produced on a timescale much shorter than the other relevant timescales (the decay time t_D and $t_{LMC} \equiv R_{LMC}/c$). SN1987A was located in the Large Magellanic Cloud, at a distance of $R_{LMC} = 160\,kpc$ from Earth. Let R_γ be the distance that the photon produced by the (radially propagating) scalar decayed after a distance $R_D = \beta t_D$ has to travel to reach Earth. Elementary geometry sets [5]

$$R_\gamma = \sqrt{R_{LMC}^2 - R_D^2 \sin^2\theta} - R_D \cos\theta$$

with θ being the production angle of the photon in the center of mass. *A priori* we do not know if the scalar decays near the SN ($R_D \ll R_{LMC}$) or near Earth (which is the opposite limit). Calling θ^* the angle of the production of the photon in the center of mass of the scalar, basic special relativity gives

$$\cos\theta = \frac{\beta + \cos\theta^*}{1 + \beta\cos\theta^*}.$$

[5] We are following the steps of Ref. [44].

Then, substituting this expression back in R_γ, one gets that the time delay between the first neutrino arrival and the photon detection is

$$t = \frac{t_D}{\gamma^2(1+\beta\cos\theta^*)} + \left[R_{LMC}^2 - R_D^2\left(1-\left(\frac{\beta+\cos\theta^*}{1+\beta\cos\theta^*}\right)^2\right)\right]^{1/2} - R_{LMC} \quad (6.12)$$

Clearly, this formula gets simplified once $R_D \ll R_{LMC}$, when we remain with the first term only. This is also true if $R_D \simeq \lambda_S \gg R_{LMC}$ (e.g. if $t_D \gtrsim \tau_H$, the Hubble time, $\tau_H \simeq 10\,Gyr$). We assume then that only the first term is relevant. We checked that if $R_D \simeq R_{LMC}$, there is at most an order one factor difference between the whole expression 6.12 and its first term.

Of course, the number of photons decaying between t_D and $t_D + dt_D$ is

$$\frac{dN}{dt_D} = \frac{1}{\gamma\tau_S} e^{-\frac{t_D}{\gamma\tau_S}}.$$

Thus, the number of photons produced per unit time of arrival becomes

$$\frac{dN}{dt} = C_\gamma B_\gamma \frac{\gamma(1+\beta\cos\theta^*)}{\tau_S}\,\exp\left\{-\frac{\gamma(1+\beta\cos\theta^*)\,t}{\tau_S}\right\} \quad (6.13)$$

with B_γ the branching ratio of processes leading to photons and C_γ the number of photons produced in the decay.

We can now interpret the LHS of Equation 6.13 as the flux of photons detected at Earth per unit time, solid angle and CoM energy ω, if we multiply the RHS by the production rate dN_S/dE_S and a normalized distribution $f(\omega, \cos\theta^*)$. Clearly, for $S \to \gamma\,\gamma$ isotropy of the decay and energy-momentum conservation can lead only to

$$f(\omega, \cos\theta^*) = \frac{1}{2}\delta\left(\omega - \frac{m_S}{2}\right).$$

Explicitly,

$$\frac{dF_\gamma}{dt\,d\cos\theta^* d\omega} = \frac{1}{4\pi R_{LMC}^2} C_\gamma B_\gamma \frac{\gamma(1+\beta\cos\theta^*)}{\tau_S}\,\exp\left\{-\frac{\gamma(1+\beta\cos\theta^*)\,t}{\tau_S}\right\}\times$$
$$\times\, f(\omega,\cos\theta^*)\int_{m_S}^{+\infty} dE_S\,\frac{dN_S}{dE_S}\,e^{-R_*/\lambda_S(E_S)}$$

Being E_γ the energy of the emitted photon in the LAB frame, one has $E_\gamma = \gamma(1+\beta\cos\theta^*)\omega$. Thus the delta function becomes accordingly

$$\delta\left(\omega - \frac{m_S}{2}\right) = \delta\left(\frac{E_\gamma}{\gamma(1+\beta\cos\theta^*)} - \frac{m_S}{2}\right)$$

If one integrates the delta in $d\cos\theta^*$, and considers the process $S \to \gamma\,\gamma$, the result obtained is ($C_\gamma = 2$)

$$\frac{dF_\gamma}{dE_\gamma\,dt} = 2\frac{2E_\gamma}{m_S}\Gamma(S\to\gamma\,\gamma)\,e^{-2E_\gamma\,t\,\Gamma_S/m_S}\int dE_S \frac{1}{p_S}\frac{d\Phi_S}{dE_S}\cdot e^{-R_*/\lambda(E_S)} \quad (6.14)$$

where we have defined $\Phi_S \equiv N_S/(4\pi R_{LMC}^2)$.

Finally, integrating this result in dt between 0 and $223.2\,s$ and in dE_γ between the extrema of Channel 3 of Table 6.1: $E_{min} = 25\,MeV$ and $E_{max} = 100\,MeV$. The use of Channel 3 of the GRS detector if justified, as in Sec. V of Ref. [42], by the fact that it leads to more restrictive bounds. Then, for the $S \to \gamma\,\gamma$ process one has[6]

$$F_\gamma(Ch.3) = 2B_{\gamma\gamma} \int_{m_S}^{+\infty} dE_S \, \frac{1}{p_S} \frac{d\Phi_S}{dE_S} \cdot e^{-R_*/\lambda(E_S)} \times \\ \times \int_{E_{min}}^{E_{max}} dE_\gamma \, \Theta\left(\gamma(1+\beta)m_S/2 - E_\gamma\right) \left(1 - \, e^{-2E_\gamma \, t_f \, \Gamma_S/m_S}\right) \tag{6.15}$$

For the produced flux Φ_S I consider a $10\,s$ production from a $20\,km$ neutron star at $T = 30\,MeV$. In the low coupling regime (where we can Taylor expand the exponential of the decays) F_γ becomes, calling $E_D^{max} \equiv \gamma(1+\beta)m_S/2$:

$$F_\gamma(Ch.3) = \frac{4\Gamma(S \to \gamma\,\gamma)\, t_f}{m_S} \int_{m_S}^{+\infty} dE_S \, \frac{1}{p_S} \frac{d\Phi_S}{dE_S} \cdot e^{-R_*/\lambda(E_S)} \int_{E_{min}}^{E_{max}} dE_\gamma \, E_\gamma \, \Theta\left(E_D^{max} - E_\gamma\right) \tag{6.16}$$

We comment an interesting difference between Equation 6.15 and its low coupling version 6.16. The first one scales as $B_{\gamma\gamma}$, while the second as $\Gamma(S \to \gamma\,\gamma)$. This happens because for low couplings the decay time is much longer than the $223\,s$ survey, so effectively most of the scalars are still decaying. Thus, the F_γ becomes $\propto B_{\gamma\gamma}\Gamma_S$, which is always increasing. For example, if the rate doubled due to the activation of new decay channels, even if these new channels are dominant and do not produce photons, naively also the number of scalars decaying doubles, thus leaving the number of photons produced the same (or greater). Instead, if all the scalars decayed before arriving at Earth, it would be important how many scalars *had decayed* into photons, which is governed only by the branching ratio of the process(es).

In our model the decay into two photons is not the only one relevant, since the scalar couples also to electrons and muons, which can produce photons by final state radiation (FSR). A good analysis of the process can be found in Ref. [45]. In particular, considering the differential rate per CoM photon energy in the FSR produced by the decay into electrons

$$\frac{d\Gamma_{FSR}}{d\omega} = \frac{2\alpha_{em}\Gamma(S \to e^+\,e^-)}{\pi\,\omega} \left[1 - 2\lambda_\gamma + (1 - 2\lambda_\gamma + 2\lambda_\gamma^2) \log\left(\frac{1-2\lambda_\gamma}{m_e^2/m_S^2}\right)\right] \tag{6.17}$$

with $\lambda_\gamma = \omega/m_S$. Being $E_\gamma = \gamma(1 + \beta\cos\theta^*)\omega$ the energy in the LAB frame and calling $\chi = \gamma(1 + \beta\cos\theta^*)$, we can write:

$$\frac{dF_\gamma}{dE_\gamma} = \int_{\gamma(1-\beta)}^{\gamma(1+\beta)} \frac{d\chi}{\gamma\beta} \frac{\tau_{TOT}}{\chi} \left(1 - e^{-\chi\, t_f/\tau_{TOT}}\right) \int dE_S \, \frac{d\Phi_S}{dE_S} \frac{1}{2} \frac{d\Gamma_{FSR,e}}{d\omega} \cdot e^{-R_*/\lambda(E_S)}$$

[6] We include the Heaviside Θ due to the fact that energy-momentum conservation constrains the domain of integration in dE_γ.

and

$$\frac{d\Gamma_{FSR}}{d\omega} = \frac{2\alpha_{em}\Gamma_{S\to e^+e^-}}{\pi\, E_\gamma}\left[\chi - 2\lambda + (\chi - 2\lambda + 2\frac{\lambda^2}{\chi})\log\left(\frac{1-2\lambda/\chi}{m_e^2/m_S^2}\right)\right]$$

where $\lambda = E_\gamma/m_S$. We now have to deal with the fact that the logarithm in Equation 6.17 requires $\lambda \leq (1-4m_e^2/m_S^2)\chi/2$ and we ask for the Channel 3 of Table 6.1. Calling $E_{D,FSR}^{max} \equiv \gamma(1+\beta)(1-4m_e^2/m_S^2)\cdot m_S/2$:

$$F_\gamma^{FSR,e} = \int_{m_S}^{+\infty} dE_S\, \frac{d\Phi_S}{dE_S}\frac{1}{2}\cdot e^{-R_*/\lambda(E_S)} \int_{E_{min}}^{E_{max}} dE_\gamma\, \Theta\left(E_{D,FSR}^{max} - E_\gamma\right)\left(1 - e^{-\chi\, t_f\, \Gamma_S}\right)\times$$
$$\times \int_{\gamma(1-\beta)}^{\gamma(1+\beta)} \frac{d\chi}{\gamma\beta}\frac{2\alpha_{em}B_{e^+e^-}}{\pi\, E_\gamma}\left[1 - 2\frac{\lambda}{\chi} + (1 - 2\frac{\lambda}{\chi} + 2\frac{\lambda^2}{\chi^2})\log\left(\frac{1-2\lambda/\chi}{m_e^2/m_S^2}\right)\right] \tag{6.18}$$

With B_i being the branching ratio of the decay channel i. Of course, we get an analogous formula for the final state radiation from muonic legs.

The exclusion plot obtained summing all the contributions ($S \to \gamma\,\gamma$, $S \to e^+\,e^-\,\gamma$ and $S \to \mu^+\,\mu^-\,\gamma$) is shown in Figure 6.3.

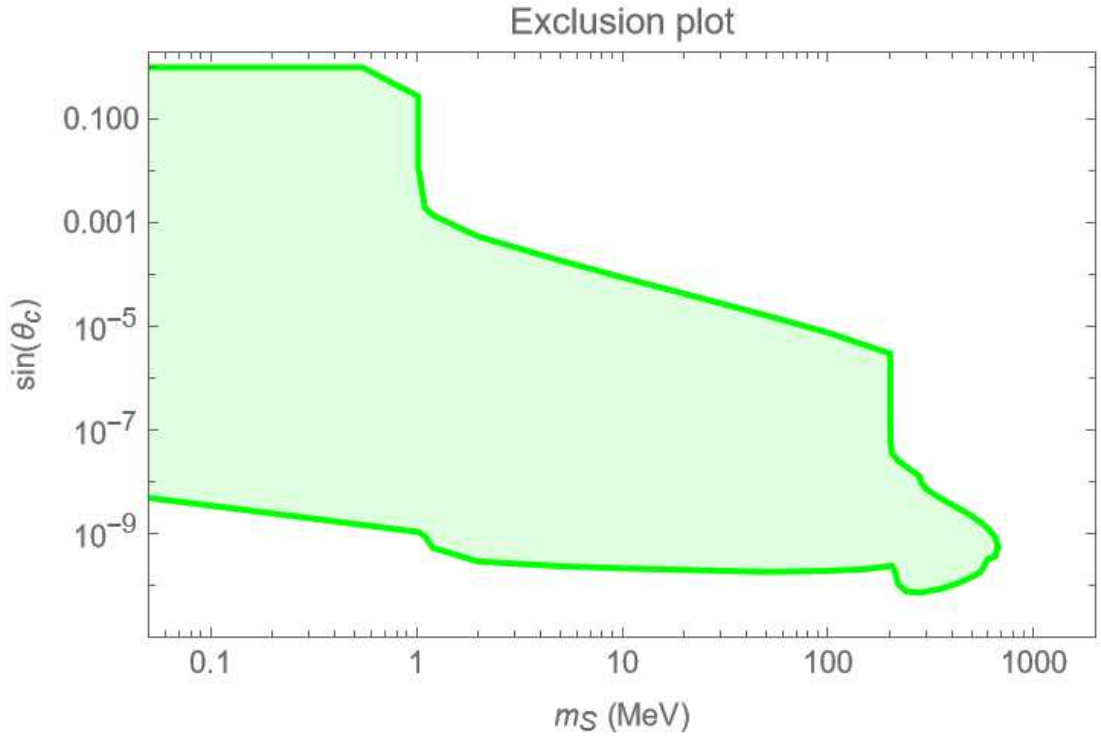

Figure 6.3: Exclusion plot from the Channel 3 of GRS (Table 6.1).

Before passing to a brief analytic interpretation, we clear out what we mean by low coupling. In the low mass limit ($m_S < 2m_e$), the low coupling condition may be rewritten as (remembering $\Gamma_{S\to\gamma\,\gamma} \propto m_S^3 s_c^2$)

$$2\frac{E_{max}}{m_S} t_f \Gamma_S << 1 \Longrightarrow s_C << 10^{-3}$$

This limit is always satisfied in the lower part of the exclusion plot. Practically speaking, linear order expansion of the low coupling regime well-describes the physics. For $m_S \to 0$, the production integral is (almost) independent from m_S and is proportional to s_C^2 and $\Gamma_S \propto m_S^3\, s_C^2$, then, we expect a behaviour like $s_C \propto m_S^{-1/2}$. The descent is milder than in the same regime for the LESNe bound (Figure 6.2), where we have $s_C \propto m_S^{-3/4}$.

Asking that $F_\gamma(25\text{—}100\,MeV) < 1.84\,cm^{-2}$, we analyze the exclusion plot in two possible regimes:

- **Low coupling**: in the low coupling limit we can neglect the exponentials accounting for the decays. Then, increasing the coupling, we increase the production of scalars and their decay into photons. Thus, we expect a decreasing exclusion boundary until $m_S \gtrsim 100\,MeV$, when the production becomes Boltzmann suppressed.
  For $m_S > 2m_e$ the decay channel into electrons activates: very soon the decay of scalars into electrons starts to dominate the total decay width (e.g. $B_{e^+e^-} \approx 10^4 B_{\gamma\gamma}$ already for $m_S = 1.023\,MeV$, that is only $1\,keV$ above the threshold for decay into electrons). However, final state radiation from electrons starts to dominate the flux a few hundredths of keV later than the threshold. The reason why it happens is because in the scalar rest frame the radiated photons takes at most (when the electrons are produced almost at rest) $m_S - 2m_e$, which in the lab frame corresponds to a maximum of $2E_S(1-2m_e/m_S)$ which for $E_S \approx 100\,MeV$ is inside the detection channel for $m_S > 1.15\,MeV$.
  Then, being $\Gamma(S \to e^+e^-) \approx 10^4\Gamma(S \to \gamma\,\gamma)$ slightly above the threshold, we expect that the flux of photons from final state radiation is ~ 100 times higher than the one from the decay into photons, since the flux goes as $\alpha_{em}\Gamma_{S\to e^+e^-}$. This creates a smooth jump for the sine which becomes very broadly speaking $100^{1/4} \sim 3$ times lower, as confirmed by the plot 6.3.
- **High coupling**: in this case we change perspective, since the flux is regulated by the exponential of the decay inside the progenitor star. Thus, the flux decreases when the sine increases, since the particles decay faster. The interpretation in this case is that the curve must be parallel to the curve for the same regime in the LESNe bound. Here, every time a new decay channel activates, the bound has to deminish because we can no more exclude the higher coupling region in which "all" the particles decay in the progenitor. It is therefore natural that in this case the energy released into low energy SNe put a better bound.

6.4 Diffuse photons bound

Radiative decays of scalars emitted in past SN events contribute to the diffuse cosmic gamma-ray background and thus can be constrained by the extra-galactic background light (see Ref. [46]). Following the discussion in Sec. VI of Ref. [42], the differential number density of photons that have accumulated due to scalars emitted

in all past CCSN explosions is

$$\frac{dn_\gamma}{d\omega} = \int_0^{+\infty} dz(1+z)n'_{cc}(z) \int_{m_S}^{+\infty} dE_z\, \Theta\left(\frac{E_z}{2}(1+\beta) - \omega_z\right) f_D(z)\, C_\gamma B_\gamma \frac{dp_\gamma}{d\omega_z}\frac{dN_S}{dE_z} \cdot e^{-\frac{R_*}{\lambda(E_S)}}$$

Here z is the red-shift at which the CCSN event happens, $n'_{cc}(z)$ is the differential number density per red-shift z, $\omega_z = (1+z)\omega$ is the blue-shifted photon energy, E_z is the blue-shifted energy of the scalar and dN_s/dE_z is the production rate per unit energy in the SN at red-shift z. Clearly, the probability to create a photon detected in the energy interval ω and $\omega + d\omega$ is

$$\frac{dp_\gamma}{d\omega}d\omega = \frac{dp_\gamma}{d\omega_z}d\omega_z = (1+z)\frac{dp_\gamma}{d\omega_z}d\omega$$

hence the jacobian factor in front of $n'_{cc}(z)$. Calling ω^* the energy of the photon in the center of mass for the scalar, one simply gets $\omega_z = \gamma(1+\beta\cos\theta^*)\omega^*$. Thus, for the process $S \to \gamma\,\gamma$ one has $C_\gamma = 2$ and

$$\begin{aligned}\frac{dp_\gamma}{d\omega_z} &= \int_{-1}^{1} d\cos\theta^* \frac{dp_\gamma}{d\omega^* d\cos\theta^*}\frac{d\omega^*}{d\omega_z} \\ &= \int_{-1}^{1} d\cos\theta^* \frac{1}{2}\delta(\omega^* - m_S/2)\frac{1}{\gamma(1+\beta\cos\theta^*)} \\ &= \frac{1}{E_z}\frac{1}{\sqrt{\beta^2 - (1-2\omega_z/E_z)^2}}\end{aligned}$$

Finally $f_D(z)$ takes into account the probability that a scalar produced by a CC event at red-shift z has now decayed. Practically speaking, f_D is 1 if the scalar lifetime is much less than the Hubble time $H^{-1} \simeq 10\,Gyr$ (order of magnitude). In our range of interest for $\sin\theta_c$, which spans down to 10^{-9}, we cannot always assume it (only for masses below the MeV).

The factor $f_D(z)$ is

$$f_D(z) = 1 - \exp\left\{-\int_0^z dz_D\, \frac{t'(z_D)}{\tau_S}\frac{m_S}{E_S(z_D)}\right\}$$

with the last quotient being the boost factor with

$$E_S(z_D) = E_S\frac{1+z_D}{1+z}.$$

To be clear z is the red-shift at which a scalar with energy E_S has been produced. Its energy now, if it had not decayed, would be $E_S/(1+z)$. z_D is the red-shift at which the scalar decays. The expression for $f_D(z)$ can be written as

$$f_D(z) = 1 - \exp\left\{-(1+z)\int_0^z dz_D\, \frac{1}{\tau_S}\frac{m_S}{E_z}g(z_D)\right\}$$

with

$$g(z_D) = \frac{1}{(1+z_D)^2}\frac{1}{H_0}\left(\Omega_M(1+z_D)^3 + \Omega_\Lambda\right)^{-1/2}.$$

So, if the lifetime of the scalar is not negligible with respect to τ_H, one has to deal with the cosmological history between the SN event and the eventual decay. Clearly, $\Omega_M = 0.32$ and $\Omega_\Lambda = 0.68$ are the nowadays contributions respectively of matter and Dark Energy. We do not consider other contributions since CCSNe events, being the spectacular end of massive stars, may happen only in Matter (or DE) dominated epochs.

Instead, for the $S \to e^+ e^- \gamma$ final state radiation processes for electrons (equivalently for the muons), we have instead $C_\gamma = 1$ (at leading order in perturbation theory) and

$$\frac{dn_\gamma}{d\omega} = \int_0^{+\infty} dz(1+z) n'_{cc}(z) \int_{m_S}^{+\infty} dE_S \int_{\gamma(1-\beta)}^{\gamma(1+\beta)} \frac{d\chi}{\gamma\beta}\, \Theta\left(\frac{m_S}{2}\left(1-\frac{4m_e^2}{m_S^2}\right) - \frac{\omega_z}{\chi}\right) \times f_D(z)\, B_{e^+e^-}\, \frac{dp_\gamma}{d\omega_z d\cos\theta^*} \frac{dN_S}{dE_S} \cdot e^{-R_*/\lambda(E_S)}$$

with χ defined as in Eq. 49 ($\chi = \gamma(1+\beta\cos\theta^*)$). The factor 2 which in Eq. 56 was before B_γ now of course disappears because we produce, at leading order in perturbation theory, only one electron. Finally, repeating the same argument as before,

$$, \frac{dp_\gamma}{d\omega_z d\cos\theta^*} = \frac{dp_\gamma}{d\omega^* d\cos\theta^*}\frac{d\omega^*}{d\omega_z}$$
$$= \frac{1}{2}\frac{2\alpha_{em}}{\pi\omega^*}\left(1 - 2\frac{\omega^*}{m_S} + (1 - 2\frac{\omega^*}{m_S} + 2(\frac{\omega^*}{m_S})^2)\log\left(\frac{1-2\omega_z/(\chi m_S)}{m_e^2/m_S^2}\right)\right)\frac{1}{\gamma(1+\beta\cos\theta^*)}$$
$$= \frac{1}{2}\frac{2\alpha_{em}}{\pi\omega_z}\left(1 - 2\frac{\omega_z}{\chi m_S} + (1 - 2\frac{\omega_z}{\chi m_S} + 2(\frac{\omega_z}{\chi m_S})^2)\log\left(\frac{1-2\omega_z/(\chi m_S)}{m_e^2/m_S^2}\right)\right).$$

Cosmic core-collapse rate

The cosmic CC density we need $n'_{cc}(z)$ is usually parametrized as

$$n'_{cc}(z) = k_{cc}\dot{\rho}_*(z)t'(z).$$

The factor $\dot{\rho}_*(z)$ is the star formation rate, which is a much explored topic in the literature (Refs. [47, 48, 49, 50]). The value of k_{cc} is well-explained in Eq. 39 of Ref. [51]: $k_{cc} \simeq (135\, M_\odot)^{-1}$. A plot with our $n'_{cc}(z)$ can be found in Fig. 9 of Ref. [42]. For our scopes, we approximate the CC density rate of function of Yüksel *et al.* (Ref. [47]) as a Dirac delta in $z = 1$. Explicitly:

$$n'_{cc}(z) \simeq 1.05 \cdot 10^7\, Mpc^{-3}\, \delta(z-1).$$

Looking at Fig. 9 of Ref. [42], it is quite evident that using different n'_{cc} profiles we do not get more than an order one factor difference, so we stick with our approximation.

Numerical bound

What is observed by Ackermann *et al.* in Ref. [46] is that the extra-galactic flux between $\omega = 2\, MeV$ and $200\, MeV$ has approximately a ω^{-2} dependence, such that

$$\omega^2 \frac{d\Phi_\gamma}{d\omega} \simeq 2 \cdot 10^{-3}\, MeV\, cm^{-2}\, s^{-1}\, ster^{-1}.$$

To pass from $dn_\gamma/d\omega$ we had computed to $d\Phi_\gamma/d\omega$ we clearly have to multiply by c and divide by the total solid angle 4π.

Keeping all this in mind we can compute the differential flux and compare with observations. Thus, we will span over photon energies ω in the (2—200) MeV range and require

$$\omega^2 \frac{d\Phi_\gamma}{d\omega}\bigg|_{max} \lesssim 2 \cdot 10^{-3}\, MeV\, cm^{-2}\, s^{-1}\, ster^{-1}$$

The obtained exclusion plot is shown in Figure 6.4. It has two main differences with its counterpart of SN1947A gamma rays in Figure 6.3. Firstly, when the decay channel into electrons activates, the production of photons gets much reduced due to the abrupt decrease of $B_{\gamma\gamma}$ (we discussed this fact below Equation 6.16). This happens because passing the MeV scale, the decay rate of the scalar becomes much larger than H_0. The second main difference, related to the first one, concerns the fact the the exclusion plot closes itself when the decay channels into muons activate, because of the combined effect leading to a scarce production of photons both for low couplings (i.e. when we neglect the probability the the particle decays in R_*) and for high coupling, when we can no more exclude strongly coupled scalars.

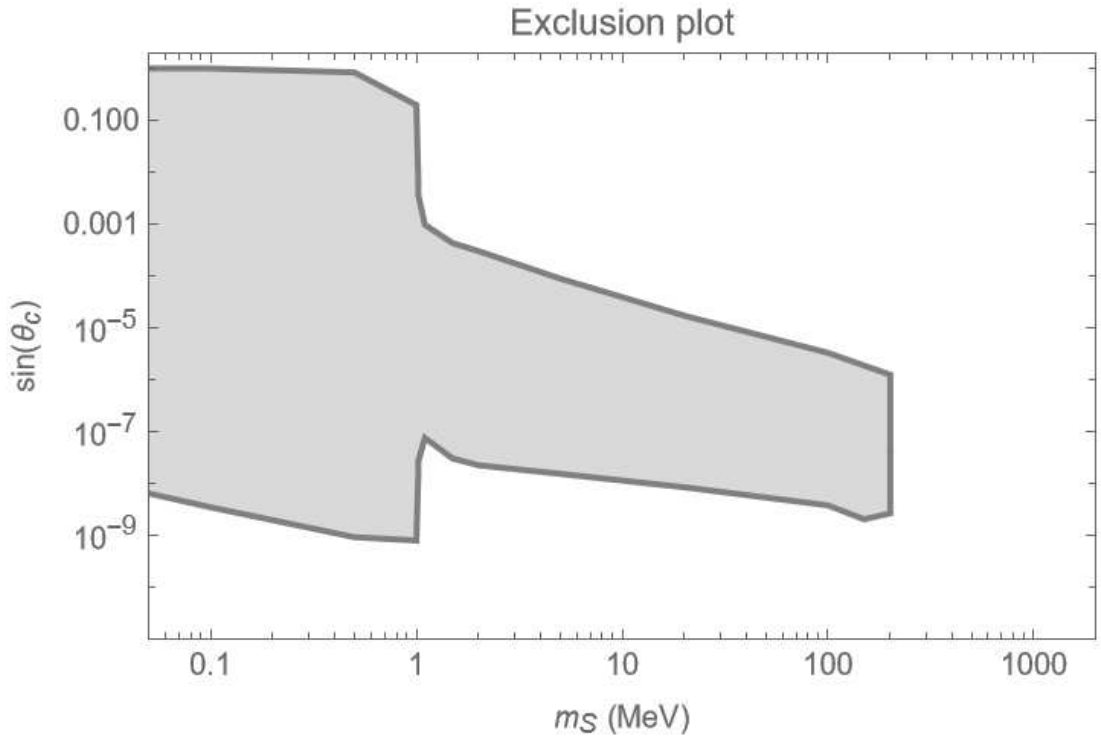

Figure 6.4: Exclusion plot from diffuse cosmic γ background.

As a final comment we notice that below the MeV scale and in the low coupling region, the slope of the excluded boundary is decreasing. Often in the literature the lower part of the plot is basically constant, as in Fig. 2 of Ref. [5]. This must straightforwardly happen if the particle has a decay rate much greater than H_0, since the factor $f_D(z)$ can be taken as 1, so basically the flux Φ_γ can depend only on the production rate dN_S/dE_Z, which is basically constant in m_S when $m_S \ll T$.

If, however, as in our case, one has that for low masses the decay time is greater than τ_H, then the factor $f_D(z)$ becomes

$$f_D(z) \simeq (1+z)\frac{m_S\,\Gamma_S}{E_z}\int_0^z dz_D\, g(z_D).$$

Of course, in this limit, $\Gamma_S = \Gamma(S \to \gamma\,\gamma)$ so that the exclusion condition implies $s_C \propto m_S^{-1}$ in this region.

Instead, when the decay into electrons is dominant, which is immediately above the threshold $m_S > 2m_e$, it is safe to say that all the scalars decay within the Hubble time, hence making the exclusion plot a combination of the effects of the branching ratios into photons (very broadly speaking $B_\gamma \simeq B_{\gamma\gamma} + \alpha_{em} B_{e^+e^-}$) and, for masses above the temperature scale $T = 30\,MeV$, of the thermal Boltzmann suppression. Below $30\,MeV$ we can say that we expect first an abrupt increase in $\sin\theta_c$ because of the suppressed B_γ, which afterward increases slowly again, as one can appreciate in the lower part of Figure 6.4.

Conclusions

We have seen in Chapter 5 that thanks to the Higgs-portal mechanism, our scalar couples to every operator to which the SM Higgs boson h is coupled and the only new parameter added is $s_C \equiv \sin\theta_C$. Thus, the lagrangian that has been used to study the production of scalars in CCSNe is given by

$$\mathcal{L} \supset -i\, f \frac{2m_N}{m_\pi} \pi^a \overline{\psi} \gamma_5 \tau^a \psi \; - \phi \sin\theta_c \left(A_\pi \left(\pi_0^2 + 2\pi^+\pi^- \right) + y_{hN} \overline{\psi_N} \psi_N \right).$$

From this lagrangian, we have computed the luminosity of ϕ emission and, imposing the Raffelt criterion $L_\phi \lesssim L_\nu$, we numerically got that at low masses (w.r.t. the temperature $T \simeq 30\, MeV$)

$$s_C \lesssim 6.6 \cdot 10^{-7}$$

which is equal to the bound in Ref. [3], only because of a coincidence of factors ≈ 2 which cancel out, as we have interpreted in Section 6.1.

However, thanks to the fact that decays of the scalar may produce photons, we can push the bound even further low to $s_C \lesssim 10^{-9}$ or even 10^{-10} (for masses above the MeV) thanks to the SN1987A photons detected by GRS a few seconds after the arrival of the first neutrino at the IMB detector (Section 6.2) and the extra-galactic photon flux measured by Ackermann *et al.* in Ref. [46], which can be constrained in both cases because of the s_C and m_S of the decay rates of the scalar and its production. The bound from all past CCSNe is however less restrictive than its counterpart of "direct" photons from SN1987A, as one can appreciate in Figure 6.5.

The upper part of the plot is better constrained by Low-Energy Supernovae, requiring that decays of the scalar deposit less energy than $0.1\, B = 10^{50}\, erg$ in the progenitor star mantle. Clearly, this bound does not exclude enormous values for s_C, because in this case the scalar may decay already inside the Proto-Neutron star, making the argument moot. However, for these values ϕ would be coupled to the SM comparably with h, leading to constraints from colliders and rare meson decays. For example, as noted in Sec. IV of Ref. [1], the kaon decays $K \to \pi\, \phi$ put a conservative bound $s_C \lesssim 10^{-4}$, which effectively exclude the upper part of Figure 6.5.

Final comments and *desiderata*

All the discussion of Chapter 6 involves a scalar that once created, freely streams away from the PNS and possibly decays. We did not consider the possibility of re-

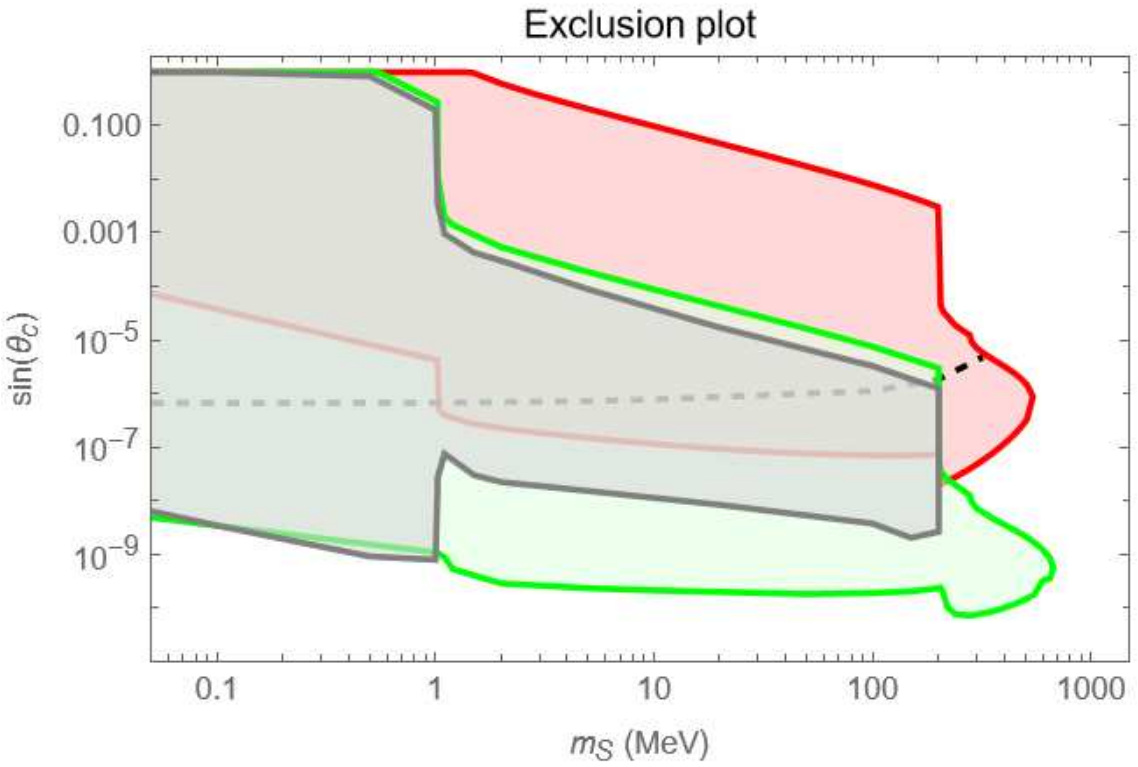

Figure 6.5: Final exclusion plot obtained by freely streaming scalars emitted by a PNS with $T \simeq 30\,MeV$. In dashed black the cooling bound (Sec. 6.1), in red the LESNe bound for $0.1\,B$ deposition (Sec. 6.2), in green gamma rays bound from SN1987A (Sec. 6.3) and in gray the cosmic diffuse γ bound (Sec. 6.4).

absorption, hence eventual trapping, inside the PNS. In practice, this would make impossible that scalars with masses above few T are efficiently produced, because they would more easily decay or be absorbed. To correctly model trapping of scalars, however, one would need more precise SN profiles and more accurate numerics (because in the trapping regime it is relevant where the scalar is produced, so that in this framework the one-zone model we have used is way too approximate), which are beyond the scopes of this thesis work.

Additionally, as pointed out in Ref. [52], decays slightly outside the progenitor star may produce particles that thermalize. This is particularly efficient when the scalar can decay into $e^+\,e^-$ directly, so that a electron-(muon-)photon plasma can be created. The creation of an expanding plasma cools the decay products, thus the energy of photons arriving at Earth (either from SN1987A or past CCSN events). Effectively, this would mean that we should not exclude (or alternatively, we should re-include) suitable values of s_c in the upper part of the green and grey plots in Figure 6.5.

Appendix A

The chiral lagrangian

The chiral lagrangian is the EFT describing QCD at the energies below $\Lambda_{QCD} \sim 1\,GeV$, which is the energy scale at which QCD becomes non-perturbative. Broadly speaking, the picture is that quarks are forced to form bound states which are color singlets, since the gluons must disappear from the theory. This is the nature of confinement and the newly formed particles are the hadrons. Clearly, the QCD lagrangian is impractical at these scales, for which we need an effective theory describing the new degrees of freedom. The idea under this discussion is that the EFT conserves the symmetries of the UV one and this guides us in writing the new lagrangian.

Below the confinement scale Λ_{QCD}, the only relevant d.o.f. are the light quarks (u, d, s) and the QCD lagrangian can be written as

$$\mathcal{L}_{\rm QCD} = -\frac{1}{4} G^a_{\mu\nu} G^{a,\mu\nu} + \bar{\Psi}_L \, i\not{D} \Psi_L + \bar{\Psi}_R \, i\not{D} \Psi_R - \bar{\Psi}_L \, M \, \Psi_R - \bar{\Psi}_R \, M \, \Psi_L \qquad \text{(A.1)}$$

upon defining $D_\mu = \partial_\mu + i g_S \, G^a_\mu \lambda^a / 2$ and

$$\Psi = \begin{pmatrix} u \\ d \\ s \end{pmatrix} \quad \text{and} \quad M = \begin{pmatrix} m_u & 0 & 0 \\ 0 & m_d & 0 \\ 0 & 0 & m_s \end{pmatrix}.$$

For a moment, let us forget about quark masses. If we set $m_q = 0$, $\mathcal{L}_{\rm QCD}$ has a global $U(3)_L \times U(3)_R$ symmetry, called chiral symmetry. The chiral symmetry group can be also written as $SU(3)_V \times SU(3)_A \times U(1)_V \times U(1)_A$. Ψ transforms under the fundamental representation of $SU(3)$ and, *a priori*, any 3×3 hermitian matrix can be taken as generator for each $U(1)$. Vectorial rotations are the ones rotating the L and R components of the same angle, while the axial ones rotate L and R by a different angle: in a compact form:

$$V: \ \Psi \to e^{i\alpha T} \Psi \qquad A: \ \Psi \to e^{i\alpha T \gamma_5} \Psi$$

The Noether currents associated with the symmetry subgroups are:

$$SU(3)_V: \ j^{a\,\mu}_V = \overline{\Psi} \, \gamma^\mu \frac{\lambda^a}{2} \, \Psi \quad SU(3)_A: \ j^{a\,\mu}_A = \overline{\Psi} \, \gamma^\mu \gamma_5 \frac{\lambda^a}{2} \, \Psi$$

$$U(1)_V:\ j_V^{0\,\mu} = \overline{\Psi}\,\gamma^\mu\, X\,\Psi \quad U(1)_A:\ j_A^{0\,\mu} = \overline{\Psi}\,\gamma^\mu\gamma_5\, X'\,\Psi$$

It is well-known that $U(1)_A$ is not a good symmetry at quantum level, since it does not leave invariant the path integral measure (see Chapter 3). Therefore, now on we will ignore it. Vafa and Witten [16] have shown that the vacuum of QCD is necessarily invariant under vectorial transformations, simply because if $|\alpha,+\rangle$ is a state of energy E_α and parity $+1$, then the same is true for $Q_V^{\widetilde{a}}\,|\alpha,+\rangle$[1], and parity is not spontaneously broken in QCD. This implies that $Q_V^{\widetilde{a}}\,|0\rangle = 0$. Instead, the fact that we do not see degenerate hadron multiplets with opposite parities, forces $Q_A^a\,|0\rangle \neq 0$.

One can use Chapter 3.2.2 of [53] as a reference to show that, defining the scalar and pseudoscalar currents

$$S_a \equiv \overline{\Psi}\frac{\lambda^a}{2}\Psi \quad \text{and} \quad P_a \equiv \overline{\Psi}\gamma_5\frac{\lambda^a}{2}\Psi,$$

symmetry arguments and a bit amount of algebra imply $\langle 0|\, S_a(y)\,|0\rangle = 0$. Thus, it is trivial that $\langle\overline{u}u\rangle = \langle\overline{d}d\rangle = \langle\overline{s}s\rangle$. Instead, there is no reason why one should take $\langle\overline{\Psi}\Psi\rangle = 0$, thus we will assume that $\langle\overline{u}u + \overline{d}d + \overline{s}s\rangle \neq 0$, as motivated by pion existence.

In fact, the quark condensate $\langle\overline{\Psi}\Psi\rangle = 0$ breakes $SU(3)_A$, thus implying its spontaneous breaking. It is well-known that the Goldstone bosons associated to the SSB of a broken symmetry may be written (CCWZ formalism) in terms of

$$U(\pi) = \exp\left\{i\frac{\pi^a T^a}{f_\pi}\right\}$$

with T^a being the broken generators. In general, the transformation of $U(\pi)$ under the full group G is complicated and, in particular, non linear. However, if we restrict to transformations only in the unbroken directions, i.e. $h \in H$ where H is the unbroken subgroup of G, the pions transform under the adjoint of H:

$$\pi^a \to h\pi^a h^\dagger.$$

For transformation along broken generators, at linear order the transformation is a shift of the pions $\pi^a \to \pi^a - \alpha^a f_\pi + \dots$. This implies that pions must couple only derivatively!

If, as in the case under study, the coset group is symmetric (i.e. the broken generators X^a algebra closes in the unbroken one T^c, $[X^a, X^b] \propto T^c$), one could instead use the the $\Sigma(\pi) \equiv U(\pi)^2$ realization of the fields, because it has much simpler transformation properties. In terms of our original $SU(3)_L \times SU(3)_R$,

$$\Sigma \to L\Sigma\, R^\dagger$$

To build the kinetic term for pions, we write the easiest invariant under G transformation, canonically normalized, 2-derivatives term, which is

$$\mathcal{L}_\chi = \frac{f_\pi^2}{4}\,\mathrm{Tr}\big\{\partial_\mu\Sigma^\dagger\partial^\mu\Sigma\big\} = \frac{1}{2}\partial_\mu\pi^a\,\partial^\mu\pi^a + \dots$$

[1] As notation, a ranges from 1 to 8, while $\widetilde{a} = 0, \dots, 8$.

In our case, a convenient parametrization for the pion fields is

$$\Sigma = \exp\left\{\frac{i\pi^a\lambda^a}{f_\pi}\right\} = \exp\left\{\begin{pmatrix} \pi^0+\eta/\sqrt{3} & \sqrt{2}\pi^+ & \sqrt{2}K^+ \\ \sqrt{2}\pi^- & -\pi^0+\eta/\sqrt{3} & \sqrt{2}K^0 \\ \sqrt{2}K^- & \sqrt{2}\,\overline{K}^0 & -2\eta/\sqrt{3}\end{pmatrix}\right\}$$

Clearly, the shift symmetry forbids any potential for the pions, which are consequently forced to be massless, as required by Goldstone theorem.

Pion masses

Pions have been observed to be massive, thus we need a mechanism that gives them their mass, trying not to give up to our EFT description.

All the previous results were obtained in the massless quark limit, where the chiral symmetry emerged. In reality quarks have masses, written in the mass matrix M. Quark masses explicitly break the chiral symmetry, but their mass is negligible with respect to Λ_{QCD}, that is when chiral symmetry spontaneously breaks. This is really accurate for the up and down quark masses, while m_s is the same order of the scale f_π coming from the quark condensate. Therefore, the EFT we will derive will be less accurate for mesons containing the strange quark. Quark masses break explicitly $SU(3)_V \times SU(3)_A \times U(1)_V$ in $SU(3)_V \times U(1)_V$ if all the quarks have the same mass, while we remain only with $U(1)_V$ if the quark have different masses. This argument implies that by symmetry if all quarks had the same masses, pions would be all forced to have the same masses.

To write a mass term in the chiral lagrangian, we adopt the spurion field description. This means that we promote the mass matrix M to be a field that has to transform under chiral symmetry in order to leave the QCD lagrangian invariant. Then, after we have written an invariant effective lagrangian, we "remember" that M is just a constant matrix From the term

$$\bar{\Psi}_L\, M\, \Psi_R$$

we evince that M has to transform as $M \to LMR^\dagger$. Thus, the simplest non vanishing invariant mass term for quarks is

$$\mathcal{L}_\chi \supset \frac{B f_\pi^2}{2}\,\mathrm{Tr}\{M\Sigma^\dagger + \Sigma\, M^\dagger\}$$

with B being a dimensional quantities, $[B] = 2$, which has to be determined by experiments.

Finding the quark masses is now a simple exercise:

$$\begin{aligned} m^2(\pi^\pm) &= B(m_u + m_d) \\ m^2(K^\pm) &= B(m_u + m_s) \\ m^2(K^0, \overline{K}^0) &= B(m_d + m_s) \end{aligned}$$

The neutral pion and the the η have a mass mixing, since their generators commute,

$$\mathcal{L}_{mix} = -\frac{B}{2}\begin{pmatrix}\pi^0 & \eta\end{pmatrix}\begin{pmatrix} m_u+m_d & (m_u-m_d)/\sqrt{3} \\ (m_u-m_d)/\sqrt{3} & (m_u+m_d+4m_s)/3\end{pmatrix}\begin{pmatrix}\pi^0 \\ \eta\end{pmatrix}$$

One diagonalizes the matrix and identifies the neutral pion as the lightest mass eigenstate. It is worth noticing that in the $m_u = m_d$ the charged pions $\pi^{\pm}$ and the π^0, have the same mass. This happens because the setting $m_u = m_d$ enhances the symmetries of the system, due to the fact that know there is a $SU(2)$ invariant subgroup of $SU(3)$!

Interaction with nucleons: the OPE potential

For our scopes we are not interested in the most general pion-nucleon lagrangian, starting from first principles (i.e. the chiral symmetry), an approach that can be appreciated in [53]. We want to derive the One-Pion Exchange potential, which is much easier. Now on, In fact, the pions are non-linear realizations of the original chiral symmetry and, restricting to $SU(2)_V$ isospin theory, we can write the nucleon doublet doublet

$$\psi = \begin{pmatrix} p \\ n \end{pmatrix}$$

which quite evidently transforms in in the fundamental of $SU(2)_V$. We know that pions, associated to the broken generators of $SU(2)_A$, must couple derivatively (for shift symmetry) to the broken current. The only possibility to have isospin and Lorentz invariance is a pseudovector coupling of the form:

$$\mathcal{L}_{OPE} = g_{\pi N} \frac{\partial_\mu \pi^a}{f_\pi} \overline{\psi} \gamma^\mu \gamma_5 \tau^a \psi$$

One can simplify the result, since integrating by parts (which leaves invariant the action) and remembering that $\partial_\mu j_A^{a\,\mu} = 2im\overline{\psi}\gamma_5\psi$, one gets

$$\mathcal{L}_{OPE} = -i\, g_{\pi N} \frac{m_N}{f_\pi} \pi^a \overline{\psi} \gamma_5 \tau^a \psi.$$

The parametrization that we use in the main text is

$$\mathcal{L}_{OPE} = -i\, f \frac{2m_N}{m_\pi} \pi^a \overline{\psi} \gamma_5 \tau^a \psi. \tag{A.2}$$

with f, or equivalently $g_{\pi N}$ to be experimentally measured.

Appendix B

Emissivity computations

The emissivity of the scalars is defined as the power of scalar emission in the process $N(p_1)\ N(p_2) \longrightarrow N(p_3)\ N(p_4)\ \phi(q)$ given a thermal bath with temperature T and chemical potential μ

$$\dot{\epsilon} = \int \frac{d^3p_1}{(2\pi)^3\,2E_1}\frac{d^3p_2}{(2\pi)^3\,2E_2}\frac{d^3p_3}{(2\pi)^3\,2E_3}\frac{d^3p_4}{(2\pi)^3\,2E_4}\frac{d^3q}{(2\pi)^3\,2E_s}\cdot S\cdot(2\pi)^4\delta^{(4)}(p_f-p_i)\cdot$$
$$\cdot\,|\mathcal{M}|^2\cdot E_S\cdot f(E_1)\,f(E_2)\,(1-f(E_3))\,(1-f(E_4))$$

Where $f(E_i) = f(E_i;T,\mu) = [\exp\{E_i-\mu/T\}+1]^{-1}$ is the usual distribution function for fermions. S is the symmetry factor associated to eventual identical particles in the initial and final state.
To solve the integral is useful to redefine 3-momenta in the CoM frame:

$$\mathbf{p}_+ = \frac{\mathbf{p}_1+\mathbf{p}_2}{2}\quad \mathbf{p}_- = \frac{\mathbf{p}_1-\mathbf{p}_2}{2}\quad \mathbf{p}_3^* = \mathbf{p}_3-\mathbf{p}_+\quad \mathbf{p}_4^* = \mathbf{p}_4-\mathbf{p}_+$$

Thus, the measure of the integral becomes $8\,d^3p_+\,d^3p_-\,d^3p_3^*\,d^3p_4^*\,d^3q$ and the Dirac delta splits in $\delta(E_1+E_2-E_3-E_4-E_S)\delta^{(3)}(\mathbf{p}_3^*+\mathbf{p}_4^*)$, since the momentum of the scalar in negligible (of order ε). We now have to write the energies in a more convenient way (already assuming $\mathbf{p}_3^*+\mathbf{p}_4^*=0$), by using the non-relativistic limit and defining $u=\mathbf{p}^2/2mT$, $\gamma_1 = \mathbf{p}_+\cdot\mathbf{p}_-/|\mathbf{p}_+||\mathbf{p}_-|$ and $\gamma_c = \mathbf{p}_+\cdot\mathbf{p}_3^*/|\mathbf{p}_+||\mathbf{p}_3^*|$:

$$E_1 = m+\frac{\mathbf{p}_1^2}{2m} = m+T(u_+ + u_- + 2\sqrt{u_+u_-}\gamma_1)$$
$$E_2 = m+\frac{\mathbf{p}_2^2}{2m} = m+T(u_+ + u_- - 2\sqrt{u_+u_-}\gamma_1)$$
$$E_3 = m+\frac{\mathbf{p}_3^2}{2m} = m+T(u_+ + u_3^* + 2\sqrt{u_+u_3^*}\gamma_c)$$
$$E_4 = m+\frac{\mathbf{p}_4^2}{2m} = m+T(u_+ + u_3^* - 2\sqrt{u_+u_3^*}\gamma_c)$$

Now we notice that all the u variables are intrinsically of order ε: therefore, at leading order $E_1E_2E_3E_4$ is is simply m^4. While the energy conservation condition

now reads $E_1 + E_2 - E_3 - E_4 - E_S = 2T(u_- - u_3^*) - E_S$.Putting all together, with the constant matrix element approximation:

$$\begin{aligned}\dot{\epsilon} &= \frac{S|\mathcal{M}|^2}{4(2\pi)^{11}}\frac{4\pi}{m^4}\int d^3p_+\, d^3p_-\, d^3p_3^* \int_{m_S}^{+\infty} dE_S\, E_S\sqrt{E_S^2 - m_S^2} \\ &\quad \times \delta(2T(u_- - u_3^*) - E_S) f(E_1) f(E_2)(1 - f(E_3))(1 - f(E_4)) \\ &= \frac{S|\mathcal{M}|^2}{4(2\pi)^{11}}\frac{4\pi}{m^4}\int d^3p_+\, d^3p_-\, d^3p_3^* \left[2T(u_- - u_3^*)\right] \sqrt{\left[2T(u_- - u_3^*)\right]^2 - m_S^2} \\ &\quad \times f(E_1) f(E_2)(1 - f(E_3))(1 - f(E_4))\end{aligned}$$

of course where we will have the condition $u_- \geq u_3^* - m_S/2T$. Now on, since $m_S \sim O(\varepsilon)$, we will neglect it. Working on the distribution functions, we have that

$$f_i \equiv f(E_i) = \left[\exp\left(\frac{E_i - \mu}{T}\right) + 1\right]^{-1} \simeq \left[\exp\left(\frac{m - \mu}{T}\right)\exp\left(\frac{\mathbf{p}_i^2}{2mT}\right) + 1\right]^{-1}$$

We now call $y = (\mu - m)/T$ and this parameter will govern the behaviour of our system.

Non-degenerate case

The ND case is defined by $y \to -\infty$. In this case

$$f_i = \frac{1}{1 + e^{u_i - y}} \sim e^{y - u_i} \ll 1$$

so that the blocking factors $1 - f_3$ and $1 - f_4$ can be neglected. Moreover, $f_1 f_2 \sim e^{2y - (u_1 + u_2)} \sim e^{2y}\, e^{-2u_+}\, e^{-2u_-}$. Thus, the integrand now does not depend on γ_1 and γ_c: therefore, $d^3p = 2\pi(2mT)^{3/2}u^{1/2}du$. Putting all together

$$\begin{aligned}\dot{\epsilon} &= \frac{S|\mathcal{M}|^2}{4(2\pi)^{11}}\frac{2(2\pi)^4}{m^4}(2mT)^{9/2}(2T)^2\, e^{2y} \\ &\quad \times \int_0^{+\infty} du_+ \int_0^{+\infty} du_- \int_0^{u_-} du_3^* (u_+ u_- u_3^*)^{1/2}\, (u_- - u_3^*)^2\, e^{-2u_+} e^{-2u_-} \\ &= \frac{32\sqrt{2}}{(2\pi)^7} S|\mathcal{M}|^2\, m^{0.5}\, T^{6.5}\, e^{2y} \\ &\quad \times \int_0^{+\infty} du_+\, u_+^{1/2} e^{-2u_+} \int_0^{+\infty} du_-\, u_-^{1/2} e^{-2u_-} \int_0^{u_-} du_3^*\, u_3^{*1/2} (u_- - u_3^*)^2\end{aligned}$$

Given that $\int_0^{+\infty} dy\, y^\alpha\, e^{-2y} = \Gamma(\alpha + 1)/2^{\alpha+1}$, we have

$$\begin{aligned}\dot{\epsilon} &= \frac{32\sqrt{2}}{(2\pi)^7} S|\mathcal{M}|^2\, m^{0.5}\, T^{6.5}\, e^{2y} \cdot \frac{\pi^{1/2}}{2^{5/2}} \cdot \int_0^{+\infty} du_-\, u_-^{1/2} e^{-2u_-} \frac{16}{105} u_-^{7/2} \\ &= \frac{32\sqrt{2}}{(2\pi)^7} S|\mathcal{M}|^2\, m^{0.5}\, T^{6.5}\, e^{2y} \cdot \frac{\pi^{1/2}}{2^{5/2}} \cdot \frac{4}{35} \\ &= \frac{S|\mathcal{M}|^2}{4 \cdot 35 \cdot \pi^{6.5}}\, m^{0.5}\, T^{6.5}\, e^{2y}\end{aligned}$$

Now, we remember that for a nucleon the number density is

$$n = 2 \int \frac{d^3p}{(2\pi)^3} \frac{1}{1 + \exp\left(\frac{m-\mu}{T}\right) \exp\left(\frac{\mathbf{p}_i^2}{2mT}\right)}$$

With the same computations and assumptions as above we easily get the very well-known

$$n = 2 \left(\frac{mT}{2\pi}\right)^{3/2} e^y$$

So, putting all together, we get

$$\dot{E} = \frac{S|\mathcal{M}|^2}{2 \cdot 35 \cdot \pi^{3.5}} m \left(\frac{T}{m}\right)^{3.5} n^2$$

The result is in beautiful accordance with expectations, since in ND conditions we expect that the process is governed both by n and T and both concur to enhance the emissivity.

Degenerate case

From the definition above

$$\dot{\epsilon} = \int \frac{d^3p_1}{(2\pi)^3\, 2E_1} \frac{d^3p_2}{(2\pi)^3\, 2E_2} \frac{d^3p_3}{(2\pi)^3\, 2E_3} \frac{d^3p_4}{(2\pi)^3\, 2E_4} \frac{d^3q}{(2\pi)^3\, 2E_s} \cdot S$$
$$\times (2\pi)^4 \delta^{(4)}(p_1 + p_2 - p_3 - p_4 - q) \cdot |\mathcal{M}|^2 \cdot E_S \cdot f(E_1)\, f(E_2)\, (1 - f(E_3))\, (1 - f(E_4))$$

leading to

$$\dot{\epsilon} = \frac{S|\mathcal{M}|^2}{32(2\pi)^{11}} \frac{1}{m^4} \int d^3p_1\, d^3p_2\, d^3p_3\, d^3p_4\, d^3q\; \delta\left(\frac{\mathbf{k} \cdot \mathbf{l}}{m} - E_S\right)$$
$$\times \delta^{(3)}(\mathbf{p}_1 + \mathbf{p}_2 - \mathbf{p}_3 - \mathbf{p}_4)\, f_1 f_2 (1 - f_3)(1 - f_4)$$

we will now use a trick that is valid in the degenerate (we use also the NR condition $E_i = m + p_i^2/2m$) limit since, by definition, $p_F^2 \gg mT$, so we can approximate the nucleons as laying on the Fermi surface:

$$d^3p_i = d^3p_i \int dE_i\, \delta(E_i - E_F) = d^3p_i \frac{m}{p_F} \delta(p_i - p_F) \int dE_i = d^3p_i \frac{mT}{p_F} \delta(p_i - p_F) \int dx_i$$

This separates the radial (on the energy) integrals and the angular ones. To manipulate the angular part, it is useful to insert the resolutions of the identity:

$$1 = \int d^3k\, \delta^{(3)}(\mathbf{k} - (\mathbf{p}_2 - \mathbf{p}_4))$$

$$1 = \int d^3l\, \delta^{(3)}(\mathbf{l} - (\mathbf{p}_2 - \mathbf{p}_4))$$

At this point the integral becomes

$$\dot{\epsilon} = \frac{S|\mathcal{M}|^2}{32(2\pi)^{11}} \frac{p_F^3\, T^3}{m} \int d^3p_2\, d^3p_3\, d^3p_4\, d^3q\, d^3k\, d^3l\; \delta\left(\frac{\mathbf{k}\cdot\mathbf{l}}{m} - E_S\right) \prod_{j=2}^{4} \delta(p_j - p_F)$$
$$\delta^{(3)}(\mathbf{k} - (\mathbf{p}_2 - \mathbf{p}_4))\; \delta^{(3)}(\mathbf{l} - (\mathbf{p}_2 - \mathbf{p}_4)) \int_{-\infty}^{\infty} dx_2\, dx_3\, dx_4 \frac{1}{e^{x_1}+1} \frac{1}{e^{x_2}+1} \frac{1}{e^{-x_3}+1} \frac{1}{e^{-x_4}+1}$$

with obviously $x_1 = x_3 + x_4 + E_S/T - x_2$. We call $\omega \equiv E_S$ and define:

$$F(\omega/T) = \int_{-\infty}^{\infty} dx_2\, dx_3\, dx_4 \frac{1}{e^{x_1}+1} \frac{1}{e^{x_2}+1} \frac{1}{e^{-x_3}+1} \frac{1}{e^{-x_4}+1} = \frac{\omega}{6T^3} \frac{4\pi^2T^2 + \omega^2}{e^{\omega/T} - 1}$$

We make the integrations over $\mathbf{p}_3$ and $\mathbf{p}_4$ via the Dirac deltas we have introduced and observe that the angular components of $\mathbf{p}_2$ and $\mathbf{q}$ are unconstrained:

$$\dot{\epsilon} = \frac{S|\mathcal{M}|^2}{32(2\pi)^{11}} \frac{T^3}{m\, p_F^3} \cdot (4\pi)^2 p_F^2 \int_0^{+\infty} d\omega\, \omega^2 F(\omega/T)\, (2\pi) \int_0^{+\infty} dk\, dl\, k^2 l^2 \int_0^{2\pi} d\phi\, \delta\left(\frac{\mathbf{k}\cdot\mathbf{l}}{m} - \omega\right)$$
$$\int_{-1}^{1} dy_3\, dy_4 \delta(\sqrt{p_F^2 + l^2 - 2lp_F y_3} - p_F)\, \delta(\sqrt{p_F^2 + k^2 - 2kp_F y_4} - p_F)$$

The integrals in the y variables just give jacobians and constrain the region of integration to $k, l \leq 2p_F$. We get:

$$\dot{\epsilon} = \frac{S|\mathcal{M}|^2}{8(2\pi)^8} \frac{T^3}{m\, p_F} \int_0^{+\infty} d\omega\, \omega^2 F(\omega/T) \int_0^{2p_F} dk\, dl\, kl \int_0^{2\pi} d\phi\, \delta\left(\frac{kl\cos\theta_{kl}}{m} - \omega\right)$$

We can parametrize the 3-momenta such that

$$\cos\theta_{kl} = \cos\phi \sqrt{1 - \frac{k^2}{4p_F^2}} \sqrt{1 - \frac{l^2}{4p_F^2}} + \frac{kl}{4p_F^2}$$

Thus:

$$\int_0^{2\pi} d\phi\, \delta\left(\frac{kl\cos\theta_{kl}}{m} - \omega\right) = \frac{2m}{kl} \frac{1}{\left[\left(1 - \frac{k^2}{4p_F^2}\right)\left(1 - \frac{l^2}{4p_F^2}\right) - \left(\frac{m\omega}{kl} - \frac{kl}{4p_F^2}\right)^2\right]^{1/2}}$$

Now, in order to arrive to an exact expression, we could make an approximation. In fact, in degenerate conditions one can very easily check that assuming all fermions on the Fermi surface, $\hat{k}\cdot\hat{l} \sim 0$. Therefore, whenever possible, one could make the assumption that $\mathbf{k}\cdot\mathbf{l} \ll kl$. Therefore, thanks to energy conservation setting $m\omega = \mathbf{k}\cdot\mathbf{l}$, we can neglect the ω term inside the square root in the previous expression.

$$\dot{\epsilon} = \frac{S|\mathcal{M}|^2}{8(2\pi)^8} \frac{T^3}{m\, p_F} \int_0^{+\infty} d\omega\, \omega^2 F(\omega/T) \int_{K^2+l^2 \leq 4p_F^2} dk\, dl\, \frac{2m}{\sqrt{1 - \frac{k^2+l^2}{4p_F^2}}} \tag{B.1}$$

Note also that the integration of the delta in $d\phi$, as it should, now constrains the region of integration, in which we can now integrate in polar coordinates. Pretty easily this becomes:

$$\dot{\epsilon} = \frac{S|\mathcal{M}|^2}{8(2\pi)^8}\frac{T^3}{m\,p_F}(4\pi)mp_F^2\int_0^{+\infty} d\omega\,\omega^2 F(\omega/T) = \frac{S|\mathcal{M}|^2}{8(2\pi)^8}4\pi p_F T^6\int_0^{+\infty} dx\,\frac{x^3}{6}\frac{4\pi^2+x^2}{e^x-1}$$

The integral results (exactly) in

$$\dot{\epsilon} = \frac{S|\mathcal{M}|^2}{8(2\pi)^8}4\pi p_F T^6\cdot\frac{124\pi^6}{6\cdot 315}$$

Substituting $p_F = (2mTy)^{1/2}$, we recast into Turner's result

$$\dot{\epsilon} = \frac{31\sqrt{2}}{64\cdot 3780\pi}S|\mathcal{M}|^2\,m^{0.5}\,T^{6.5}\,y^{1/2}$$

Appendix C

Non-Relativistic expansion of scalar products

We want to study the process $N_1(p_1) + N_2(p_2) \longrightarrow N_3(p_3) + N_4(p_4) + \phi(q)$ in an environment in which the kinetic energy of the nucleons is much smaller then their rest mass: we will be interested therefore in expansions in the parameter $\varepsilon = T/m_N$. Therefore the four-momenta of the nucleons can be expanded as

$$p_i^\mu = \left(m_N + \frac{\mathbf{p}_i^2}{2m_N}\varepsilon - \frac{\mathbf{p}_i^4}{8m_N^3}\varepsilon^2 + O(\varepsilon^3),\ \mathbf{p}_i \varepsilon^{\frac{1}{2}} \right)$$

We define also the classical kinetic energy as $K = \mathbf{p}^2/2m$, which is of course the same order of T, thus the 3-momentum is $O(\varepsilon^{\frac{1}{2}})$. Since the mass difference between protons and neutrons is higher order in ε than the difference between K_i, we assume isospin invariance. Therefore, the energy of the scalar must be at most of order ε, constraining the scalar mass to be also at most of order ε. So we write

$$q^\mu = (E_S\, \varepsilon,\ \mathbf{q}\, \varepsilon)$$

of course with $\mathbf{q}^2 = E_S^2 - m_S^2$. Our goal is now to consistently parametrize the scalar products between the 4-momenta up to order ε^2, where we expect the scalar mass to appear. We begin defining $k = p_2 - p_4$ and $l = p_2 - p_3$. Therefore, by definition $k^2 = 2m_N^2 - 2p_2 \cdot p_4$, but also

$$\left((K_2 - K_4)\varepsilon + O(\varepsilon^2),\ \mathbf{k}\, \varepsilon^{\frac{1}{2}} \right) \ = \ -\mathbf{k}^2\, \varepsilon + (K_2 - K_4)^2\, \varepsilon^2$$

So, $p_2 \cdot p_4 = m_N^2 + \frac{\varepsilon}{2}\mathbf{k}^2 - \frac{\varepsilon^2}{2}(K_2 - K_4)^2$. We proceed for all the products between

the p_i:

$$
\begin{aligned}
p_1 \cdot p_2 &= m_N^2 + \frac{\varepsilon}{2}(\mathbf{k}^2 + \mathbf{l}^2 + 2\mathbf{k}\cdot\mathbf{l}) - \frac{\varepsilon^{\frac{3}{2}}}{2}(\mathbf{q}\cdot\mathbf{k} + \mathbf{q}\cdot\mathbf{l}) + \frac{\varepsilon^2}{2}\mathbf{q}^2 - \frac{\varepsilon^2}{2}(K_1 - K_2)^2 \\
p_1 \cdot p_3 &= m_N^2 + \frac{\varepsilon}{2}\mathbf{k}^2 - \varepsilon^{\frac{3}{2}}\,\mathbf{q}\cdot\mathbf{k} - \frac{\varepsilon^2}{2}(m_S^2 + (K_2 - K_4)(K_2 - K_4 - 2E_S)) \\
p_1 \cdot p_4 &= m_N^2 + \frac{\varepsilon}{2}\mathbf{l}^2 - \varepsilon^{\frac{3}{2}}\,\mathbf{q}\cdot\mathbf{l} - \frac{\varepsilon^2}{2}(m_S^2 + (K_2 - K_3)(K_2 - K_3 - 2E_S)) \\
p_2 \cdot p_3 &= m_N^2 + \frac{\varepsilon}{2}\mathbf{l}^2 - \frac{\varepsilon^2}{2}(K_2 - K_3)^2 \\
p_2 \cdot p_4 &= m_N^2 + \frac{\varepsilon}{2}\mathbf{k}^2 - \frac{\varepsilon^2}{2}(K_2 - K_4)^2 \\
p_3 \cdot p_4 &= m_N^2 = \frac{\varepsilon}{2}(\mathbf{k}^2 + \mathbf{l}^2 - 2\mathbf{k}\cdot\mathbf{l}) - \frac{\varepsilon^2}{2}(K_3 - K_4)^2
\end{aligned}
$$

We made use of the additional relation $p_1 - p_2 = -(k + l - q)$ (4-momenta!). Now, to pass to the products $p_i \cdot q$, first of all we define the parameters β_i from $\mathbf{q}\cdot\mathbf{p}_i = m_N\,|\mathbf{q}|\,\beta_i$ then we exploit the useful relations of the kind $2p_1 = p_1 + p_2 - k - l + q$ and we get

$$
\begin{aligned}
p_1 \cdot q &= (m_N + K_1\,\varepsilon)\,E_S\,\varepsilon - \varepsilon^{\frac{3}{2}}|\mathbf{q}|\,m_N\left(\frac{\beta_1 + \beta_2}{2}\right) - \frac{\varepsilon^{\frac{3}{2}}}{2}(-\mathbf{q}\cdot\mathbf{k} - \mathbf{q}\cdot\mathbf{l} + \mathbf{q}^2\varepsilon^{\frac{1}{2}}) \\
p_2 \cdot q &= (m_N + K_2\,\varepsilon)\,E_S\,\varepsilon - \varepsilon^{\frac{3}{2}}|\mathbf{q}|\,m_N\left(\frac{\beta_1 + \beta_2}{2}\right) - \frac{\varepsilon^{\frac{3}{2}}}{2}(+\mathbf{q}\cdot\mathbf{k} + \mathbf{q}\cdot\mathbf{l} - \mathbf{q}^2\varepsilon^{\frac{1}{2}}) \\
p_3 \cdot q &= (m_N + K_3\,\varepsilon)\,E_S\,\varepsilon - \varepsilon^{\frac{3}{2}}|\mathbf{q}|\,m_N\left(\frac{\beta_1 + \beta_2}{2}\right) - \frac{\varepsilon^{\frac{3}{2}}}{2}(+\mathbf{q}\cdot\mathbf{k} - \mathbf{q}\cdot\mathbf{l} - \mathbf{q}^2\varepsilon^{\frac{1}{2}}) \\
p_4 \cdot q &= (m_N + K_4\,\varepsilon)\,E_S\,\varepsilon - \varepsilon^{\frac{3}{2}}|\mathbf{q}|\,m_N\left(\frac{\beta_1 + \beta_2}{2}\right) - \frac{\varepsilon^{\frac{3}{2}}}{2}(-\mathbf{q}\cdot\mathbf{k} + \mathbf{q}\cdot\mathbf{l} - \mathbf{q}^2\varepsilon^{\frac{1}{2}})
\end{aligned}
$$

Finally, demanding that $(p_1 + p_2 - p_3 - p_4)\cdot p_i - q\cdot p_i$ is 0 at each order in ϵ, we get some useful relations between the variables:

$$
\begin{aligned}
\mathbf{k}\cdot\mathbf{l} &= m_N\,E_S \\
\beta_1 + \beta_2 &= \frac{\mathbf{q}\cdot\mathbf{k} + \mathbf{q}\cdot\mathbf{l}}{m_N\,|\mathbf{q}|} \\
0 &= -\frac{1}{2}E_S^2 - (K_2 + K_3 - K_4)E_S + (K_2 - K_3)(K_2 - K_4)
\end{aligned}
$$

Appendix D

Squared amplitude and comparison with existing literature

Using the notation of Appendix C, taking the degenerate limit means that one can neglect the $\mathbf{k}\cdot\mathbf{l} = m_N \cdot E_S$ whenever this does not lead to inconsistent results. Thus, the squared amplitude is computed and the relations in Appendix C are substituted in the scalar products. Then, averaging over the scalar directions means that

$$\begin{aligned}
\langle \hat{k}\cdot\hat{q}\rangle &= 0 \\
\langle (\hat{k}\cdot\hat{q})^2\rangle &= \frac{1}{3} \\
\langle (\hat{k}\cdot\hat{q})^4\rangle &= \frac{1}{5} \\
\langle (\hat{k}\cdot\hat{q})^2(\hat{l}\cdot\hat{q})^2\rangle &= \frac{1+\langle(\hat{k}\cdot\hat{l})^2\rangle}{15}
\end{aligned}$$

Let $M_{nuc} \equiv M_a + M_b + M_c + M_d + M'_a + M'_b + M'_c + M'_d$ and $M_\pi = M_e + M'_e$ (remember that $M' = -M(p_3 \leftrightarrow p_4)$), then

$$|M_{nuc} + M_\pi|^2 = G^2\left[I_{nuc} + I_{int} + I_\pi\right]$$

with $G = (2m_N/m_\pi)^2 f^2 \sin\theta_c$, $G^2 I_\pi = |M_\pi|^2$ (idem for I_{nuc}) and $G^2 I_{int} = 2\,\mathrm{Re}\{M_{nuc}M_\pi^*\}$. Explicitly, in the degenerate limit:

$$I_\pi = 4A_\pi^2\left[\frac{\mathbf{k}^4}{(\mathbf{k}^2+m_\pi^2)^4} + \frac{\mathbf{l}^4}{(\mathbf{l}^2+m_\pi^2)^4} + \frac{\mathbf{k}^2\mathbf{l}^2}{(\mathbf{k}^2+m_\pi^2)^2(\mathbf{l}^2+m_\pi^2)^2}\right] \tag{D.1}$$

$$\begin{aligned}
I_{int} = &-\frac{16m_\pi^2 A_\pi\, y_{hN}}{3m_N}\left[\frac{\mathbf{k}^4}{(\mathbf{k}^2+m_\pi^2)^4} + \frac{\mathbf{l}^4}{(\mathbf{l}^2+m_\pi^2)^4} + \frac{\mathbf{k}^2\mathbf{l}^2}{(\mathbf{k}^2+m_\pi^2)^2(\mathbf{l}^2+m_\pi^2)^2}\right] \\
&+ \frac{m_S^2}{E_S^2}\frac{4A_\pi\, y_{hN}}{m_N}\left[\frac{10m_\pi^2}{3}\left(\frac{\mathbf{k}^4}{(\mathbf{k}^2+m_\pi^2)^4} + \frac{\mathbf{l}^4}{(\mathbf{l}^2+m_\pi^2)^4} + \frac{\mathbf{k}^2\mathbf{l}^2}{(\mathbf{k}^2+m_\pi^2)^2(\mathbf{l}^2+m_\pi^2)^2}\right)\right. \\
&\left. + \left(\frac{2\mathbf{k}^6}{(\mathbf{k}^2+m_\pi^2)^4} + \frac{2\mathbf{l}^6}{(\mathbf{l}^2+m_\pi^2)^4} + \frac{\mathbf{k}^2\mathbf{l}^2\,(\mathbf{k}^2+\mathbf{l}^2)}{(\mathbf{k}^2+m_\pi^2)^2(\mathbf{l}^2+m_\pi^2)^2}\right)\right]
\end{aligned} \tag{D.2}$$

$$
\begin{aligned}
I_{nuc} = \frac{16y_{hN}^2}{15m_N^2}\Bigg[& \left(\frac{\mathbf{k}^8}{(\mathbf{k}^2+m_\pi^2)^4}+\frac{\mathbf{l}^8}{(\mathbf{l}^2+m_\pi^2)^4}-\frac{\mathbf{k}^4\mathbf{l}^4}{(\mathbf{k}^2+m_\pi^2)^2(\mathbf{l}^2+m_\pi^2)^2}\right) \\
& + m_\pi^2\left(\frac{2\mathbf{k}^6}{(\mathbf{k}^2+m_\pi^2)^4}+\frac{2\mathbf{l}^6}{(\mathbf{l}^2+m_\pi^2)^4}-\frac{\mathbf{k}^2\mathbf{l}^2\,(\mathbf{k}^2+\mathbf{l}^2)}{(\mathbf{k}^2+m_\pi^2)^2(\mathbf{l}^2+m_\pi^2)^2}\right) \\
& + 4m_\pi^4\left(\frac{\mathbf{k}^4}{(\mathbf{k}^2+m_\pi^2)^4}+\frac{\mathbf{l}^4}{(\mathbf{l}^2+m_\pi^2)^4}\right)\Bigg] \\
- \frac{8y_{hN}^2}{15m_N^2}\frac{m_S^2}{E_S^2}\Bigg[& 4\left(\frac{\mathbf{k}^8}{(\mathbf{k}^2+m_\pi^2)^4}+\frac{\mathbf{l}^8}{(\mathbf{l}^2+m_\pi^2)^4}-\frac{\mathbf{k}^4\mathbf{l}^4}{(\mathbf{k}^2+m_\pi^2)^2(\mathbf{l}^2+m_\pi^2)^2}\right) \\
& + m_\pi^2\left(\frac{18\mathbf{k}^6}{(\mathbf{k}^2+m_\pi^2)^4}+\frac{18\mathbf{l}^6}{(\mathbf{l}^2+m_\pi^2)^4}+\frac{\mathbf{k}^2\mathbf{l}^2\,(\mathbf{k}^2+\mathbf{l}^2)}{(\mathbf{k}^2+m_\pi^2)^2(\mathbf{l}^2+m_\pi^2)^2}\right) \\
& + m_\pi^4\left(\frac{26\mathbf{k}^4}{(\mathbf{k}^2+m_\pi^2)^4}+\frac{26\mathbf{l}^4}{(\mathbf{l}^2+m_\pi^2)^4}+\frac{80\mathbf{k}^2\mathbf{l}^2}{(\mathbf{k}^2+m_\pi^2)^2(\mathbf{l}^2+m_\pi^2)^2}\right)\Bigg] \\
- \frac{4y_{hN}^2}{15m_N^2}\frac{m_S^4}{E_S^4}\Bigg[& \left(\frac{19\mathbf{k}^8}{(\mathbf{k}^2+m_\pi^2)^4}+\frac{19\mathbf{l}^8}{(\mathbf{l}^2+m_\pi^2)^4}-\frac{44\mathbf{k}^4\mathbf{l}^4}{(\mathbf{k}^2+m_\pi^2)^2(\mathbf{l}^2+m_\pi^2)^2}\right) \\
& + m_\pi^2\left(\frac{58\mathbf{k}^6}{(\mathbf{k}^2+m_\pi^2)^4}+\frac{58\mathbf{l}^6}{(\mathbf{l}^2+m_\pi^2)^4}+\frac{84\mathbf{k}^2\mathbf{l}^2\,(\mathbf{k}^2+\mathbf{l}^2)}{(\mathbf{k}^2+m_\pi^2)^2(\mathbf{l}^2+m_\pi^2)^2}\right) \\
& + m_\pi^4\left(\frac{204\mathbf{k}^4}{(\mathbf{k}^2+m_\pi^2)^4}+\frac{204\mathbf{l}^4}{(\mathbf{l}^2+m_\pi^2)^4}+\frac{140\mathbf{k}^2\mathbf{l}^2}{(\mathbf{k}^2+m_\pi^2)^2(\mathbf{l}^2+m_\pi^2)^2}\right)\Bigg] \\
+ \frac{16y_{hN}^2}{15m_N^4}\frac{1}{E_S^2}\left(1-\frac{1}{2}\frac{m_S^2}{E_S^2}+\frac{m_S^4}{E_S^4}\right) & \frac{3\mathbf{k}^6\mathbf{l}^6+3m_\pi^2\mathbf{k}^4\mathbf{l}^4(\mathbf{k}^2+\mathbf{l}^2)+m_\pi^4\mathbf{k}^2\mathbf{l}^2(\mathbf{k}^4+\mathbf{l}^4+\mathbf{k}^2\mathbf{l}^2)}{(\mathbf{k}^2+m_\pi^2)^2(\mathbf{l}^2+m_\pi^2)^2}
\end{aligned}
\tag{D.3}
$$

D.1 Comparison with previous literature

Having expressed the squared amplitudes, we can focus on the difference between the matrix element squared we obtain and the previous literature.

Ref. [3][1]

The BMZ term of pure emission from nucleon legs should be 0 in the limit of vanishing scalar mass, which is not our case, as it is manifest from their Eq. A.15. In terms of the non-relativistic expansion in the previous section, Mohapatra forgets terms that are relevant at the NLO level. At leading order in ε (defined as in Appendix C as our NR expansion parameter) in fact we can write:

$$
\frac{1}{k^2-m_\pi^2}\sim-\frac{1}{\mathbf{k}^2+m_\pi^2}\quad\text{and}\quad\frac{1}{(p_i\pm q)^2-m_N^2}\sim\frac{1}{\pm 2m_N E_S}
$$

With this simplification it is easy to verify that $\widetilde{M}_{nuc}=M_a+M_b+M_c+M_d$ is zero at leading order due to Dirac equation. Namely,

$$
\widetilde{M}_{nuc}^{LO}\propto[\overline{u}(p_3)\gamma_5 u(p_1)]\left[\overline{u}(p_4)(\not{p}_4+\not{p}_2)\gamma_5 u(p_2)\right]+\left[\overline{u}(p_3)(\not{p}_3+\not{p}_1)\gamma_5 u(p_1)\right][\overline{u}(p_4)\gamma_5 u(p_2)]=0
$$

[1] We indicate the authors as BMZ

So, we must go beyond leading order and see what happens:

- for the pionic propagator (all the kinematic variables are defined in Appendix C):

$$\frac{1}{k^2-m_\pi^2} \sim -\frac{1}{\mathbf{k}^2+m_\pi^2}\frac{1}{\varepsilon}\left(1+\frac{(K_2-K_4)^2\varepsilon}{\mathbf{k}^2+m_\pi^2}\right)$$

- for the nucleon propagator:

$$\begin{aligned}
\frac{1}{(p_1-q)^2-m_N^2} &\sim -\frac{1}{2m_N E_S\varepsilon}\left(1+\frac{E_S-2K_1}{2m_N}\varepsilon\right)\\
\frac{1}{(p_2-q)^2-m_N^2} &\sim -\frac{1}{2m_N E_S\varepsilon}\left(1+\frac{\mathbf{q}\cdot\mathbf{k}+\mathbf{q}\cdot\mathbf{l}}{E_S m_N}\varepsilon^{\frac{1}{2}}\right.\\
&\qquad\left.-\frac{E_S^3 m_N+2E_S^2K_2m_N-2E_S m_N m_S^2-2(\mathbf{q}\cdot\mathbf{k}+\mathbf{q}\cdot\mathbf{l})^2}{2m_N^2E_S^2}\varepsilon\right)\\
\frac{1}{(p_3+q)^2-m_N^2} &\sim +\frac{1}{2m_N E_S\varepsilon}\left(1+\frac{\mathbf{q}\cdot\mathbf{k}}{E_S m_N}\varepsilon^{\frac{1}{2}}-\frac{E_S^3 m_N+2E_S^2K_3m_N-2(\mathbf{q}\cdot\mathbf{k})^2}{2m_N^2E_S^2}\varepsilon\right)\\
\frac{1}{(p_4+q)^2-m_N^2} &\sim +\frac{1}{2m_N E_S\varepsilon}\left(1+\frac{\mathbf{q}\cdot\mathbf{l}}{E_S m_N}\varepsilon^{\frac{1}{2}}-\frac{E_S^3 m_N+2E_S^2K_4m_N-2(\mathbf{q}\cdot\mathbf{l})^2}{2m_N^2E_S^2}\varepsilon\right)
\end{aligned}$$

However, this is not what BMZ get in their expansion. This is because they overlook terms that are dominant or comparable with respect to m_S^2. Concretely what they do is an expansion of the form:

$$\frac{1}{(p_i\pm q)^2-m_N^2} \sim \frac{1}{\pm 2m_N E_S\varepsilon}\left(1\mp\frac{m_S^2}{2m_N E_S}\varepsilon\right)$$

We have checked that with this expansion and neglecting *every* other term (both in the nucleon and in the pion propagators), we cast back into their expression for the amplitude squared, which goes as:

$$|M_{nuc}^{NLO}+M_{nuc}^{\prime NLO}|^2 \propto \frac{m_S^4}{E_S^4}\left[\frac{\mathbf{k}^4}{(\mathbf{k}^2+m_\pi^2)^2}+\frac{\mathbf{l}^4}{(\mathbf{l}^2+m_\pi^2)^2}+\frac{\mathbf{k}^2\mathbf{l}^2-2(\mathbf{k}\cdot\mathbf{l})^2}{(\mathbf{k}^2+m_\pi^2)(\mathbf{l}^2+m_\pi^2)}\right]$$

Actually, there is a minus sign in their Eq. A.8 in front of the mixed term because they overlooked the minus sign arising from exchange of fermion legs between t and u channels.

Ref. [39]

We averaged the amplitude in Eqs. 20 and 21 of Ishizuka and Yoshimura over the scalar direction and considered the degenerate case. We got (they used a different notation on momenta so that their q is our k, their q' is out l and their k is our q):

$$\begin{aligned}
\sum_{spins}|\mathcal{M}|^2 = g_D^2\left(\frac{f}{m_\pi}\right)^4\cdot\left[\frac{16}{15m_N^4}\frac{1}{E_S^2}\left(\frac{\mathbf{k}^2\mathbf{l}^6}{(\mathbf{l}^2+m_\pi)^2}+\frac{\mathbf{l}^2\mathbf{k}^6}{(\mathbf{k}^2+m_\pi)^2}+\frac{\mathbf{k}^4\mathbf{l}^4}{(\mathbf{k}^2+m_\pi)(\mathbf{l}^2+m_\pi^2)}\right)+\right.\\
\left.+\frac{1}{3m_N^2}\left(\frac{32\mathbf{k}^2\mathbf{l}^2}{(\mathbf{k}^2+m_\pi)(\mathbf{l}^2+m_\pi^2)}+\frac{464\mathbf{k}^4}{5(\mathbf{k}^2+m_\pi)^2}+\frac{464\mathbf{l}^4}{5(\mathbf{l}^2+m_\pi)^2}\right)\right]
\end{aligned}$$

By direct evaluation we see that the term that goes as E_S^{-2} is identical to our term, while the other is not. It seems that their formula for the emissivity neglects the second term (going as E_S^0) as we can see from the T^4 dependence in their Eq. 20:

$$\dot{\epsilon}_D = y_{hNN}^2 \sin^2\theta_C \left(\frac{f}{m_\pi}\right)^4 T^4 p_F^5 \frac{11}{(15\pi)^3} G_D(m_\pi/p_F)$$

This is exactly equal to $\dot{\epsilon}_S$ (Equation 6.4) once we evaluate $\dot{\epsilon}_D$ for $m_\pi/p_F \to 0$. The equivalence is also valid when $\dot{\epsilon}_S$ is numerically evaluated for $y_\pi \approx 0.24$. Basically, it seems evident to us that in Ref. [39] they overlooked the computation of the emissivity for the E_S^0 term and, in any case, their somehow disappeared piece is different from ours.

Appendix E

Non-thermal emission spectrum

In this Appendix we show that a (dominant) term going as $E_S{-}2$ in the full amplitude, implies that the emission spectrum for free-streaming scalars is non thermal, since they do not in general respect a properly normalized Maxwell-Boltzmann (it is quasi-thermal only for scalars that have masses $m_s \simeq T$)

$$\frac{dN}{dE_s} = \zeta_S \frac{E_s\sqrt{E_s^2 - m_s^2}}{T^3} \exp\left\{\left(-\frac{Es}{T}\right)\right\}$$

This can be appreciated in the plots below (Figure E.1).

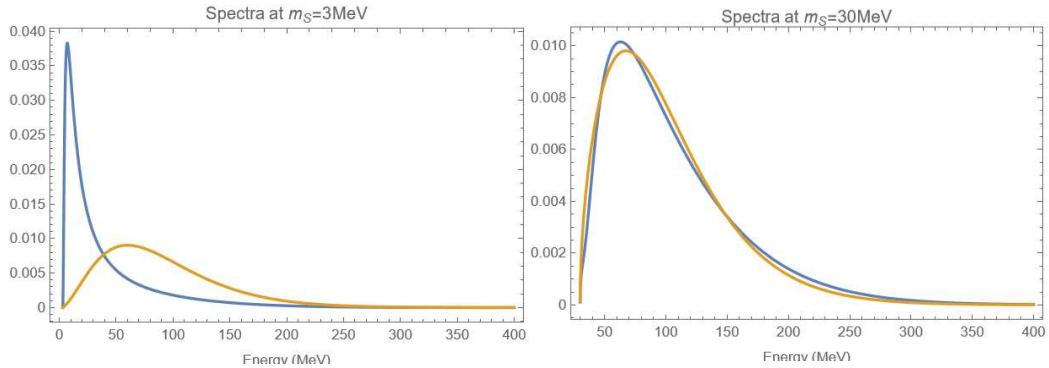

Figure E.1: Emission spectra: in blue the free-streaming one, in yellow the thermal one

This implies that the average emission energy $\langle E_S \rangle$ depends on the mass of the scalar, as it is possible to see in Figure E.2.

The consequences of this fact may be seen e.g. in the low coupling region of the LESNe bound (Figure 6.2) for the MeV region (i.e. dominated by the decays int electrons). Naively, for a thermal spectrum where the emitted energy is almost constant, we would expect that $s^4 m_S^2 \simeq const$, due to the fact that the production goes as s^2, the decay rate as $s^2 m_S$ and the boost factor as $\langle E_S \rangle / m_S$ (which is at the denominator). This would produce the dashed black line in Fig. E.3, which at high masses is wrong by a factor of 5—6. If we correct this line accounting for the fact that dN/dE_S is now dependent on the mass through the dependency of $\langle E_S \rangle$, and

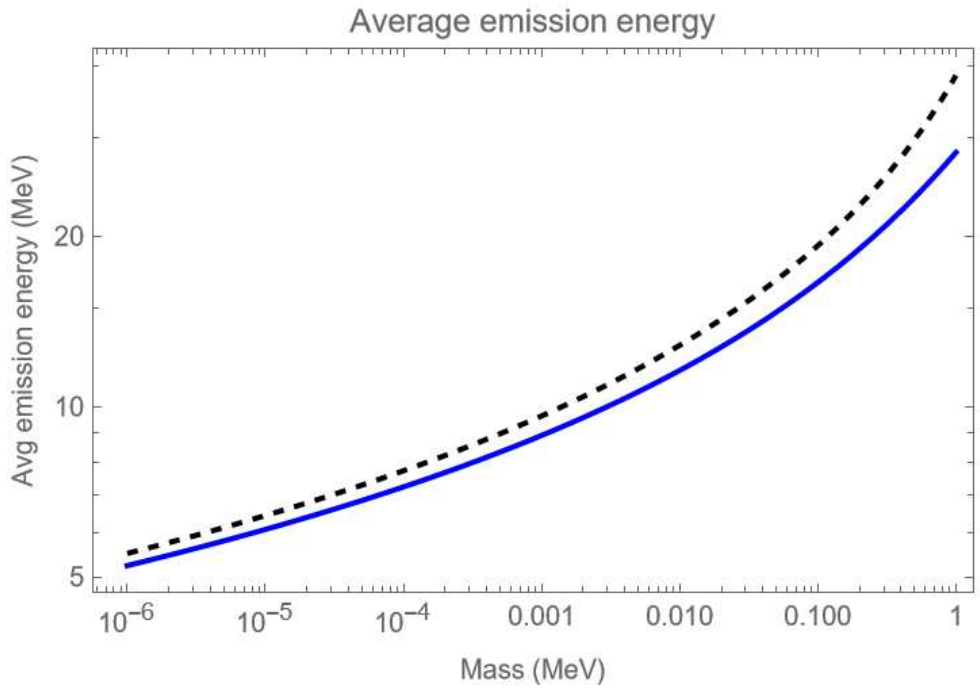

Figure E.2: Average emission energy as a function of the mass.

the same consideration holds for the boosted factor, we get the dashed blue line, which is always very close to the numerical curve except up to numerical factors of order 1—1.5.

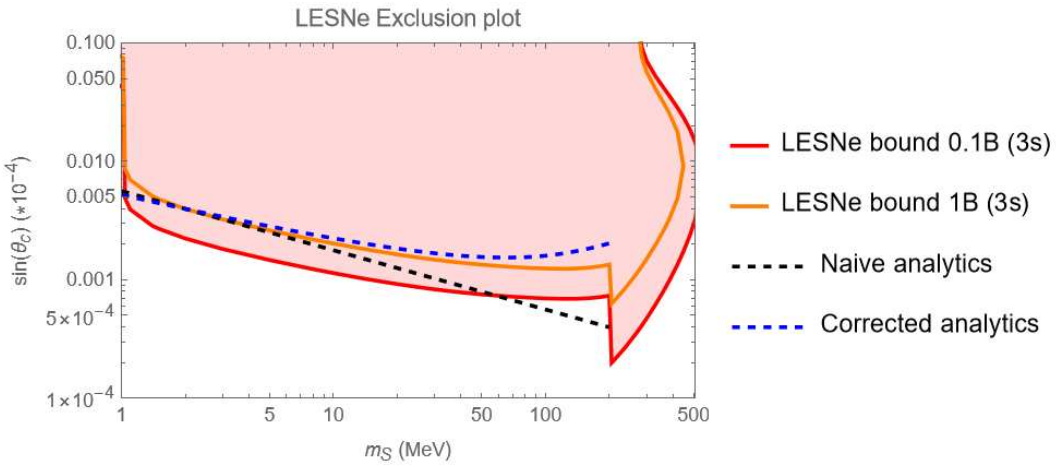

Figure E.3

The same considerations apply to the SN 1987A gamma ray bound in the same region and low coupling limit. In fact, by a look to formulae in Equations 6.16 and 6.18, we have that

$$F_\gamma \propto \frac{dN}{dE_S}\chi\Gamma_S\frac{1}{\gamma\beta} \simeq \frac{dN}{dE_S}m_S$$

since $\chi \simeq \gamma, \beta \simeq 1$ and $\Gamma_S \approx \Gamma_{S\to e^+e^-} \propto m_S$. Correcting the expected behaviour of $s \propto m_S^{-1/4}$ with the non-thermal emission considerations, we reproduce the be-

haviour of the numerics (in Figure E.4 the corrections make the flux of photons produced by the decay into electrons a constant).

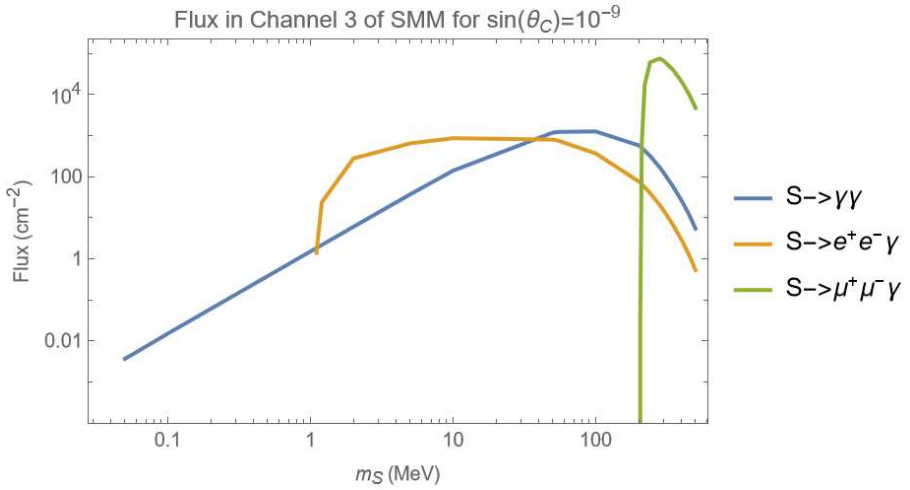

Figure E.4

We delve a little more into why we have a mass dependence of $\langle E_S \rangle$ even for masses $m_S \ll T$. If one takes Equation 6.3 and applies it to the scalar emission, one easily sees (plugging all the numbers) that the dominant contribution in the $m_S \ll T$ limit comes from the E_S^{-2} term. In this case the emissivity goes as

$$\dot{\epsilon} \propto \int_{m_S}^{+\infty} dE_S \sqrt{E_S^2 - m_S^2} \frac{4\pi^2 T^2 + E_S^2}{e^{E_S/T} - 1}$$

If $m_S \ll T$ it is trivial that $\dot{\epsilon}$ is constant in m_S. The problems come when one tries to compute the production rate per unit volume, which is simply

$$\dot{r} \propto \int_{m_S}^{+\infty} dE_S \frac{\sqrt{E_S^2 - m_S^2}}{E_S} \frac{4\pi^2 T^2 + E_S^2}{e^{E_S/T} - 1}.$$

For $m_S \to 0$ there is a divergence now. If one splits the integral at an energy value of $10\,MeV$, the two contributions behave very differently:

$$\dot{r} \propto \int_{m_S}^{10\,MeV} dE_S \frac{4\pi^2 T^3}{E_S} + \int_{10\,MeV}^{+\infty} dE_S \frac{4\pi^2 T^2 + E_S^2}{e^{E_S/T} - 1} \simeq 4\pi^2 T^3 \log \frac{10\,MeV}{m_S} + const. \tag{E.1}$$

The average emission energy can be computed as $\dot{\epsilon}/\dot{r}$. Using Equation E.15, one can see that for low enough masses the average energy goes as $\langle E_S \rangle \propto \log m_S$. This must happen, since when the emissivity is independent of the mass, we cannot expect the same for the rate of production. In other words: in our theory and in the massless limit the energy taken away from the PNS is effectively independent of the mass, but, because of the E_S^{-2} the scalars "prefer" to be produced with low energies, thus leading to an increased production rate. These considerations can be appreciated in Figure E.2, where we have approximated (dashed black line) the emission energy using only the E_S^{-2} term and in the massless limit, which is less a 10% away from the numerical value at low masses.

Bibliography

[1] G. Krnjaic. "Probing Light Thermal Dark-Matter with a Higgs-Portal Mediator". In: *Phys. Rev. D* 94 (2016). arXiv: 1512.04119v2 [hep-ph].

[2] N. Iwamoto. "Axion Emission From Neutron Stars". In: *Phys. Rev. Lett.* 53 (1984). DOI: 10.1103/PhysRevLett.53.1198.

[3] P.S. Bhupal Dev, R.N. Mohapatra, and Y. Zhang. "Revisiting supernova constraints on a light CP-even scalar". In: *JCAP08(2020)003* (2020). arXiv: 2005.00490v3 [hep-ph].

[4] G.G. Raffelt. "Astrophysical axion bounds". In: *Lect.Notes Phys.* 741 (2008), pp. 51–71. arXiv: hep-ph/0611350.

[5] A. Caputo et al. "Low-Energy Supernovae Severely Constrain Radiative Particle Decays". In: (2022). arXiv: 2201.09890v2 [astro-ph.HE].

[6] H. Georgi and S. Glashow. "Unity of All Elementary Particle Forces". In: *Phys. Rev. Lett.* (1974).

[7] F. Capozzi et al. "Neutrino masses and mixings: Status of known and unknown 3ν parameters". In: *Nuclear Physics B* (2016). arXiv: 1601.07777 [hep-ph].

[8] J. Billard et al. "Direct detection of dark matter—APPEC committee report". In: *Rep. Prog. Phys.* (2021). arXiv: 2104.07634 [hep-ex].

[9] B.W. Lee and S. Weinberg. "Cosmological lower bound on heavy-neutrino masses". In: *Phys.Rev.Lett.* (1977).

[10] S. Dodelson and L.M. Widrow. "Sterile neutrinos as dark matter". In: *Phys. Rev. Lett.* (1994). arXiv: hep-ph/9303287 [hep-ph].

[11] K. Petraki and R. R. Volkas. "Review of asymmetric dark matter". In: *PoS* (2013). arXiv: hep-ph/1305.4939.

[12] M.E. Peskin and D.V. Shroeder. *An Introduction to Quantum Field Theory.* CRC Press, 1995.

[13] A. A. Belavin et al. "Pseudoparticle solutions of the Yang-Mills Equations". In: *Physics Letters B* (1975).

[14] M.K. Gaillard J.R. Ellis. "Strong and Weak CP violation". In: *Nucl. Phys. B* (1979).

[15] A. Hook. "TASI Lectures on the Strong CP Problem and Axions". In: *arXiv: 1812. 02669 [hep-ph]* (2023).

[16] E. Witten C. Vafa. "Parity Conservation in QCD". In: *Phys. Rev. Lett. 53* (1984).

[17] S. Weinberg. "A new light boson?" In: *Phys. Rev. Lett. 40* (1978).

[18] F. Wilczek. "Problem of Strong P and T Invariance in the Presence of Instantons". In: *Phys. Rev. Lett. 40* (1978).

[19] M. Dine, W. Fischler, and M. Srednicki. "A Simple Solution to the Strong CP Problem with a Harmless Axion". In: *Phys. Lett. B* 104 (1981), pp. 199–202. URL: http://doi.org/10.1016/0370-2693(81)90590-6.

[20] A. R. Zhitnitsky. "On Possible Suppression of the Axion Hadron Interactions. (In Russian)". In: *Sov. J. Nucl. Phys.* 31 (1980). [Yad. Fiz.31,497(1980)], p. 260.

[21] M. A. Shifman, A. I. Vainshtein, and V. I. Zakharov. "Can Confinement Ensure Natural CP Invariance of Strong Interactions?" In: *Nuclear Physics B* 166.3 (1980), p. 493.

[22] J. E. Kim. "Weak Interaction Singlet and Strong CP Invariance". In: *Physical Review Letters* 43.2 (1979), p. 103.

[23] A. Bazavov et al. "The chiral and deconfinement aspects of the QCD transition". In: *Phys. Rev. D* 85 (2012), p. 054503. arXiv: 1111.1710.

[24] A. Caputo and G. Raffelt. "Astrophysical Axion Bounds: The 2024 Edition". In: *PoS* 454 (2024). DOI: 10.48550/arXiv.2401.13728. arXiv: 2401.13728 [hep-ph].

[25] M.S. Turner R.P. Brinkmann. "Numerical rates for nucleon-nucleon, axion bremsstrahlung". In: *Physical Review D* (1988).

[26] P. Goldreich and S. Weber. "Homologously collapsing stellar cores". In: *Ap. J.* 238 (1980), pp. 991–997.

[27] G.G. Raffelt. *Stars as Laboratories for Fundamental Physics*. 2nd ed. The University of Chicago Press, 2021.

[28] R. Kippenhahn, A. Weigert, and A. Weiss. *Stellar Structure and Evolution*. Springer, 2012.

[29] H.T. Janka. "Neutrino Emission from Supernovae". In: (2017). arXiv: 1702.08713 [astro-ph].

[30] A. Burrows. "On detecting stellar collapse with neutrinos". In: *Ap. J.* 238 (1984). DOI: 10.1086/162371.

[31] K. Hirata et al. "Observation of a neutrino burst from the supernova SN1987A". In: *Phys. Rev. Lett.* 58 (1987). DOI: 10.1103/PhysRevLett.58.1490.

[32] C.B. Bratton et al. "Angular distribution of events from SN1987A". In: *Phys. Rev. D* 37 (1988). DOI: 10.1103/PhysRevD.37.3361.

[33] E:N: Alexeyev et al. "Detection of the neutrino signal from SN 1987A in the LMC using the INR Baksan underground scintillation telescope". In: *Phys. Lett. B* 205 (1988). DOI: 10.1016/0370-2693(88)91651-6.

[34] L.J. Hall et al. "Freeze-In Production of FIMP Dark Matter". In: *JHEP 1003:080,2010* (2009). arXiv: 0911.1120v2 [hep-ph].

[35] S. Knapen, T. Lin, and K.M. Zurek. "Light Dark Matter: Models and Constraints". In: *Phys. Rev. D* 96 (2017). arXiv: 1709.07882v2 [hep-ph].

[36] M.A. Shifman, A.I. Vainshtein, and V.I. Zakharov. "Remarks on Higgs-boson interactions with nucleons". In: *Phys. Lett. B* 78 (1978).

[37] H.-Y. Cheng and C.-W. Chiang. "Revisiting Scalar and Pseudoscalar Couplings with Nucleons". In: (2012). arXiv: 1202.1292v2 [hep-ph].

[38] R.S. Chivukula et al. "Couplings of a light Higgs boson". In: *Phys. Lett. B* 222 (1989).

[39] N. Ishizuka and M. Yoshimura. "Axion and Dilaton Emissivity from Nascent Neutron Stars". In: *Prog. Theor. Phys.* 84 (1990). DOI: https://doi.org/10.1143/ptp/84.2.233.

[40] H. Yang and R.A. Chevalier. "Evolution of the Crab nebula in a low energy supernova". In: (2015). arXiv: 1505.03211v1 [astro-ph.HE].

[41] D. Slominski. "Higgs Boson Decay to Two Photons". MA thesis. Stockholm University, 2022.

[42] A. Caputo, G. Raffelt, and E. Vitagliano. "Muonic Boson Limits: Supernova Redux". In: (2021). arXiv: 2109.03244 [hep-ph].

[43] E.L. Chupp, W.T. Vestrand, and C. Reppin. "Experimental Limits on the Radiative Decay of SN 1987A Neutrinos". In: *Phys.Rev.Lett.* 62 (1989). DOI: https://doi.org/10.1103/PhysRevLett.62.505.

[44] L. Oberauer et al. "Supernova bounds on neutrino radiative decays". In: *Astropart. Phys.* 1 (1993). DOI: https://doi.org/10.1016/0927-6505(93)90004-W.

[45] R. Essig et al. "Constraining Light Dark Matter with Diffuse X-Ray and Gamma-Ray Observations". In: (2013). arXiv: 1309.4091v3 [hep-ph].

[46] Fermi LAT collaboration. "The spectrum of isotropic diffuse gamma-ray emission between 100 MeV and 820 GeV". In: *M. Ackermann et al. 2015 ApJ 799 86* (2014). arXiv: 1410.3696v1 [astro-ph.HE].

[47] H. Yüksel et al. "Revealing the High-Redshift Star Formation Rate with Gamma-Ray Bursts". In: *Astrophys.J.683:L5-L8* (2008). arXiv: 0804.4008v2 [astro-ph].

[48] G.J. Mathews et al. "Supernova Relic Neutrinos and the Supernova Rate Problem: Analysis of Uncertainties and Detectability of ONeMg and Failed Supernovae". In: (2014). arXiv: 1405.0458v1 [astro-ph.CO].

[49] B.E. Robertson et al. "Cosmic reionization and early star-forming galaxies: A joint analysis of new constraints From Planck and the Hubble Space Telescope". In: (2015). arXiv: 1502.02024v2 [astro-ph.CO].

[50] P. Madau and M. Dickinson. "Cosmic star formation history". In: (2014). arXiv: 1403.0007v3 [astro-ph.CO].

[51] E. Vitagliano, I. Tamborra, and G. Raffelt. "Grand Unified Neutrino Spectrum at Earth: Sources and Spectral Components". In: *Rev. Mod. Phys.* 92 (2020). arXiv: 1910.11878v3 [astro-ph.HE].

[52] M. Diamond et al. "Axion-sourced fireballs from supernovae". In: *Phys.Rev.D* 10 (2023). arXiv: 2303.11395v2 [hep-ph].

[53] S. Scherer and M.R. Schindler. *A Primer for Chiral Perturbation Theory.* Springer, 2012.